

Molecular Genetics of Lissencephaly
and
Functions of LIS1 in Cell Division

by

Hyang Mi Moon

DISSERTATION

Submitted in partial satisfaction of the requirements for the degree of

DOCTOR OF PHILOSOPHY

in

Biomedical Sciences

in the

GRADUATE DIVISION

of the

UNIVERSITY OF CALIFORNIA, SAN FRANCISCO

Dedication and Acknowledgments

Dedication

This thesis is dedicated to the mentors, friends, and family who have supported me through graduate school and life.

UCSF

Tony Wynshaw-Boris : A great mentor of my PhD graduate study. This thesis would not have been possible without your support and guidance. I am grateful to have him as the best advisor in my long journey in bioscience. I would like to express my deepest gratitude to him.

John Rubenstein and Arnold Kriegstein : Members of my thesis committee. It is my great pleasure and honor to have them in my thesis committee. Thank you so much for sharing your knowledge and giving me inspiration to become a better scientist.

Biomedical Sciences PhD program : *Lisa Magargal, Monique Piazza, Kevin Luong, Caroline Rutland*. It was grateful to meet you and get help in my graduate school at UCSF. They were such friendly and wonderful people for me, a lonely transfer student from UCSD.

Tony's Lab Members : *YongHa Youn*, I appreciate all his help and advice in my graduate school days. He was one of the best laboratory colleagues that I have ever met. I learned so many things from him about mouse genetics/care and felt lucky to have another good teacher from Korea.

Jin Nakatani, He was a great labmate who shares not only the lab benches but also his ideas and skills. I miss you so much and hope you will become a good and successful professor in Japan. You were such a good person with friendships and kindness.

Marina Bershetyn, She is the role model of working mom, a female bioscientist that I met in the same lab. Thank you for sharing all your experiences in your graduate school days and gave me advice on my future career.

Former lab members, *Tiziano Prampero, Yuichiro Ihara, JeeHee Hong, Sailaja Peddada*

Current lab members, *Kazuhito Toyo-oka, Tomoka Toyo-oka, Haim Belinson, Lana Bogdanova, Brooke Babineau* : I would like to thank all of you to be great lab colleagues who give helps in experiments/mouse works and exchange scientific ideas.

Torsten Wittmann lab : *Torsten Wittmann, Hayley Pemble, Samantha Stehbens, Sarah Gierke*, It was a great joy for me to meet you as a collaborating team, experienced cell biology research group. Liqun Luo lab at Stanford : *Liqun Luo, Simon Hippenmeyer*, Thanks for providing me a chance to participate in successful collaborating project.

Institute for Human Genetics : Thank you so much for help settle down Tony's lab at UCSF IHG. They were helpful administrators for every aspect.

HSE 901 Floormates, (Nadav Ahituv lab) *Nadav Ahituv, Ramon Birnbaum, Meej Kim, Julia VanderMeer, Nir Oksenberg, Robin Smith (Jane Gitscher lab) Jane Gitscher, Elizabeth Theusch (Bob Nussbaum lab) Bob Nussbaum, Ianai Fishbein* : Although I do not have so many people known from my class at UCSF, luckily I met all of you as floormates to have lunch chat/discussion and happy hour events together. You were all wonderful.

Yien Kuo, Special thanks to you to share all my graduate years in UCSF. You were the first person I met in this school who is a great human being to have such a positive energy.

Kolis in UCSF, Korean bioscientist group in UCSF. I would like to keep these relationships with many of you in the future and in my life. Thank you for all support and helps.

Family and friends

My parents : I love you so much. My father (*MyoungYoung Moon*), I always respect you. My mother (*KapSuk Youn*), I know that you keep praying for me and us. I was so happy to have you in my PhD dissertation seminar and commencement in this year. God bless you and I sincerely believe in miracle.

My brother (HongIl Moon) : Thank you for being a supportive brother who takes care parents in Korea instead of me. I will look forward to meeting again my nephew, *Geonhee Moon* and sister-in-law in US in the future.

My husband's family, in-laws : I am happy to have another family members in my life. I am a not a good daughter-in-law and sister-in-law but I hope we will have good time when we all meet together again.

Beverly Chen : My best classmate from UCSD. I miss you and San Diego La Jolla very much. It was so nice to have you in my commencement. Thanks for coming and celebrating an important moment of my life together. You are the best friend that I met in US.

UCSD Biomedical Sciences PhD classmates : I am sorry that I only spent my 1st year of graduate school together with you at UCSD because of my transfer to UCSF. I will keep all great memories about my classmates, all events near the beautiful shores at La Jolla. I hope all of you will be also successful in your career.

Annie Arguello : It was very nice to meet you as a classmate in UCSF. You were a wonderful listener and counselor. It was always good to have some friend to share Korean heritage and cultures as well.

Seoul National University Lab (MS) : *JaeBum Kim*, my MS thesis advisor and Korean mentor, Thank you for making me step up the first level as a bioscientist in my graduate school in Korea.

Hokyung Rho and *KangHo Kim* : You have been such best friends who share joys and sorrows for a long time since college days. Although we are all far away in Korea, Houston and San Francisco, I hope we will be in the same as we were in Kim's lab to help and inspire each other.

Stanford Lab (Technician lab) : *Jeffrey Glenn*, my first PI in US and the best role model of young professor. I always keep in mind your advice about the balance between happiness and science.

My husband (Juanghae Alex Lee) : The best of the best. My soulmate and a life-long companion. Without you, all things would have been impossible for me, as a married woman and female scientist. I love you and hope to complete our family in next year.

Acknowledgements

The text of this dissertation includes a reprint of the material as it appears in:

Moon HM and Wynshaw-Boris A. 'Cytoskeleton in action: lissencephaly, a neuronal migration disorder.' *WIREs Dev Biol* 2012. doi: 10.1002/wdev.67

And the partial manuscripts of two research papers:

Moon HM, Youn YH, Pemble H, Yingling J, Wittmann T and Wynshaw-Boris A. 'LIS1 controls mitosis and mitotic spindle organization via the LIS1-NDE1/NDEL1-dynein complex.'

Moon HM and Wynshaw-Boris A. 'LIS1 is required for cleavage furrow positioning at the equatorial cortex during cytokinesis by regulating cortical contractility through RhoA-actomyosin and contractile ring components.'

I would like to thanks to Graduate Student Research Award (GSRA) from UCSF Graduate Division to support this study. These studies were also supported by the grants from NIH-R01 NS41030 and NIH-R01 HD047380.

Molecular Genetics of Lissencephaly
and
Functions of LIS1 in Cell Division

Hyang Mi Moon

Abstract

Lissencephaly (smooth brain) is a brain malformation disorder resulted from defective neuronal migration during early development. Deletion or mutation of many genes involved in the regulation of the microtubule (MT) and actin cytoskeletons have been identified as a direct causes of lissencephaly, including the human *LIS1* (lissencephaly-1) gene. Loss-of-function phenotypes of lissencephaly-causing protein are linked with MT-actin dysfunction in post-mitotic neurons, which disrupts nucleokinesis and leading process dynamics. Haploinsufficiency of human *LIS1* is responsible for reduced gyri/sulci in the brains from isolated lissencephaly sequence patients. We are particularly interested in mouse LIS1 functions in early development and used mouse embryonic fibroblasts (MEFs) and neural progenitors (NPs) to investigate molecular mechanisms regulated by LIS1. Previously, we demonstrated that loss of LIS1 in these cells led to cell death of these progenitors. However, the understanding of the detailed cellular processes regulated by LIS1 has been limited thus far. By performing timelapse live-imaging from *Lis1* mutant MEFs, we demonstrate here that LIS1 is required for the spatiotemporal regulation of the mitotic spindle during mitotic cell division to dictate proper spindle orientation, anchored to the cell cortex by astral MT plus-end tips. Furthermore, LIS1 is also essential for normal centrosome number maintenance in MEFs. Surprisingly, we found that *Lis1* mutant MEFs displayed severe defects in cytokinesis, a final critical step of cell separation. RhoA-actomyosin-contractile ring components

and signaling pathways important for cleavage furrow specification were misregulated in *Lis1* mutant MEFs, suggesting that mouse LIS1 mainly suppress RhoA GTPase activity to precisely control actomyosin-mediated cortical contractility at the cell cortex. Taken together, we concluded that LIS1 is a key molecular switch to balance MTs and actomyosin cytoskeletons to coordinate the interaction between mitotic spindle-associated cellular machinery and actin-based cell cortex membranes throughout the mitotic cell division. These results further suggest that LIS1 particulates in critical protein networks that determine cell survival or death of NPs through the regulation of mitosis and cytokinesis.

Table of Contents

Chapter One : General Introduction - Neuronal Migration Disorder and LIS1

1-1. Introduction.....	1
1-2. PAFAH1B1 (LIS1).....	7
1-3. Deletion of human chromosome 17p13.3.....	12
1-4. DCX (Doublecortin).....	13
1-5. Tubulin – TUBA1A, TUBB2B, TUBB3.....	16
1-6. RELN (Reelin).....	17
1-7. VLDLR / APOER2 (LRP8).....	20
1-8. ARX (Aristaless-related homeobox).....	20
1-9. NDE1 and NDEL1.....	21
1-10. CDK5.....	24
1-11. Conclusion.....	27

Chapter Two : Function of LIS1 in Mitosis

2-1. Introduction.....	29
2-2. Results.....	32
2-3. Discussion.....	57

Chapter Three : Function of LIS1 in Cytokinesis

3-1. Introduction.....	64
3-2. Results.....	67
3-3. Discussion.....	78

Chapter Four : Conclusions

4-1. Cytoskeletal regulation of microtubules and actin by lissencephaly-causing genes.....82

4-2. Mouse LIS1 is required for maintaining normal centrosome number and proper mitotic spindle orientation during mitotic cell division.....82

4-3. LIS1 integrates RhoA-actomyosin-contractile ring component signaling to restrict the cleavage furrow positioning at the equatorial cortex during cytokinesis.....83

4-4. Conclusions.....84

4-5. Implications.....85

Material and Methods.....87

References.....94

List of Table

Table 1. The genes implicated in human neuronal migration disorders.....	6
--	---

List of Figures

Chapter 1.

Figure 1-1. Schematic representation of the developing mammalian brain.....	2
Figure 1-2. Cytoskeletal features of migrating neurons during central nervous system (CNS) development.....	4
Figure 1-3. PAFAH1B1 (LIS1)-binding partners.....	10
Figure 1-4. PAFAH1B1 (LIS1) and RELN (Reelin)-mediated actin regulation.....	19
Figure 1-5. NDE1 and NDE1-like (NDEL1) are key proteins integrating several signals in neuronal migration.....	23
Figure 1-6. CDK5 phosphorylation substrates during neuronal migration.....	26

Chapter 2.

Figure 2-1. Loss of LIS1 results in a prolonged mitotic cell cycle to induce anaphase onset delay.....	33
Figure 2-2. Endogenous LIS1 in <i>Lis1</i> mutant MEFs is less distributed in the mitotic spindles and the cell periphery.....	36
Figure 2-3. Loss of LIS1 leads to extra centrosomes formation and centrosome number abnormality.....	38
Figure 2-4. <i>Lis1</i> mutant MEFs exhibit centrosome clustering phenotype during mitosis.....	40
Figure 2-5. Loss of LIS1 causes frequent multiple cilia formation in interphase.....	42
Figure 2-6. Loss of LIS1 induces chromosome misalignment in metaphase and chromosome missegregation in anaphase during mitosis.....	43

Figure 2-7. Loss of LIS1 causes less recruitment of kinetochore proteins to kinetochores on the chromosomes during mitosis.....	45
Figure 2-8. Loss of LIS1 impairs spindle orientation during mitosis of MEFs.....	47
Figure 2-9. Normal cell shape and morphology in metaphase of <i>Lis1</i> mutant MEFs.....	48
Figure 2-10. Loss of LIS1 results in less cortical dynein/dynactin complex recruitment to the cell cortex during mitosis.....	49
Figure 2-11. Loss of LIS1 causes aberrant interactions between astral microtubule plus ends and the cell cortex.....	51
Figure 2-12. Reduced frequency of movement of EB1-labeled astral MT plus-ends near the cell cortex.....	53
Figure 2-13. Spindle misorientation and centrosome clustering phenotype in <i>Lis1</i> mutant MEFs are restored by overexpression of several components of LIS1-NDEL1/NDE1-dynein complex.....	56
Figure 2-14. Proposed working model of LIS1 function in mitotic cell divisions.....	58

Chapter 3.

Figure 3-1. Loss of LIS1 disrupts normal cytokinesis and leads to increased formation of binucleated daughter cells.....	68
Figure 3-2. Loss of LIS1 results in cell shape oscillation and spindle rocking to cause cytokinetic failure with aberrant cleavage furrow positioning.....	70,71
Figure 3-3. <i>Lis1</i> mutant MEFs display mislocalization of RhoA-actomyosin and contractile ring components.....	74
Figure 3-4. Myosin-II (MRLC1) was abnormally distributed in <i>Lis1</i> mutant MEFs during cytokinesis.....	75
Figure 3-5. Contractile ring component (SEPT6) was not properly maintained at the equatorial cortex in <i>Lis1</i> mutant MEFs.....	76

Chapter 1. General introduction -

Neuronal Migration Disorder and LIS1

1-1. Introduction

During mammalian central nervous system (CNS) development, the migration of newly born neurons to the appropriate areas within the brain, and the differentiation of postmitotic neurons are essential for the proper establishment of synaptic circuits and their electrophysiological functions. Failure or delay in neuronal migration in the developing human neocortex results in cortical layer malformations and devastating neurological diseases. Human lissencephaly ('smooth brain') is a severe brain malformation disorder found in 1/30,000 births (Dobyns et al., 1993; Reiner et al., 1993). Clinically, lissencephaly is characterized by a smooth cerebral surface of the brain without the convolutions known as gyri or sulci. Lissencephaly is always associated with mental retardation and lissencephaly patients suffer from epilepsy and motor function impairment. The most common type of lissencephaly is classical lissencephaly (Type 1), characterized by disorganized or less-defined layering of cortical neuronal lamina rather than the well-defined distinct six neuronal layers formed during normal development. Reduced thickness of the cerebral cortex is also found in the brains of classical lissencephaly patients. This cortical malformation is mainly caused by the misregulation of neuronal migration during early development. During neocortical development, neurons are born from neural progenitors (NPs) in the ventricular zone (VZ) that divide again as they pass through the subventricular zone (SVZ) and intermediate zone (IZ), as intermediate or basal progenitors. After extensive migration toward the pial surface above the marginal zone (MZ), neurons become integrated into defined positions within neuronal layers in the cortical plate (CP) (Fig. 1-1). Therefore, the defects in neuronal migration result in the mispositioning of neurons in the neocortex.

There are two different types of neuronal migration that occur during mammalian forebrain

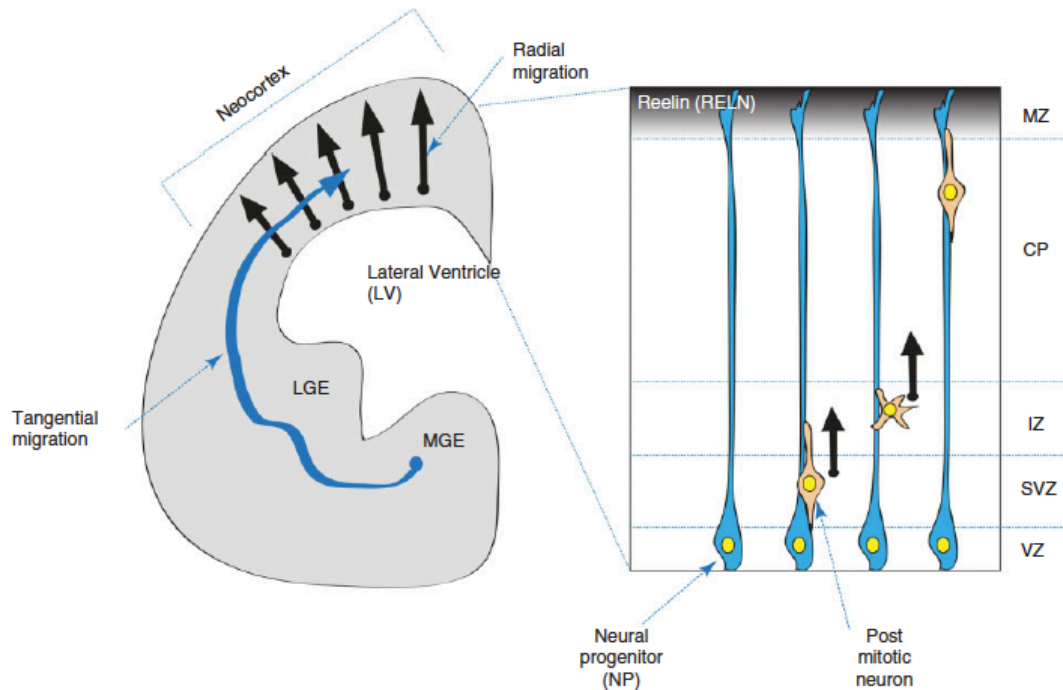


Figure 1-1. Schematic representation of the developing mammalian brain.

In the coronal section of one half of the mammalian developing forebrain there are two main migratory streams of postmitotic neurons: the radial migration of excitatory cortical pyramidal neurons from the ventricular zone (VZ) to the cortical plate (CP) (black arrow) and the tangential migration of inhibitory GABAergic interneurons from lateral and medial-ganglionic eminences (LGE/MGE) into the neocortex (blue arrow). The developing cerebral cortex in mammals is multilayered with different neuronal cell populations. Near the lateral ventricle (LV) surface, neural progenitors (NPs) reside in the ventricular zone (VZ). This progenitor zone is extended to subventricular and intermediate zones (SVZ and IZ, respectively). Newly born neurons from the division of NPs undergo extensive radial neuronal migration to enter the cortical plate (CP). The marginal zone (MZ) is the most superficial layer to contain Cajal-Retzius cells secreting the RELN (Reelin) glycoprotein.

development: (1) radial migration and (2) tangential migration. During radial migration, the excitatory cortical pyramidal neurons are born from NPs in the VZ and migrate to the CP. In a sequential migration stream, later-born neurons bypass early-born neurons and occupy more superficial layers of the CP, which generates an ‘inside-out’ pattern of cortical layers (Rakic et al., 1974). Radial migration occurs extensively in the cerebral cortex and hippocampus during embryonic brain development. During tangential migration, inhibitory interneurons are generated from the different types of progenitors at the medial or lateral ganglionic eminence (MGE/LGE) and migrate to the neocortex (Fig. 1-1). Radially migrating neurons generally display bipolar morphologies along radial glia with only a few branch points (although they do display transient multipolar morphologies in the IZ layer). By contrast, tangentially migrating neurons frequently change the directions of migration and display dynamic morphological transitions. When postmitotic neurons migrate, cytoskeletal remodeling of microtubules (MTs) and actin is evident in these cells. The volume of the nucleus (also called the soma) compared to those of extended processes is dramatically increased in the migrating neurons. The nucleus is surrounded by MT-enriched arrays in front of (fork-like MTs) and behind (cage-like MTs) the nucleus. In the leading process, the extended bundles of MTs emanate from the MT-organizing center (MTOC, also called centrosome) in front of the nucleus. Positioning of the centrosome defines the direction of movements of migrating neurons. The most anterior part of the leading process is the growth cone that senses extrinsic guidance cues and extends to the migration site. This protruded membrane structure is composed of filamentous actin (F-actin) stress fibers that establish new contacts with adhesion substrates (focal adhesion). Migration proceeds during neuronal locomotion in two modes of movements as a two-stroke action, with asynchronous movements of the centrosome (C) and later the nucleus (N). The centrosome first moves into a swelling in the leading process and then the nucleus follows (nuclear translocation, also called somal translocation or nucleokinesis) due to a pulling force from MTs and dynein motors located at the centrosome. Centrosome movement forward into the leading process precedes nuclear movement and this

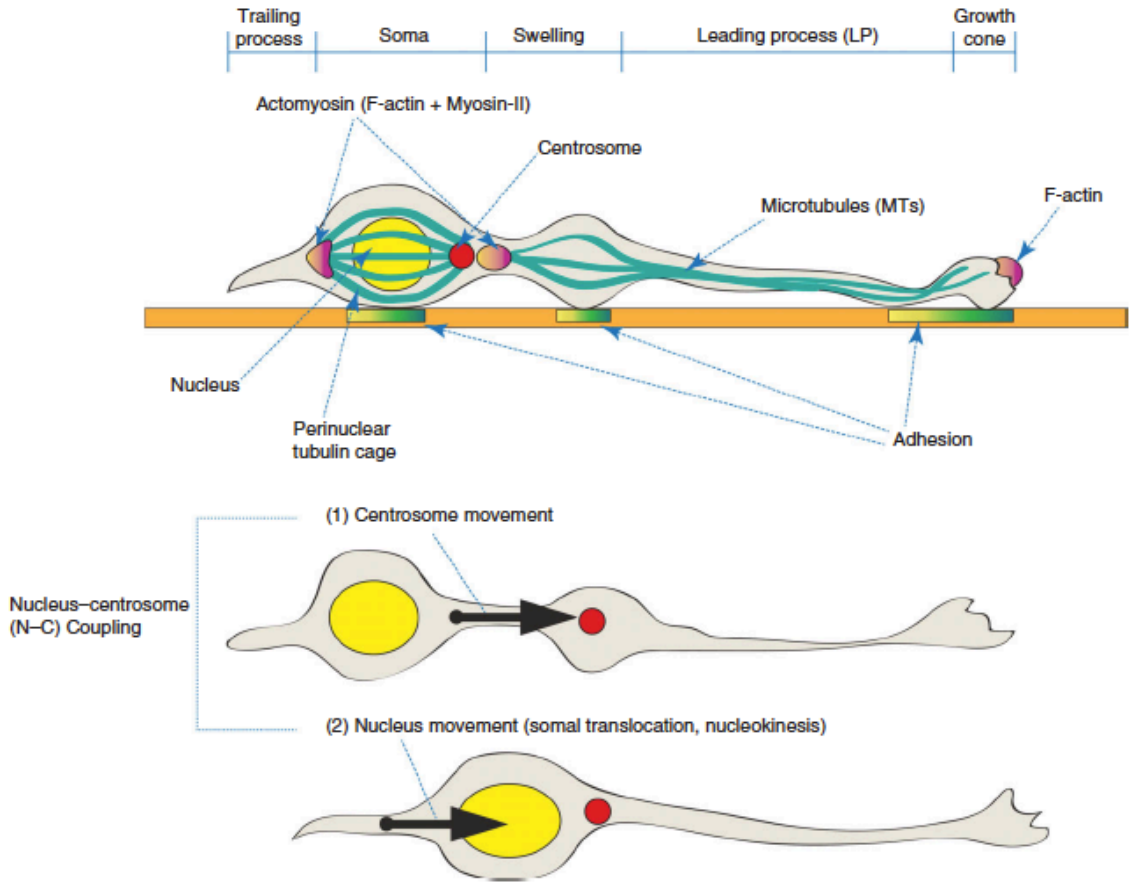


Figure 1-2. Cytoskeletal features of migrating neurons during central nervous system (CNS) development.
 Migrating neurons are polarized from the growth cone, which is the migrating tip of the leading process (LP) to the trailing process (TP). The nucleus is surrounded by a perinuclear tubulin cage and the rear side of the nucleus is enriched with actomyosin (filamentous actin, F-actin + Myosin-II) that generates pushing forces of nuclear movement (somal translocation, nucleokinesis). Migration occurs in two distinct modes of movements in a two-stroke model: (1) centrosome (C) movement toward the swelling in the LP and (2) nuclear (N) movement in the direction of migration. This N-C coupling consequently provides the pulling force on microtubules (MTs) along the LP, which establishes new contacts to adhesion substrates.

coordinated relationship is called nucleus–centrosomal (N–C) coupling (Tsai et al., 2005; Solecki et al., 2004). Eventually, the trailing process is retracted due to actomyosin (F-actin + Myosin-II)-dependent motor functions, which leads to net movement of the neuron. Myosin-II-dependent motors play a dual role in nuclear movement by generating a forward MT pushing force and a pulling force from behind (Solecki et al., 2009) (Fig. 1-2). This repetitive MT-actin remodeling is dynamically regulated during radial migration. Similarly, MGE-derived tangentially migrating cells also undergo MT and actomyosin-dependent migratory cycles during nucleokinesis (Bellion et al., 2005; Schaar et al., 2005). These dramatic cytoskeletal changes are major common characteristics of neuronal cell migration.

A diverse collection of cytoskeletal proteins is involved in the tight control of neuronal migration during neocortical development. Extensive studies on the genes mutated in human neuronal migration defects have uncovered critical roles of their protein products in the regulation of cytoskeleton dynamics during neuronal migration and development (Table 1). In this review, we will focus on some of the genetic studies in humans and mouse model system that identified those genes. We will also highlight recent approaches focusing on cellular mechanisms of action of these key proteins working in neuronal migration in the context of the MT and actin cytoskeletons.

Gene	Chromosomal locus in human	Human clinical presentation	Migration defects in mouse	Regulation mechanisms
<i>PAFAH1B1</i>	17p13.3	ILS	Abnormal lamination of cortex and hippocampus	MT / Dynein Actin
<i>YWHAE</i>	17p13.3	MDS (with LIS1 deletion)	Abnormal lamination of cortex and hippocampus	MT
<i>NDE1</i>	16p13.11	Micro-lissencephaly	Microcephaly Moderate lamination defects in cortex	MT
<i>DCX</i>	Xq22.3-q23	ILS (male) SBH (female)	Mild disorganization of hippocampus, Modest cortical lamination defects	MT Actin
<i>Tubulin</i> (<i>TUBA1A</i> , <i>TUBB2B</i> , <i>TUBB3</i>)	TUBA1A, 12q13.12 TUBB2B, 6p25.2 TUBB3, 16q24.3	ILS with cerebellar hypoplasia TUBB2B—asymmetric PMG	Abnormal lamination of cortex	MT
<i>RELN</i> (<i>Reelin</i>)	7q22	ILS with cerebellar hypoplasia	Inverted layering of CP in cortex	MT Actin
<i>VLDLR</i> [LRP8 (APOER2), mutations not found in human]	VLDLR, 9p24	ILS with cerebellar dysfunction	Inverted layering of CP in cortex	MT Actin
<i>ARX</i>	Xp21.3	XLAG	Absence of cortical interneurons and lamination defects	Transcriptional regulation

ILS, isolated lissencephaly sequence; MDS, Miller–Dieker syndrome; SBH, subcortical band heterotopia; PMG, polymicrogyria; XLAG, X-linked lissencephaly with abnormal genitalia; CP, cortical plate; MT, microtubule.

Table 1. The genes implicated in human neuronal migration disorders

1-2. *PAFAH1B1* (*LIS1*)

Human and Mouse Genetics

Human *PAFAH1B1* (platelet-activating factor acetylhydrolase isoform 1b regulatory subunit 1, formerly known as *LIS1*, Lissencephaly-1) was the first identified causal gene of neuronal migration disorders in any organism. Heterozygous de novo mutation or deletion of the human *PAFAH1B1* gene on chromosome 17p13.3 is responsible for 40% of patients with isolated lissencephaly sequence (ILS) (Dobyns et al., 1993; Reiner et al., 1993; Reiner et al., 2006; Wynshaw-Boris, 2010). Thus far, more than 70 distinct intragenic heterozygous mutations have been identified from human genetic studies (Friocourt et al., 2011). Severe brain malformations are the main characteristics of these patients, including simplified gyration in the cerebral cortex (agyria, pachygyria), disrupted cortical lamination, enlarged ventricles, and neuronal heterotopias, leading to short lifespan of ILS patients (Reiner et al., 2009).

PAFAH1B1 (*LIS1*) protein is evolutionarily conserved from yeast to mammals. In order to study the *in vivo* function of mouse *Pafah1b1* (*Lis1*), our group generated *Pafah1b1* knockout (*ko*, null) and hypomorphic conditional knockout (*hc*) alleles by gene targeting. *Pafah1b1* heterozygous (*Pafah1b1*^{ko/+}) mice display mild neuronal migration defects in the cortex and hippocampus (Hirotsune et al., 1998). Further reduction of *PAFAH1B1* (*LIS1*) protein levels by producing compound heterozygous (*Pafah1b1*^{hc/ko}) mice results in enhanced anatomical abnormalities in cortical and hippocampal structures. *Pafah1b1* compound heterozygous (*Pafah1b1*^{hc/ko}) mice display severe thinning of the cerebral cortex and broadly diffuse CP laminar organization. The hippocampal structures in these mice were also markedly disorganized due to neuronal migration defects during hippocampal development (Gambello et al., 2003). These *PAFAH1B1* dosage-dependent phenotypes in mouse animal models support a haploinsufficiency model for lissencephaly resulting from heterozygous deletion or mutation of *PAFAH1B1* in humans. Epileptic phenotypes and deficits in learning and motor function were also observed in

these Pafah1b1 mouse models, which have been seen in most human ILS patients (Paylor et al., 1999; Fleck et al., 2000).

PAFAH1B1 (LIS1), a Member of NUD Family Proteins and a Subunit of PAFAH

PAFAH1B1 (LIS1) is a 45 kDa protein with an N-terminal, homodimerization, and coiled-coil domain. The C-terminus of PAFAH1B1 contains seven WD40 (tryptophan-aspartic acid-40) repeats that are required for dynein/MT binding. The *PAFAH1B1* homolog *nudF* was identified as one of the nuclear distribution *nud* mutants in the bread mold *Aspergillus nidulans*. The *nud* mutants exhibit defects in nuclear movement into fungal hyphae during sporulation. Several *nud* mutants were genetically identified in *A. nidulans* and one of the *nud* mutants was cytoplasmic dynein, a MT minus end-directed motor. Cytoplasmic dynein is a MT motor that plays a key role in generating the pulling power of retrograde cargo transport along MTs. In addition, dynactin, a dynein-regulatory accessory protein, was also identified as a *nud* mutant, confirming the participation of dynein in nuclear movements. Several NUD protein–dynein interactions are evolutionarily conserved, supporting the critical functions of PAFAH1B1–NUD proteins in cytoplasmic dynein-regulatory pathways that control nuclear movement and nucleus positioning. Among mammalian NUD family proteins, NUDE (*nudE* nuclear distribution gene E homolog) and NUDC (*nudC* nuclear distribution gene C homolog) were identified as PAFAH1B1 (mammalian *nudF* homolog protein)-binding partners. Mammalian *nudE* homologues are now termed *NDE1* (mammalian *NudE*, *mNudE*) and *NDEL1* (*mNudE*-like) [see section 1-9, nuclear distribution gene E homolog 1 (NDE1) and NDE1-like (NDEL1)]. NUDC directly binds to PAFAH1B1 and dynein/dynactin complex and plays a chaperonin-like role for PAFAH1B1 stabilization (Morris et al., 1998; Aumais et al., 2001). A recent study demonstrated that *Nudc* siRNA-mediated knockdown (KD) in rat brain also results in neuronal migration defects (Capello et al., 2011).

Interestingly, the PAFAH1B1 protein was first discovered to be a noncatalytic subunit of PAFAH (platelet-activating factor acetylhydrolase). The fully functional PAFAH complex is

composed of two PFAH catalytic subunits (PFAH1B2 and PFAH1B3, formerly known as PFAH α 2 and PFAH α 1, respectively) and homodimers of regulatory subunits, PFAH1B1. This PFAH complex inactivates the intracellular messenger PAF (platelet-activating factor) by removing the acetyl moiety (Hattorri et al., 1994) (Fig. 1-3). The PAF receptor-encoding gene *PTAFR* expressed in the developing brain and PAF receptor-deficient mice (*Ptafr*^{-/-}) show cerebellum disorganization. Importantly, the speed of neuronal migration is significantly slower in double mutants for *Pafah1b1* and the PAF receptor (*Ptafr*^{-/-}; *Pafah1b1*^{ko/+}) than *Pafah1b1* heterozygous (*Pafah1b1*^{ko/+}), suggesting the crucial role of PAF signaling pathway in neuronal migration (Tokuoka et al., 2003).

MT Regulation

PFAH1B1 (LIS1) directly binds to tubulin and stabilizes MTs by regulating MT dynamics (Sapir et al., 1997; Sasaki et al. 2000). Most importantly, PFAH1B1 has been implicated in cytoplasmic dynein/dynactin-mediated MT cytoskeletal changes (Wynshaw-Boris, 2007). Dynein is a MT minus end-directed motor protein that regulates MT dynamics and generates MT pulling forces in the cells. This dynein/MT modulation by PFAH1B1 (LIS1) is evolutionarily conserved from *Aspergillus* to mammals. The *Aspergillus* PFAH1B1 homolog (*nudF*) mutants exhibit less MT dynamics with reduced rates of MT polymerization at MT plus ends (Han et al., 2001). Mammalian PFAH1B1 directly binds to several subunits of cytoplasmic dynein and dynactin (Sasaki et al., 2000; Faulkner et al., 2000; Smith et al., 2000). *Pafah1b1*-deficient cells display an increase in perinuclear localization of MT arrays and a decrease in MT plus end distribution at the cell periphery. These phenotypes seen in PFAH1B1 deficiency are consistent with a loss of cytoplasmic dynein/dynactin complex at plasma membranes in these cells (Sasaki et al., 2000; Smith et al., 2000; Yingling et al., 2008). In addition to this, PFAH1B1 protein is enriched at MT-concentrated intracellular compartments such as the centrosome in mammalian cells (Faulkner et al., 2000; Smith et al., 2000). A decrease in PFAH1B1 protein levels causes defects in N–C coupling with reduced distance between nucleus and centrosome during neuronal

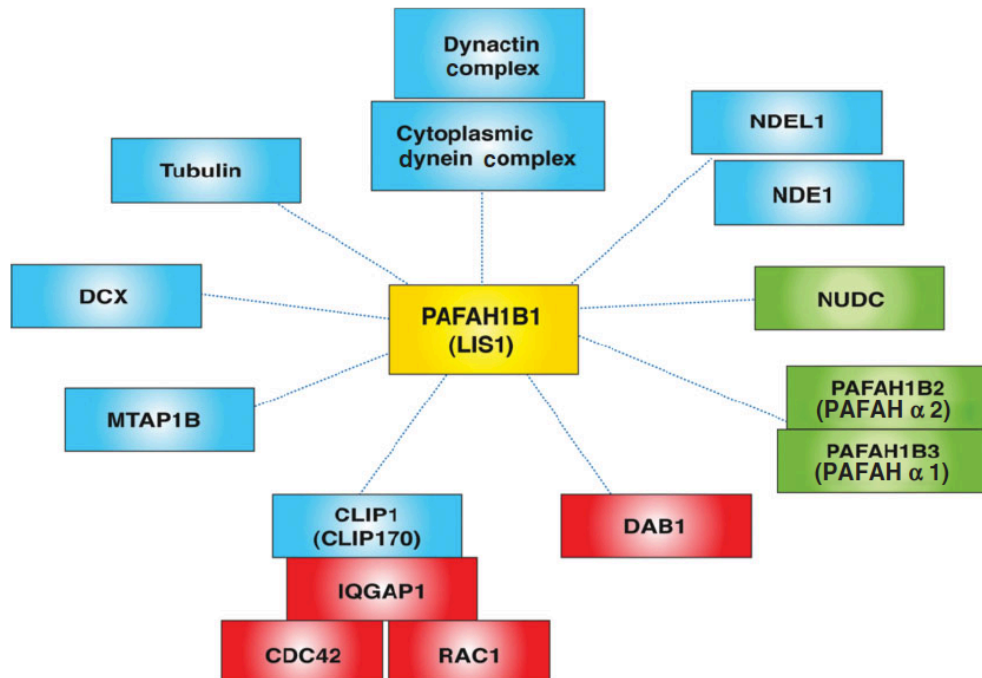


Figure 1-3. PAFAH1B1 (platelet-activating factor acetylhydrolase 1 regulatory subunit 1, formerly known as LIS1)-binding partners.

The binding of PAFAH1B1 (LIS1) to the cytoplasmic dynein/dynactin complex is evolutionarily conserved from fungi to mammals. Nuclear distribution proteins such as nuclear distribution gene E homolog 1 (NDE1), NDE1-like (NDEL1), and nuclear distribution gene C homolog (NUDC) interact directly with PAFAH1B1. PAFAH1B1 itself is a microtubule-associated protein (MAP) and is localized at tubulin/microtubule (MT)-rich subcellular compartments in cells like centrosomes. Other MAPs, such as doublecortin (DCX) and microtubule-associated protein 1b (MTAP1B), are also PAFAH1B1-binding partners. PAFAH1B1 was also identified as a noncatalytic subunit of PAFAH and PAFAH1B1 associates with PAFAH catalytic subunits such as PAFAH1B2 (PAFAH α 2) and PAFAH1B3 (PAFAH α 1). When PAFAH1B1 binds to CLIP1 (CLIP170), a MT plus end protein, it forms a complex with IQGAP1 and CDC42/RAC1. Through this interaction, PAFAH1B1 participates in F-actin dynamics in growth cones during neuronal migration. Interestingly, PAFAH1B1 also binds to disabled homolog 1 (DAB1), an actin-regulatory protein acting in RELN (Reelin) signaling pathway. PAFAH1B1 has dual roles in distinct regulatory pathways of MT and actin cytoskeletons. (Blue proteins, MT regulators; red proteins, actin regulators; green proteins, unclear detailed function in MT/actin regulation).

cell migration (Tsai et al., 2005; Tanaka et al., 2004). The pulling force of nuclear movement during nucleokinesis is generated by the PAFAH1B1/dynein complex at the centrosome. Therefore, defects in N–C coupling of *Pafah1b1*-deficient neurons result in slower migration speeds of these cells. PAFAH1B1 and dynein KD cells display similar migration defects in rat cortical cultures, suggesting that PAFAH1B1 and dynein converge on the same MT regulatory pathways in cortical development (Tsai et al., 2005). PAFAH1B1 itself is an atypical MT-associated protein (MAP), and interacts with other MAPs such as doublecortin (DCX) (Caspi et al., 2000) and MT-associated protein 1b (MTAP1B) (Jimenez-Mateos et al., 2005). DCX binding to MTs elevates the rate of MT polymerization and stabilizes MT arrays. Similarly, MTAP1B binding on MTs enhances the growth of dynamic MTs (Caspi et al., 2000; Jimenez-Mateos et al., 2005). PAFAH1B1 also binds to CLIP1 (formerly known as CLIP170), a MT plus end binding protein that helps loading of vesicle cargoes along MT arrays to the cell periphery (Coquelle et al., 2002; Tai et al., 2002) (Fig. 1-3).

Actin Regulation

Interestingly, PAFAH1B1–CLIP1 at MT plus ends is part of another large complex with CDC42 and RAC1, members of the small GTPase family proteins that function as actin-regulatory proteins. An effector of these small GTPases, IQGAP1, participates in this interaction and further stabilizes this complex.³³ PAFAH1B1 promotes F-actin polymerization at distal ends of leading processes by modulating CDC42/RAC1-dependent actin stabilization. PAFAH1B1 has critical roles in regulating these small GTPases by activating CDC42/RAC1 and antagonistically inactivating RhoA (encoded by *RhoA* gene). *Pafah1b1* deficiency in heterozygous cells (*Pafah1b1*^{ko/+}) leads to the misregulation of actin cytoskeleton at the growth cones in the leading processes of migrating neurons. *Pafah1b1*-deficient neurons have reduced F-actin in the leading edge and less numbers of filopodia, which results in slower migration of these cells (Kholmanskikh et al., 2003; Kholmanskikh et al., 2006). This actin cytoskeleton remodeling by PAFAH1B1 also contributes to proper neuronal migration. Intriguingly, PAFAH1B1 binds to

DAB1 (disabled homolog 1), a scaffold adaptor protein downstream of RELN (see 1-6. RELN section). By interacting with phosphorylated-DAB1 (P-DAB1) in a phosphorylation-dependent manner, PFAFH1B1 controls F-actin polymerization in the growth cones of the migrating neurons (Assadi et al., 2003) (Fig. 1-3). DAB1-mediated crosstalk between PFAFH1B1 and RELN pathways has pivotal roles linking cytoskeletal dynamics of actin to those of MTs.

1-3. Deletion of human chromosome 17p13.3

Human and Mouse Genetics

Large deletions of human chromosome 17p13.3 cause Miller–Dieker syndrome (MDS), a severe form of lissencephaly (often complete agyria) accompanied by craniofacial dysmorphisms.² In contrast to ILS patients, where 40% display *PFAFH1B1* deletions, 100% MDS patients have larger contiguous gene deletions consisting of both *PFAFH1B1* and *YWHAE*. More than 20 genes are located in this deleted region. Among these genes, the human *YWHAE* gene is located near the telomeric tip of chromosome 17p about 1Mb from the *PFAFH1B1* gene. *YWHAE* gene encodes the 14-3-3 ϵ (tyrosine 3-monooxygenase 5-monooxygenase activation protein, ϵ peptide) protein, a member of 14-3-3 protein family that is an evolutionarily conserved signaling molecule (Lo Nigro et al., 1997; Chong et al., 1997). The location of mouse *Ywhae* gene is also conserved on mouse chromosome 11 where mouse *Pafah1b1* gene is located, and these are conserved synteny regions on human chromosome 17p13.3 region and mouse chromosome 11.

Mouse *Ywhae* null homozygous mutants display hippocampal and cerebral disorganization. Double compound heterozygous mice with both *Pafah1b1* and *Ywhae* mutations (*Pafah1b1*^{ko/+}; *Ywhae*^{-/-}) display more severe migration defects than those of single mutants, consistent with the more severe brain phenotypes seen in MDS patients (Toyo-oka et al, 2003). This synergistic effects of reduced YWHAE protein levels on the severity of neuronal migration in *Pafah1b1*-deficient mice suggest that YWHAE may modulate components of the PFAFH1B1 pathway to

control the motility of neurons.

YWHAE-mediated MT Regulation

YWHAE protein binds to CDK5 (cyclin-dependent kinase 5)-phosphorylated-NDEL1 (P-NDEL1) directly. CDK5 plays a key role in the regulation of neuronal migration in mice (see section of 1-10. CDK5). YWHAE binding to NDEL1 protects P-NDEL1 from protein phosphatase 2 (PPP2, formerly known as PP2A)-dependent dephosphorylation and enhances P-NDEL1 stability.³⁸ These CDK5-mediated phosphorylation sites of NDEL1 are involved in dynein and PAFAH1B1 interaction. Hence, the P-NDEL1/YWHAE complex binds tightly to cytoplasmic dynein and PAFAH1B1 along MTs. Loss of the YWHAE protein results in mislocalization of NDEL1 and PAFAH1B1 offloaded from MT plus end tips (Toyo-oka et al., 2003), suggesting that YWHAE also converges on PAFAH1B1/NDEL1/dynein-regulated MT remodeling pathway during neuronal migration.

CRK-mediated Actin Regulation

CRK (v-crk sarcoma virus CT10 oncogene homolog) is one of the genes located within the MDS critical region at the telomeric end of human chromosome 17p (Carsodo et al., 2003), adjacent to *YWHAE*, and additional loss of CRK may contribute to the more severe phenotype of MDS. CRK family proteins function as adaptor molecules to reorganize the actin cytoskeleton by regulating adhesion signals (Feller et al., 2001). Intriguingly, CRK and CRKL (CRK-like) interact with P-DAB1 that is implicated in RELN-mediated actin-regulatory pathway (Park et al., 2008). *Crk* null mice display craniofacial defects during early development (Park et al., 2006) and *Crk/Crkl* KD prevents RELN-induced dendrite extension in hippocampal neurons (Matsuki et al., 2008), which are consistent with the severe craniofacial and neurological phenotypes seen in MDS patients.

1-4. DCX (Doublecortin)

Human and Mouse Genetics

DCX (doublecortin) is the most common genetic cause of X-linked lissencephaly and the human gene is located in Xq22.3-q23. Clinically, heterozygous *DCX* mutations in females (*DCX*^{+/-}) result in subcortical band heterotopia (SBH, misplaced neurons in the white matter rather than the CP), while hemizygous mutation in males (*DCX*^{y/-}) results in ILS. Female phenotypes with *DCX* mutation are variable due to random X-inactivation, resulting in genetic mosaicism in these patients (Gleeson et al., 1998; des Portes et al., 1998). One distinct feature in *DCX*-associated ILS compared to that of *PAFAH1B1*-associated ILS is that *PAFAH1B1* has a more severe posterior (P) cortical abnormality, while *DCX* has a more severe anterior (A) phenotype (*DCX* P > A versus *PAFAH1B1* P < A).

Mouse *Dcx* genetic male mutants (*Dcx*^{y/-}) display mild histological defects in the cortex and more notable disorganization of the hippocampus (Corbo et al., 2002), probably due to compensatory mechanisms from doublecortin-like kinase (*Dclk*). In support of this, *Dcx/Dclk* double knockout (DKO) mice display severe defects in neuronal migration with abnormal lamination in the CP with the accumulation of multipolar neurons in the IZ (Deule et al., 2006; Tanaka et al., 2006). More careful analysis of neuronal migration by live imaging of brain slices from *Dcx* genetic male mouse mutants (*Dcx*^{y/-}) (Pramparo et al., 2008) or acute *Dcx* KD cells in rat brain slices (Bai et al., 2003) uncovered significant migration defects in *Dcx*-deficient migrating neurons.

MT Regulation

DCX is a MAP expressed in NPs and differentiating neurons. *DCX* protein has two evolutionarily conserved tandem repeat domains that are required for MT binding and stabilization. *DCX* stabilizes MTs and enhances MT polymerization as well as the bundling capacity of MTs. *Dcx* mutant and *Dcx* KD immature neurons exhibit weakened N–C coupling and ultimately delayed centrosomal and nuclear movement (Tanaka et al., 2004; Sapir et al., 2008). *DCX* is also a phosphoprotein that serves as a substrate of several kinases, including MT affinity-regulating kinase 1 (MARK1) and protein kinase A (PRKA, formerly known as PKA) at residue Ser47

(Schaar et al., 2004), and CDK5 mainly at residue Ser297 (Tanaka et al., 2004). MARK1 and PRKA-mediated phosphorylation of DCX reduces its MT binding activity. P-Ser47-DCX (phosphorylated form of DCX at Ser47) is required for proper localization of DCX protein at the leading processes of migrating neurons. Ser297 of DCX is the *in vivo* phosphorylation target of CDK5 and this phosphorylation event enhances the MT binding ability of DCX. DCX may directly interact with PAFAH1B1 (Caspi et al., 2000), and this interaction may contribute to MT stabilization near perinuclear regions in migrating neurons to provide power for nuclear translocation (nucleokinesis). Thus, DCX increases MT stabilization and MT nucleation by increasing tubulin polymerization, and is one of the key MT regulators in corticogenesis during early development.

Actin Regulation

DCX is also phosphorylated by mitogen-activated protein kinase 8 (MAPK8, formerly known as JNK) at residue Thr321, Thr331, and Ser334. Phosphorylation of these DCX sites are responsible for DCX recruitment to the growth cones of leading processes, the F-actin-rich zone. MAPK8-mediated DCX phosphorylation is essential for neurite outgrowth of migrating neurons (Gdalyahu et al., 2004). Through binding to MAPK8-interacting protein 1 (MAPK8IP1, formerly known as JIP-1), DCX may control actin dynamics by regulating the RELN pathway, since MAPK8IP1 directly binds to LRP8 (APOER2), a RELN receptor. DCX interaction with PPP1R9B (protein phosphatase 1 regulatory subunit 9B, formerly known as Spinophilin or Neurabin-II) may also provide a mechanism linking actin and DCX. DCX itself is cosedimented with F-actin *in vitro* and adding PPP1R9B elevates DCX-F-actin binding affinity (Tsukada et al., 2005). PPP1R9B is an actin-binding protein functioning as a protein phosphatase-1 (PPP1)-adaptor protein. PPP1R9B-mediated PPP1 targeting of DCX induces dephosphorylation of the residue Ser297. PPP1R9B and DCX colocalize at the growth cones where MT and actin dynamically interact. Dephosphorylation of Ser297 of DCX by PPP1R9B/PPP1 is important for DCX distribution at neurite tips during neuronal migration (Bielas et al., 2005).

1-5. Tubulin—*TUBA1A*, *TUBB2B*, *TUBB3*

Given that PAFAH1B1, DCX and YWHAE are all MT-associated proteins, it is not a surprising finding that tubulin mutations themselves, including *TUBA1A*, *TUBB2B*, and *TUBB3* can cause neuronal migration disorders and cortical malformations.

TUBA1A

TUBA1A (tubulin α -subunit 1A isoform) was first reported to have key roles in cortical development in both mouse and human (Keays et al., 2007). The mouse model, first described in an ENU mutagenesis study, displayed hippocampal disorganization and behavioral deficits with no overt cortical phenotype, while in human *TUBA1A* mutation-harboring patients, cortical laminar organization was disrupted and hypoplastic cerebellum and brainstem regions were also observed. Mutations found in the mouse and humans were located either within GTP binding pocket or structurally close to the motif participating in β -tubulin subunit interaction, suggesting that GTP-dependent incorporation of α - and β -tubulin in heterodimer was impaired and resulted in defective MT polymerization (Keays et al., 2007). A subsequent study demonstrated that tubulin-related cortical malformations have a very broad phenotypic spectrum in human patients (Poirer et al., 2007).

TUBB2B* / *TUBB3

Heterozygous mutation in human *TUBB2B* (tubulin β -subunit 2B isoform) causes asymmetric polymicrogyria (PMG), characterized by multiple small gyri separated by shallow sulci. Halting of neuronal migration within IZ in *Tubb2b* KD rat embryo brains suggests that *TUBB2B* contributes to neuronal migration during development (Jaglin et al., 2009). More recently, other β -tubulin *TUBB3* (tubulin β -subunit 3 isoform) human heterozygous mutations were identified that lead to cortical malformation and perturbation of axon guidance by altering MT dynamics (Tischfield et al., 2010).

1-6. *RELN* (Reelin)

Human and Mouse Genetics

RELN (Reelin), a large extracellular matrix glycoprotein (~400 kDa), is expressed and secreted by Cajal-Retzius cells at the MZ layer of the developing brain. Mutation of the human *RELN* gene located on chromosome 7q22 causes an autosomal recessive form of lissencephaly syndrome with cerebellar hypoplasia as well as malformations in the hippocampus and brainstem (Hong et al, 2000). The mouse *Reeler* mutant (*RELN* mutation) was the first mouse mutant described with neuronal migration defects and widely studied. Homozygous *Reeler* mice display ataxia, cerebellar hypoplasia and inverted ‘outside-in’ cortical layering, composed of superficial early-born neurons and deep positioning later-born neurons (opposite to the normal CP layering) (Caviness et al., 1982; D’Arcangelo et al., 1995). The absence of a well-defined MZ layer is another characteristic of *Reeler* mouse cortex due to overmigration of neurons. This observation suggests that RELN functions as a ‘stop’ signal of migrating neurons (Frotscher et al., 1998). The finding that RELN induces the detachment of migrating neuron from radial glial fibers (Dulabon et al., 2000) is consistent with the idea that RELN acts as a ‘stop and detach’ signal during radial migration (Cooper et al., 2008).

MT Regulation

RELN binds to the transmembrane receptors VLDLR (very low-density lipoprotein receptor) and LRP8 (low-density lipoprotein-related receptor 8, formerly known as APOER2). [see 1-7. APOER2 section]. RELN enhances the interaction between RELN receptors and DAB1, an intracellular adaptor protein and further induces the phosphorylation of DAB1 by SRC family kinases (SRC, FYN) activation. Upon RELN binding, tyrosine phosphorylation of DAB1 activates the downstream PI3K pathway that mediates PI3K-AKT-GSK3 β signaling and consequently the CDK5-dependent phosphorylation of its substrates, MT-associated protein tau

(MAPT) and MTAP1B is increased (Beffert et al., 2002; Gonzalez-Billault et al., 2005). Through this phosphorylation cascade, RELN–DAB1 regulates MT stability and dynamics in migrating neurons. Consistent with this, *Dab1* KO mice display a *Reeler*-like phenotype with neuronal migration defects (Howell et al., 1997). Intriguingly, P-DAB1 also binds to PAFAH1B1, a key regulator of MT/dynein in phosphorylation-dependent manner. Compound heterozygous of *Dab1/Pafah1b1* mouse mutant (*Dab1*^{+/-}; *Pafah1b1*^{ko/+}) display more severe cortical migration defects than single heterozygous mutants, suggesting important crosstalk between RELN and PAFAH1B1 signaling pathways *in vivo* and *in vitro* (Assadi et al., 2003) (Fig. 1-4).

Actin Regulation

RELN-induced activation of the DAB1–PI3K pathway elevates LIMK1 (LIM-domain containing protein kinase 1) kinase activity, which phosphorylates CFL1 (formerly known as cofilin), a F-actin-severing protein. Since P-CFL1 (phosphorylated cofilin) is an inactive form, the RELN–DAB1–PI3K–LIMK1–P-CFL1 signaling cascade increases the stability of F-actin stress fibers and consequently reduces actin cytoskeleton turnover. Therefore, *Reeler* mutants fail to transmit a DAB1–PI3K–LIMK1 signal and display reduced P-CFL1 levels in migrating neurons, resulting in misregulation of the actin cytoskeleton (Fig. 1-4). P-CFL1 may be enriched in the leading processes when migrating neurons reach the MZ layer. By elevating P-CFL1, RELN stabilizes the actin cytoskeleton and helps anchor the leading processes to the basal lamina of developing cortex. Therefore, reduced P-CFL1 in the absence of RELN results in destabilization of actin dynamics in the leading processes and leads to somal translocation failure. The *Reeler* mutant mouse cortex displays defects in somal translocation at the final stage of migration near the MZ, suggesting that the RELN pathway mediates a ‘detach and go (somal translocation)’ signal in this stage of radial migration (Cooper et al., 2008).

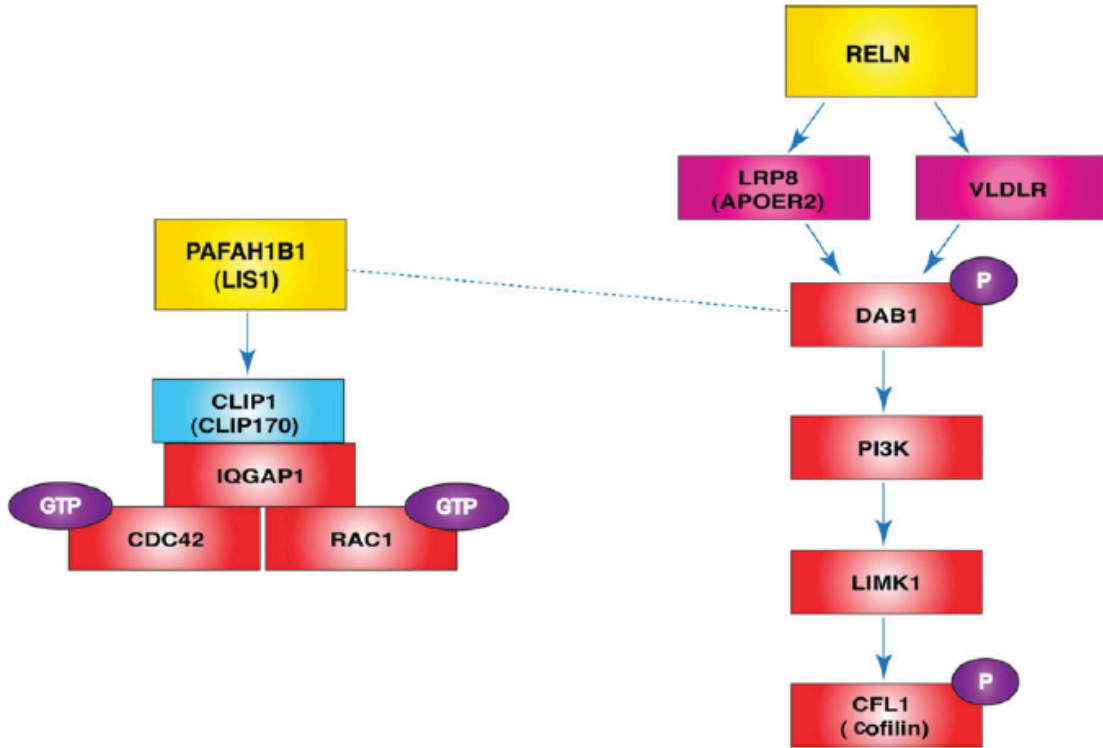


Figure 1-4. Platelet-activating factor acetylhydrolase 1 regulatory subunit 1 (PAFAH1B1) and RELN (Reelin)-mediated actin regulation.

Formation of the PAFAH1B1-CLIP1-IQGAP1-CDC42/RAC1 complex stabilizes and sustains the GTPase activities of CDC42 and RAC1. RELN, a large glycoprotein secreted from the marginal zone (MZ) area in the cortex, directly binds to lipoprotein receptors such as very low-density lipoprotein receptor (VLDLR) and low-density lipoprotein-related receptor 8 (LRP8) (APOER2). This binding recruits the disabled homolog 1 (DAB1) adaptor protein to the membrane where DAB1 is phosphorylated. P-DAB1 activates PI3K-LIM-domain containing protein kinase 1 (LIMK1) signaling and LIMK1 phosphorylates CFL1 (cofilin), an actin-severing protein, which keeps CFL1 in an inactive state. This further stabilizes F-actin stress fibers in migrating neurons. Since the dynamic regulation of the actin cytoskeleton is required for neuronal motility, a balance between actin polymerization and depolymerization is essential for neuronal migration processes. (Dashed line, direct interaction between PAFAH1B1 and P-DAB1; blue protein, microtubule (MT) regulator; red proteins, actin regulators).

1-7. *VLDLR* (Very low-density lipoprotein receptor) / *APOER2* (Low-density lipoprotein-related receptor 8, *LRP8*)

Human *VLDLR* mutations cause severe lissencephaly with cerebellar malformation (Ozcelik et al., 2008). Homozygous mutant patients display mental retardation and gyral simplification in the cortex. As noted above, *VLDLR* and *LRP8* are the members of the lipoprotein receptor family proteins at the plasma membrane and act as coreceptors for *RELN* (D'Arcangelo et al., 1999; Hiesberger et al., 1999). Compound DKO mice of *VLDLR/LRP8* display perturbation of neuronal migration that phenocopies the *Reeler* mutant (Trommsdorff et al., 1999).

VLDLR/LRP8 play critical roles in actin-MT regulation by interacting with *DAB1* through their cytosolic domain and *VLDLR/LRP8-DAB1* interaction triggers cytoskeletal remodeling during neuronal polarization and migration (Fig. 1-4) (see also 1-6. *RELN* section).

1-8. *ARX* (Aristaless-related homeobox)

ARX (aristaless-related homeobox) is an X-linked gene that encodes a transcription factor required for interneuron function and neuronal migration (Bonneau et al., 2002). Missense and truncation mutations of *ARX* lead to X-linked lissencephaly with abnormal genitalia (XLAG), and patients display epilepsy and severe mental retardation. Mouse *Arx* KO mutants similarly display neuropathological phenotypes such as GABAergic interneuron dysfunction due to tangential migration defects (Kitamura et al., 2002). *Arx* KO mice display disorganized pyramidal neuronal layering, suggesting *ARX* may play important role not only in tangential migration but radial migration as well (Bonneau et al., 2002; Kitamura et al., 2002). Since *ARX* can act as a transcriptional repressor and activator depending on promoter specificity, *Arx* mutation is accompanied by downregulation or upregulation of downstream target genes such as *Lmo1*, *Ebf3*, and *Shox2* to influence the regionalization process of the developing brain (Fulp et al., 2008;

Colasante et al., 2009). Genome-wide Chip-ChIP (chromatin immunoprecipitation) promoter analysis from *Arx* mutant cells revealed that ARX binds to the promoters of genes in regulatory pathways important for axonal guidance and neurite extension (Quille et al., 2011) suggesting that ARX is involved in cytoskeletal control of migration of postmitotic neurons by transcriptional regulation.

1-9. *NDE1* and *NDEL1*

Evolutionarily conserved PAFAH1B1 (LIS1)-binding partners

NDE1 (nuclear distribution gene E homolog 1) and NDEL1 (NDE1-like), mammalian homologues of NudE proteins, directly interact with PAFAH1B1 through its conserved coiled-coil domain (Sasaki et al., 2000; Niethammer et al., 2000). PAFAH1B1-dynein-NDE1 forms a complex that generates a persistent force of transport (McKenney et al., 2010). In recent human genetic studies, *NDE1* frame-shift mutations with protein decay have been reported and these mutations cause micro-lissencephaly (brain size reduction with cortical gyral simplification). *NDE1*-mutated patients have abnormal cortical gyral pattern and partial cortical layering defects in the brain. Similar mutation-carrying NDE1 proteins *in vitro* cannot localize to the kinetochores or centrosomes where normal NDE1 protein is recruited (Alkuraya et al., 2011; Bakircioglu et al., 2011). *Nde1* homozygous KO mice (*Nde1*^{-/-}) display microcephaly (small brain) with a fairly well-preserved CP. Detailed examination of the *Nde1* KO mouse cortex revealed that migrating neurons exhibited moderately retarded migration with thin superficial CP layers (Feng et al., 2004). By contrast, *Ndel1* heterozygous (*Ndel1*^{ko/+}) mice display no obvious phenotype but further reduction of NDEL1 protein level in compound heterozygous (*Ndel1*^{hc/ko}) mice leads to cortical patterning abnormalities such as irregularly diffuse CP neuronal layering. In addition, *Ndel1* mutants (*Ndel1hc/ko*) display significant splitting of the hippocampal pyramidal cell layer, suggesting neuronal migration defects in radial migration during hippocampal development. *Nde1*

and *Pafah1b1* double mutants (*Ndel1*^{-/-}; *Pafah1b1*^{ko/+}) display synergistic effects on neuronal migration (Sasaki et al., 2005), while *Ndel1* and *Pafah1b1* double mutants (*Ndel1*^{hc/ko}; *Pafah1b1*^{ko/+}) display synergistic effects on brain size and organization (Pawlisz et al., 2008). Thus, the phenotypes of loss-of-function of NDE1 and NDEL1 are somewhat different, suggesting that NDE1 and NDEL1 may play distinct roles in PAFAH1B1 pathway during brain development.

MT Regulation

We recently demonstrated that *Ndel1* and *Pafah1b1* have distinct dosage-dependent effects on neuronal migration, neurite outgrowth, and N-C coupling (Youn et al., 2009; Hippenmeyer et al., 2010). However, cellular functions of NDEL1 in migrating neurons seem to be mediated by MT cytoskeleton regulation that is somewhat similar to PAFAH1B1/dynein-dependent MT reorganization. In postmitotic migrating neurons, CDK5-mediated phosphorylation of NDEL1 enhances PAFAH1B1/dyneinregulated MT dynamics and promotes the binding to YWHAE. Importantly, both NDE1 and NDEL1 proteins are primarily localized to the centrosomes in mammalian cells, which suggests these NUD family proteins are important for MT reorganization by mediating central functions of PAFAH1B1 at the centrosomes. Together, NDE1 and NDEL1 have key roles in cortical neuronal migration by integrating signals from centrosome/MT-associated proteins (Fig. 1-5).

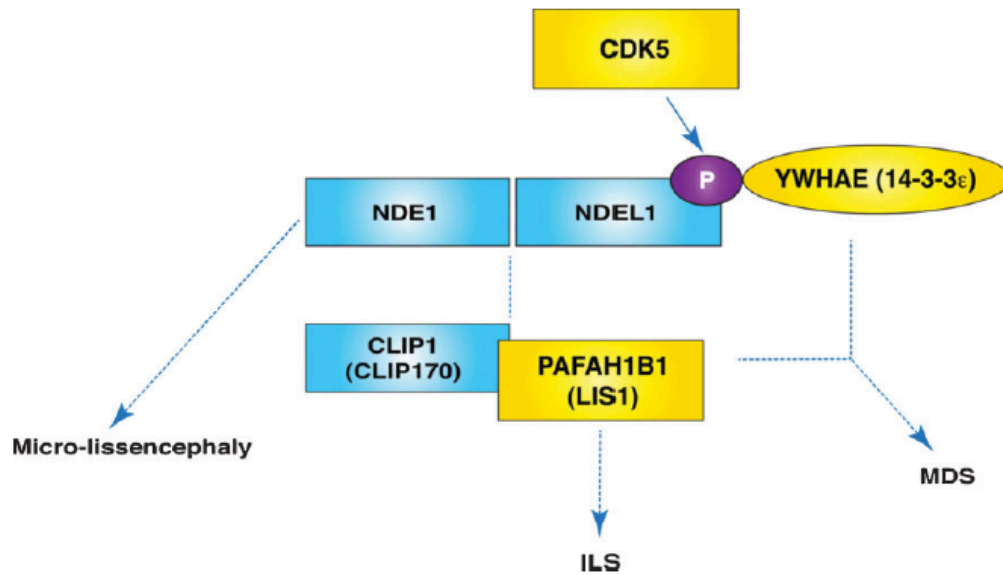


Figure 1-5. Nuclear distribution gene E homolog 1 (NDE1) and NDE1-like (NDEL1) are key proteins integrating several signals in neuronal migration.

NDE1 and NDEL1 are two mammalian homologues of *Aspergillus nidulans* nude. Upon cyclin-dependent kinase 5 (CDK5)-mediated phosphorylation of NDEL1, P-NDEL1 binds to YWHAE (formerly known as 14-3-3 ϵ). Isolated lissencephaly sequence (ILS) is caused by the haploinsufficiency of human PFAH1B1 (LIS1) gene. Simultaneous chromosomal deletion of the regions including YWHAE and PFAH1B1 in human causes Miller–Dieker syndrome (MDS), a severe case of lissencephaly with craniofacial malformation. Human NDE1 heterozygous mutations result in micro-lissencephaly.

1-10. CDK5

A key kinase to regulate neuronal migration in mice

CDK5 is a multifunctional serine/threonine kinase involved in neuronal migration by regulating phosphorylation events of several substrates. Upon binding of neuronal activators CDK5R1 (CDK5 regulatory subunit 1, formerly known as p35) and CDK5R2 (CDK5 regulatory subunit 2, formerly known as p39), CDK5 becomes enzymatically active in the developing brain. Cdk5 KO mice and Cdk5r1/Cdk5r2 DKO mice display inverted cortical layering, suggesting that the CDK5–CDK5R1/CDK5R2 pathway is essential for normal cortical development and neuronal migration (Su et al., 2011).

MT Regulation

CDK5 phosphorylates NDEL1, a PAFAH1B1-binding MT/dynein regulator and P-NDEL1 increases peripheral MT polymerization (Sasaki et al., 2000; Niethammer et al., 2000). DCX is also a substrate of CDK5 phosphorylation. P-DCX reduces the affinity of DCX binding to MT arrays, which results in DCX localization at perinuclear MTs (Tanaka et al., 2004). MTAP1B is phosphorylated by CDK5 and P-MTAP1B regulates MT-enriched axon elongation in migrating neurons (Pigino et al., 1997). Finally, CDK5-mediated PTK2 (protein tyrosine kinase 2, formerly known as FAK) phosphorylation is required for MT organization, nuclear movement, and neuronal migration (Xie et al., 2003).

Actin Regulation

Another important substrate of CDK5 in neuronal migration is CDKN1B (cdk inhibitor 1B, formerly known as p27^{kip1}), an actin regulatory protein. P-CDKN1B (phosphorylated form of CDKN1B) is stabilized and suppresses RhoA–GTPase activity (Ozcelik et al., 2008). RhoA has critical roles in actin cytoskeleton regulation by two major pathways: RhoA–ROCK(Rho kinase)–LIMK1–CFL1 phosphorylation and RhoA–ROCK–MLC (myosin light chain) phosphorylation. Therefore, CDK5-dependent CDKN1B phosphorylation is required for the inhibition of RhoA

activity to reorganize the actomyosin network during neuronal migration (Fig. 1-6).

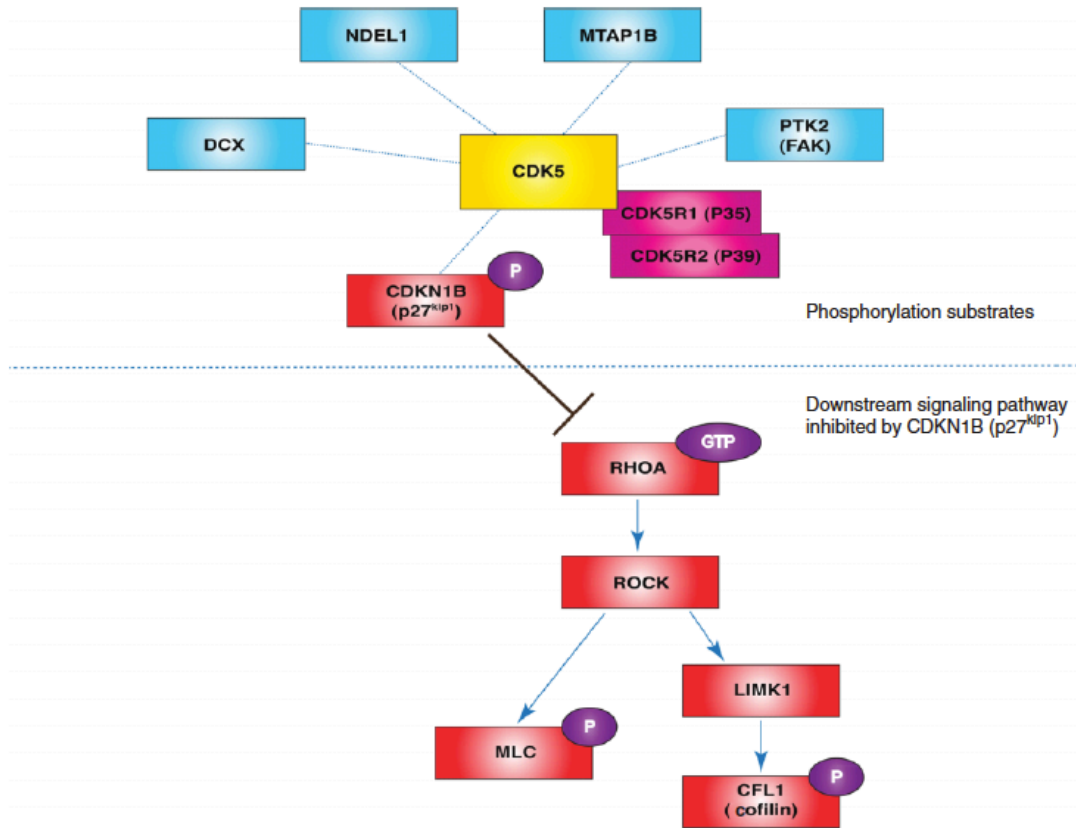


Figure 1-6. Cyclin-dependent kinase 5 (CDK5) phosphorylation substrates during neuronal migration.

When CDK5 is activated by binding of CDK5R1 (p35)/ CDK5R2 (p39), this kinase phosphorylates multiple substrates in migrating neurons. Among those substrates, doublecortin (DCX), Nuclear distribution gene E homolog 1 (NDEL1), microtubule-associated protein 1b (MTAP1B), and protein tyrosine kinase 2 (PTK2, also called FAK) are microtubule (MT)-regulating proteins. A very interesting phosphorylation substrate of CDK5 is CDKN1B (p27^{Kip1}). P-CDKN1B suppresses RhoA GTPase activity. RhoA–ROCK–LIM-domain containing protein kinase 1 (LIMK1)–CFL1 and RhoA–ROCK–MLC (myosin light chain) signaling pathways have been implicated in actin cytoskeletal remodeling during neuronal migration. CDK5 indirectly affects these actin-regulating signaling pathways by modulating CDKN1B function. (Blue proteins, MT regulators; red proteins, actin regulators).

1-11. Conclusion

Cytoskeletal remodeling of actin/MTs and the dynamic regulation of transport on these cellular structures are critical processes to induce neuronal polarization from the leading process to the trailing process and N–C coupling that drives nuclear and neuronal migration during CNS development. Several tubulin isoforms (TUBA1A, TUBB2B, TUBB3) are key components of neuronal MT arrays and DCX is tightly associated with MTs in migrating neurons. Loss of these proteins produces imbalances in MT dynamics, which causes lissencephaly or other cortical brain malformation in human. *PAFAH1B1* (*LIS1*) is a key regulator of MT stability and dynamics by modulating cytoplasmic dynein localization and motor function, while *YWHAE* binds to *P-NDEL1* to promote its function in dynein localization. Concomitant deletion of *PAFAH1B1* and *YWHAE* genes in chromosome 17p13.3 is the cause of MDS in human, suggesting that misregulation of MT stability and dynein dysfunction are the causes of MDS in human. Since deletion of *CRK*, an actin-regulatory protein on chromosome 17p, also occurs in MDS, actin dynamics may also play a role in this severe phenotype. Interestingly, *PAFAH1B1*, *DCX*, and *RELN* have central functions in the interplay between actin and MT cytoskeletons by affecting different downstream cellular pathways. *PAFAH1B1* specifically activates *RAC1/CDC42* GTPase activity to promote F-actin polymerization. The binding of *RELN* to its receptors, *VLDLR/LRP8* (*APOER2*) recruits *DAB1* adaptor protein to stabilize F-actin. Since *P-DAB1* also interacts with *PAFAH1B1*, while *DCX* interacts with *LRP8* through binding to *MAPK8IP1* (*JIP-1*), the effects of *PAFAH1B1/DCX* on MT dynamics converge to *RELN–VLDLR/LRP8–DAB1* actin regulatory pathway, which allows crosstalk between the actin and MT cytoskeletons. *PAFAH1B1*, *DCX*, and *RELN* are important organizational nodes to coordinate neuronal migration. Lastly, *ARX* mutation in human results in interneuron dysfunction and this gene is implicated in tangential migration of GABAergic neurons in the developing brain. The finding that *ARX* binds to the promoters of genes in regulatory pathways important for axonal guidance

and neurite extension (Quille et al., 2011), suggests that ARX is involved in cytoskeletal control of migration of postmitotic neurons by transcriptional regulation.

Although these previous studies have unraveled some key functions of several genes during neuronal migration in human and mouse, there are still many questions to be answered. It is likely that there is coordinate regulation between neuronal migration and neurogenesis/neuronal differentiation processes. Since many neuronal migration genes also encode centrosome-associated proteins (NDE1, NDEL1, and PFAFH1B1), cell cycle-dependent proliferation of NPs and the differentiation of daughter neurons and/or cell fates may be controlled by these centrosomal proteins. Recent studies of the human WDR62 gene demonstrated that deficiency of this centrosome-associate protein also causes micro-lissencephaly (Nicholas et al., 2010; Yu et al., 2010; Bilguvar et al., 2011). Emerging evidence strongly supports the notion that subcellular components other than centrosome (critical for N–C coupling) participate in neuronal migration processes during cortical development. These candidates include gap junction proteins, adhesion molecules and proteins involved in vesicle trafficking or recycling pathways. However, it is not clear whether these proteins contribute to neuronal migration through actin/MT cytoskeletal regulation or via distinct processes. To further understand the exact molecular and cellular mechanisms underlying neuronal migration during mammalian cerebral cortex development, additional *in vivo* and *in vitro* studies are needed for the accurate mapping of genetic and physical interactions in protein–protein networks and the proper positioning of individual protein components within detailed signaling pathways. Future studies of neuronal migration will likely explore many aspects of cytoskeletal regulation in migratory processes to further understand neuropathological pathways responsible for neurodevelopmental brain malformation disorders caused by neuronal migration defects in human. Delineation of these pathways will aid in the identification of potential new therapeutic targets to ultimately cure these devastating diseases.

Chapter 2. Function of LIS1 in Mitosis

2-1. Introduction

Mitotic cell divisions are essential for the accurate partitioning of genetic molecules into two daughter cells. Inappropriate segregation of chromosomes during mitosis leads to aneuploidy and genomic instability (Holland and Cleveland, 2009). During the mitotic cell cycle phase (M phase), microtubules (MTs) undergo dynamic reorganization to coordinate chromosome separation. Mitotic spindles are assembled by dramatic MT remodeling and emanate from the centrosome, a microtubule-organizing center (MTOC), also called the spindle pole (Bornens, 2002). The centrosome participates in MT nucleation and anchoring MT minus-ends. The core component of the centrosome is a centriole pair composed of a mother centriole and a daughter centriole, which recruits pericentriolar material components (Doxsey et al., 2005; Zimmerman and Doxsey, 2000). The centrosome duplication cycle is precisely controlled to preserve centrosome number and proper centriole assembly (Nigg and Stearns, 2011). Importantly, mammalian cell division planes are mainly determined by positioning of bipolar mitotic spindles (Glotzer, 1996). In addition, the spatiotemporal interactions between the cell cortex and astral MT plus-ends have critical roles in mitotic spindle regulation (Glotzer, 2009; Kirschner and Mitchison, 1986; Kline-Smith and Walczak, 2004). On the plus-ends of astral MTs, several MT plus-end binding proteins mediate dynamic contacts of astral MT plus-ends to the cell cortex by interacting with cortical force generators on the membrane (Moore and Cooper, 2010).

Many of the proteins important for mitosis have been discovered, although much remains to be understood the detailed mechanisms employed by each protein involved in cell division. Among those mitotically important proteins, LIS1 is part of a complex that interacts with diverse cortical factors and centrosomal proteins at kinetochores on the chromosomes, the mitotic spindles and

the cell cortex, and it has been implicated in the regulation of the mitotic spindles and chromosome segregation during mitosis (Coquelle et al., 2002; Faulkner et al., 2000; Yingling et al., 2008). The human *LIS1* gene was first identified as a causative gene of human lissencephaly ('smooth brain'), a severe neuro-developmental disease (Hattori et al., 1994; Reiner et al., 1993). Heterozygous mutation or deletion of human *LIS1* leads to this brain malformation due to defects in neuronal migration. LIS1 is also part of a highly conserved protein complex first discovered in *Aspergillus nidulans* that is responsible for nuclear distribution and functions in cytoplasmic dynein regulation (Morris et al., 1998; Xiang et al., 1995). LIS1 homologues from *Aspergillus* to mammals form a complex with cytoplasmic dynein and nuclear distribution (NUD) proteins (Sasaki et al., 2000; Smith et al., 2000; Tai et al., 2002). Cytoplasmic dynein is a MT minus-end-directed motor involved in mitotic spindle assembly by regulating MT dynamics especially at astral MTs and mediating poleward transport of spindle assembly checkpoint proteins (Busson et al., 1998; Howell et al., 2001; Merdes et al., 1996; Nguyen-Ngoc et al., 2007; O'Connell and Wang, 2000). Through its motor activity, cytoplasmic dynein exerts pulling forces on the chromosomes. Dynactin, an accessory linker protein complexed with dynein subunits, also contributes to these cellular functions by assisting cargo loading and increasing processivity (Schroer, 2004). Cortically anchored cytoplasmic dynein/dynactin complexes are important cortical force generators along MTs (Gonczy, 2002; Nguyen-Ngoc et al., 2007) and those are essential for mitotic spindle formation and positioning in M phase (Busson et al., 1998; Dujardin and Vallee, 2002). Intriguingly, LIS1 has been implicated in dynein targeting at MT plus-ends along astral MTs during cell division of various cell types (Coquelle et al., 2002; Sheeman et al., 2003; Tai et al., 2002). In addition, several NUD family proteins associate with both LIS1 and cytoplasmic dynein. Two mammalian *NudE* homologues, NDE1 and NDEL1, interact with LIS1/cytoplasmic dynein complex (Derewenda et al., 2007; Efimov and Morris, 2000; Liang et al., 2004; Niethammer et al., 2000; Sasaki et al., 2000; Stehman et al., 2007). NDE1 and NDEL1 display prominent centrosomal localization, as does LIS1 (Feng et al., 2000; Niethammer et al.,

2000; Sasaki et al., 2000). NDE1 is required for targeting of LIS1 to the cytoplasmic dynein complex to generate persistent motor forces (McKenney et al., 2010; McKenney et al., 2011), while NDEL1 has been implicated the process of LIS1/dynein recruitment, serving as a scaffold (Coquelle et al., 2002; Li et al., 2005; Zylkiewicz et al., 2011). In addition, a subset of NDE1 and NDEL1 proteins is also observed in close proximity to the cell cortex where LIS1 accumulates (Lam et al., 2010; Sumigray et al., 2011; Yingling et al., 2008). These previous studies support the notion that LIS1-NDE1/NDEL1-dynein/dynactin complex is likely part of the protein machinery needed to coordinate various signals from the cell cortex to mitotic spindles by generating pulling forces on spindle MTs. Despite these studies, the precise functions of LIS1 and its complex during mitosis remain elusive. Furthermore, it is unclear whether other components of LIS1 protein complex are involved in LIS1-dependent spindle regulation during mammalian cell division.

We took advantage of genetic null (knock-out, KO) and hypomorphic-conditional (HC) alleles of *Lis1* (Gambello et al., 2003; Hirotsune et al., 1998) to uncover the critical dose-dependent roles of LIS1 in MEFs and mouse neural progenitors (NPs). Previously we found that *Lis1*-deficiency in mouse brains resulted in apoptosis and mitotic spindle orientation defects in NPs, while in MEFs loss of *Lis1* led to severe defects in cell growth and MT capture at the cell cortex in interphase cells (Yingling et al., 2008). In a current study using *Lis1* mutant MEFs, we demonstrated that mouse LIS1 plays essential roles in chromosome movements and MT/MTOC function to instruct proper spindle formation and orientation during mitotic cell division. Further, we determined that mouse LIS1 in mitosis has dual functions to maintain the integrity and number of centrosomes in which MT minus-ends attached and simultaneously to mediate the crosstalk between MT plus-ends along astral MTs and the cell cortex. These mitotic functions of LIS1 appear to be mediated by LIS1-NDE1/NDEL1-dynein/dynactin complex, suggesting essential functions of these components to form proper mitotic spindle during mammalian cell division.

2-2. Results

Perturbed mitotic progression in mitosis of *Lis1* mutant MEFs

To investigate cellular functions of mouse LIS1 during mitotic cell division, we employed various genetic tools to completely and reproducibly reduce LIS1 expression levels in primary MEFs. We performed time-lapse live cell imaging of mitosis of *Lis1* mutant MEFs isolated from *Lis1* mutant conditional knock-out (CKO) mice that harbor HC alleles of mouse *Lis1*. Tamoxifen (TM)-inducible Cre (Hayashi and McMahon, 2002) mice were mated to produce homozygous *Lis1* CKO mice (*CreERTM*; *Lis1^{hc/hc}*, hereafter termed *Lis1*-CKO-Cre) to acutely delete the *Lis1* gene upon TM treatment, which reduced LIS1 protein level close to <10% of wild-type levels after 72 h incubation described in previous study (Yingling et al., 2008). Control mice contained two normal wild-type (WT) *Lis1* alleles with Cre transgene (*CreERTM*; *Lis1^{+/+}*, hereafter termed WT-Cre). To visualize dynamic movements of chromosomes and MTs simultaneously during mitotic progression, we infected MEFs with retroviruses encoding histone 2B (H2B)-GFP (Kanda et al., 1998) and mCherry- α -tubulin, followed by treatment with 4-hydroxy-TM for 12 h. Live cell imaging revealed that *Lis1*-CKO-Cre MEFs treated with TM (*CreERTM*; *Lis1^{hc/hc}* + TM) exhibited a high frequency of abnormalities during mitosis that were not observed in WT-Cre MEFs. In prophase, *Lis1*-CKO-Cre MEFs often formed extra centrosomes (e.g. 4 MTOCs) (Fig. 2-1 A) (See below). In prometaphase, loss of LIS1 resulted in a kinked and curved morphology of the mitotic spindle. As the mitotic cell cycle eventually proceeded into metaphase, *Lis1*-CKO-Cre MEFs displayed chromosomes roughly aligned near the metaphase plate along with pseudo-bipolar spindles. In anaphase, *Lis1*-CKO-Cre MEFs retained several misaligned and unattached chromosomes, which ultimately results in defective chromosome separation and lagging chromosomes in telophase. Surprisingly, the average time from nuclear envelope breakdown to metaphase plate formation was not significantly extended in *Lis1*-CKO-Cre MEFs (17.2 ± 0.8 min) compared to those of WT-Cre MEFs (16.2 ± 0.9 min), indicating that acute loss of LIS1 did

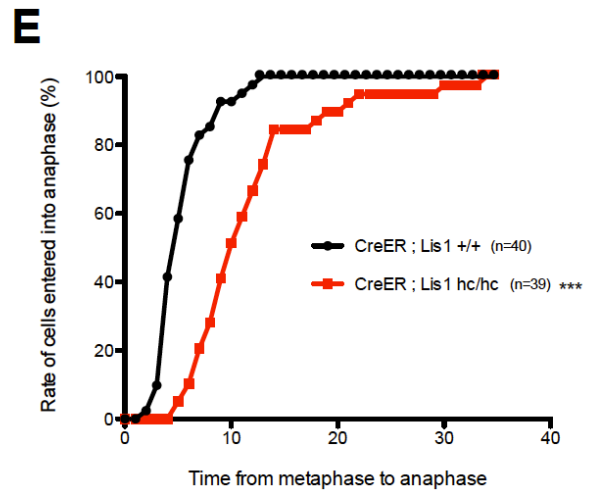
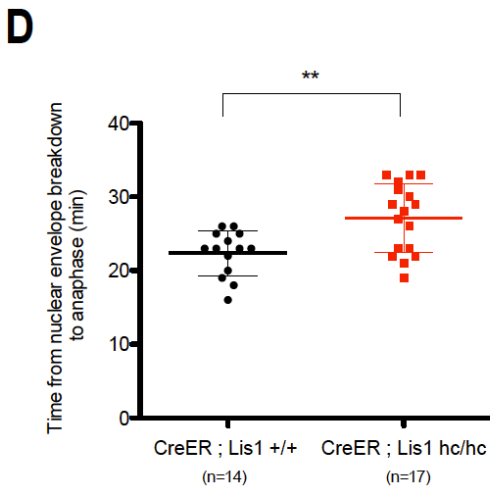
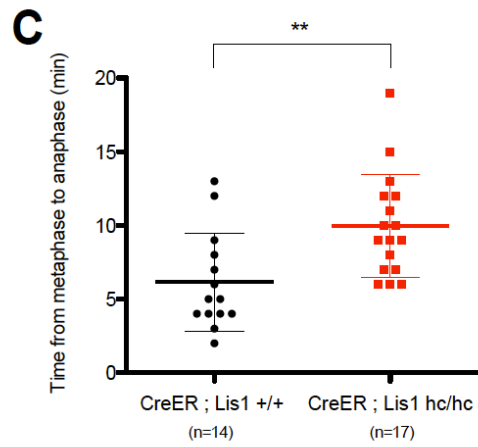
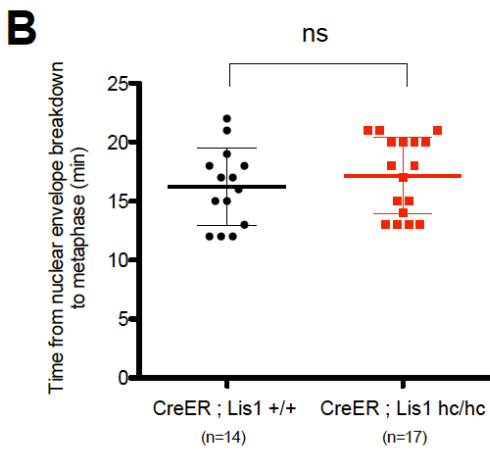
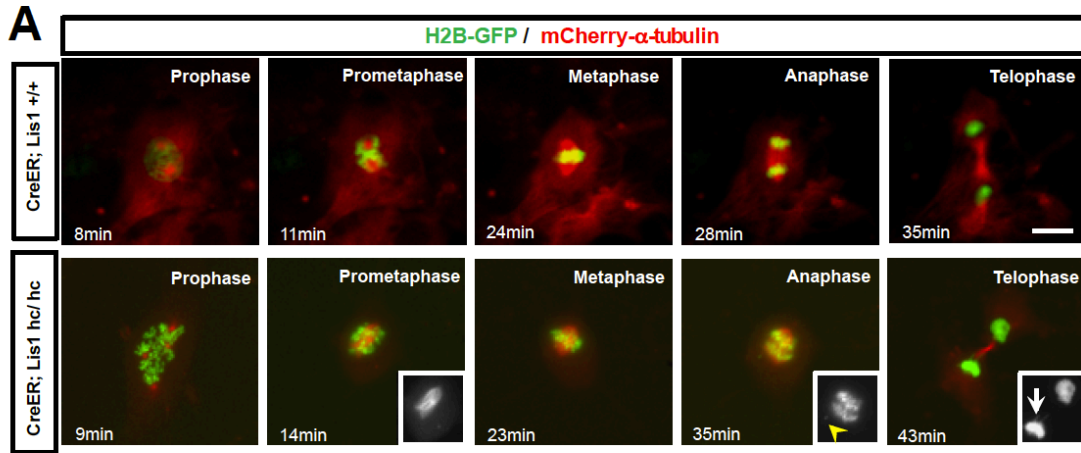


Figure 2-1. Loss of LIS1 results in a prolonged mitotic cell cycle to induce anaphase onset delay. (A) Frame series of time-lapse live imaging movies from *Lis1*-conditional knock-out (CKO)-Cre MEFs (*CreER* ; *Lis1*^{hc/hc}) and WT-Cre MEFs (*CreER* ; *Lis1*^{+/+}). MEFs were co-infected with histone2B-GFP (H2B-GFP, green) and mCherry- α -tubulin (red) retroviruses. Cre activation was induced by treatment of 4-hydroxy-tamoxifen for 12 h. Insets from *Lis1*-CKO-Cre; Prometaphase – kinked and curved spindle morphology, Anaphase – Arrowhead: unattached chromosomes, Telophase – Arrow: lagging chromosomes. Minutes indicate the time from nuclear envelope breakdown. Scale bar: 10 μ m. (B) Time from nuclear envelope breakdown to metaphase plate formation. (C) Time from metaphase plate formation to anaphase onset. (D) Time from nuclear envelope breakdown to anaphase onset. (E) Accumulated percentage of cells entered into anaphase from metaphase. Lines in (B-D): mean \pm s.d., Asterisks: *p < 0.05, ***p < 0.001 by student's *t*-test. ns: not significant.

not severely impair metaphase plate formation (Fig. 2-1 B). However, the average time from metaphase to anaphase onset was significantly delayed from *Lis1*-CKO-Cre MEFs (9.9 ± 0.9 min) compared to those of WT-Cre MEFs (6.1 ± 0.9 min) (Fig. 2-1 C). We obtained similar results of mitotic delay from a distinct analysis of anaphase onset timing. The time when 50% cells entered anaphase in *Lis1*-CKO-Cre MEFs ($t_{50\%} = \sim 10$ min) was longer than WT-Cre MEFs ($t_{50\%} = \sim 5$ min) by 2-fold (Fig. 2-1 E). The total duration of mitosis from nuclear envelope breakdown to anaphase onset was delayed in *Lis1*-CKO-Cre MEFs (27.1 ± 1.1 min) compared to WT-Cre (22.4 ± 0.8 min) by about 1.2-fold (Fig. 2-1 D).

To investigate the effects of stably reduced LIS1 protein levels on its intracellular distribution during mitotic cell cycle progression, we compared endogenous LIS1 localization in WT MEFs and *Lis1*^{hc/ko} MEFs with 35% of WT LIS1 protein levels (Fig. 2-2 A and B) (See (Yingling et al., 2008)). In WT MEFs, LIS1 was enriched at centrosomes and kinetochores from prophase to metaphase. A majority of LIS1 was cytosolic, but a small fraction of LIS1 was also observed near the cell cortex as puncta. From metaphase to anaphase, LIS1 immunostaining overlapped with MTs along the mitotic spindles. Prior to telophase, the majority of LIS1 co-localized with centrosomes in WT MEFs. By contrast, *Lis1*^{hc/ko} MEFs displayed significant reduction of LIS1 distribution in the cytoplasm, although centrosome-specific localization of LIS1 appeared to be maintained. In metaphase, LIS1 accumulated at the kinetochores on chromosomes near the metaphase plate in *Lis1*^{hc/ko} MEFs. However, mitotic spindle-associated LIS1 mostly disappeared in these cells (Fig. 2-2 A). These observations support critical mitotic functions of LIS1 at centrosomes, the mitotic spindles and the cell cortex in M phase (Faulkner et al., 2000), suggesting that the LIS1 protein complex may mediate mitotic functions in these specific cellular compartments.

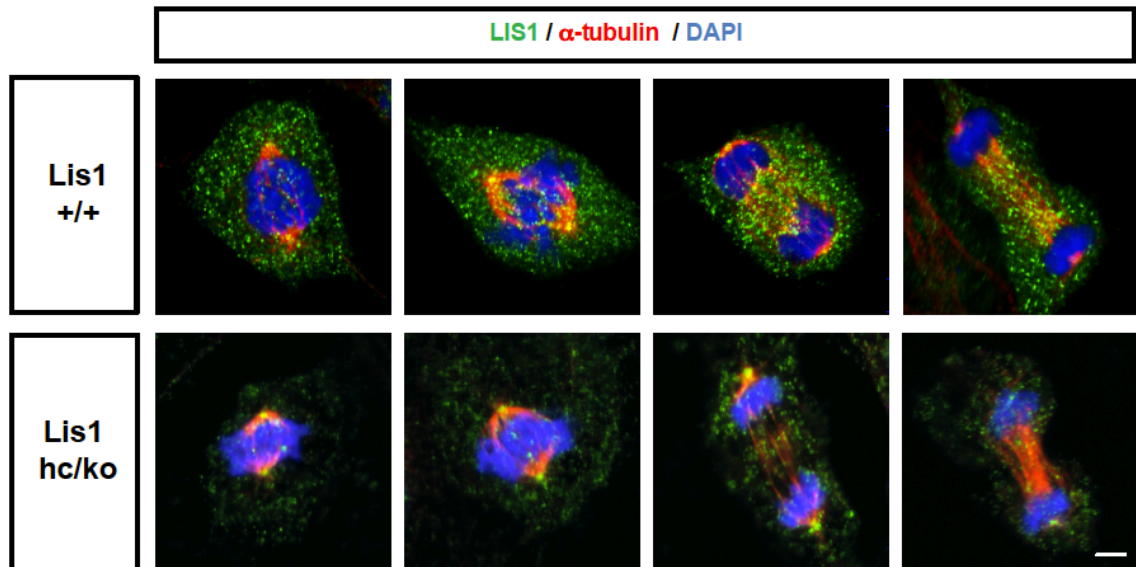
A**B**

Figure 2-2. Endogenous LIS1 in *Lis1* mutant MEFs is less distributed in the mitotic spindles and the cell periphery. (A) Localization of endogenous LIS1 (green) in different phases of mitotic cell cycle from WT MEFs and *Lis1*^{hc/ko} MEFs. MEFs were co-stained with α -tubulin (red) and DAPI (blue). Scale bars: 5 μ m. (B) Western blot of cell lysates from MEFs.

Formation of extra centrosomes caused by loss of *Lis1*

Time-lapse imaging revealed that the incidence of multiple centrosomes (more than two centrosomes) was dramatically increased in *Lis1* mutant MEFs (Fig. 2-3 A). *Lis1*-CKO-Cre MEFs had a greater than 5-fold increase in the occurrence of centrosome amplification (*Lis1*-CKO-Cre: 28.1% vs. WT-Cre: 5.1%). However, this rarely resulted in multipolar spindle formation during mitosis, since only 1.4% of *Lis1*-CKO-Cre MEFs displayed multipolar division (1/73) compared with none in WT-Cre MEFs (0/39) (Fig. 2-3 B).

To determine whether centrosome amplification is a common feature resulting from the reduction of LIS1, we performed γ -tubulin staining in WT and *Lis1*^{hc/ko} MEFs. Similar to *Lis1*-CKO-Cre, *Lis1*^{hc/ko} MEFs often displayed centrosome amplification. *Lis1*^{hc/ko} had a nearly 2-fold increase in the occurrence of multiple centrosomes (*Lis1*^{hc/ko}: 18.7% vs. WT: 10.8%) (Fig. 2-3 C and D). Notably, the occurrence of cells with 3 and 4 MTOCs was increased about 3-fold and 2-fold in *Lis1*^{hc/ko} MEFs, respectively. The frequency of 6 MTOCs was also increased in *Lis1*^{hc/ko} MEFs (Fig. 2-3 E). Thus, these results support that LIS1 reduction results in centrosome amplification.

Abnormal centrosome integrity by centrosome clustering in *Lis1* mutant MEFs

One possible mechanism to induce spindle misorientation is the mislocalization of critical centrosomal proteins. We first investigated NDE1 localization in *Lis1*^{hc/ko} MEFs, since NDE1 and LIS1 form a functional complex at centrosomes (Feng et al., 2000). We observed moderate reduction in centrosome-associated NDE1 in metaphase of *Lis1*^{hc/ko} MEFs (Fig. 2-4 A). NDEL1, a second mammalian *nudE* homolog, is important for LIS1-dynein-dependent MT regulation at the cell cortex (Yingling et al., 2008), and primarily accumulates at centrosomes during mitosis (Mori et al., 2007; Niethammer et al., 2000). In contrast to reduced centrosomal NDE1, we found a comparable amount of NDEL1 at centrosomes in *Lis1*^{hc/ko} MEFs (Fig. 2-4 B). However, spindle MT-associated NDEL1 was dramatically decreased in *Lis1*^{hc/ko} MEFs compared to the substantial

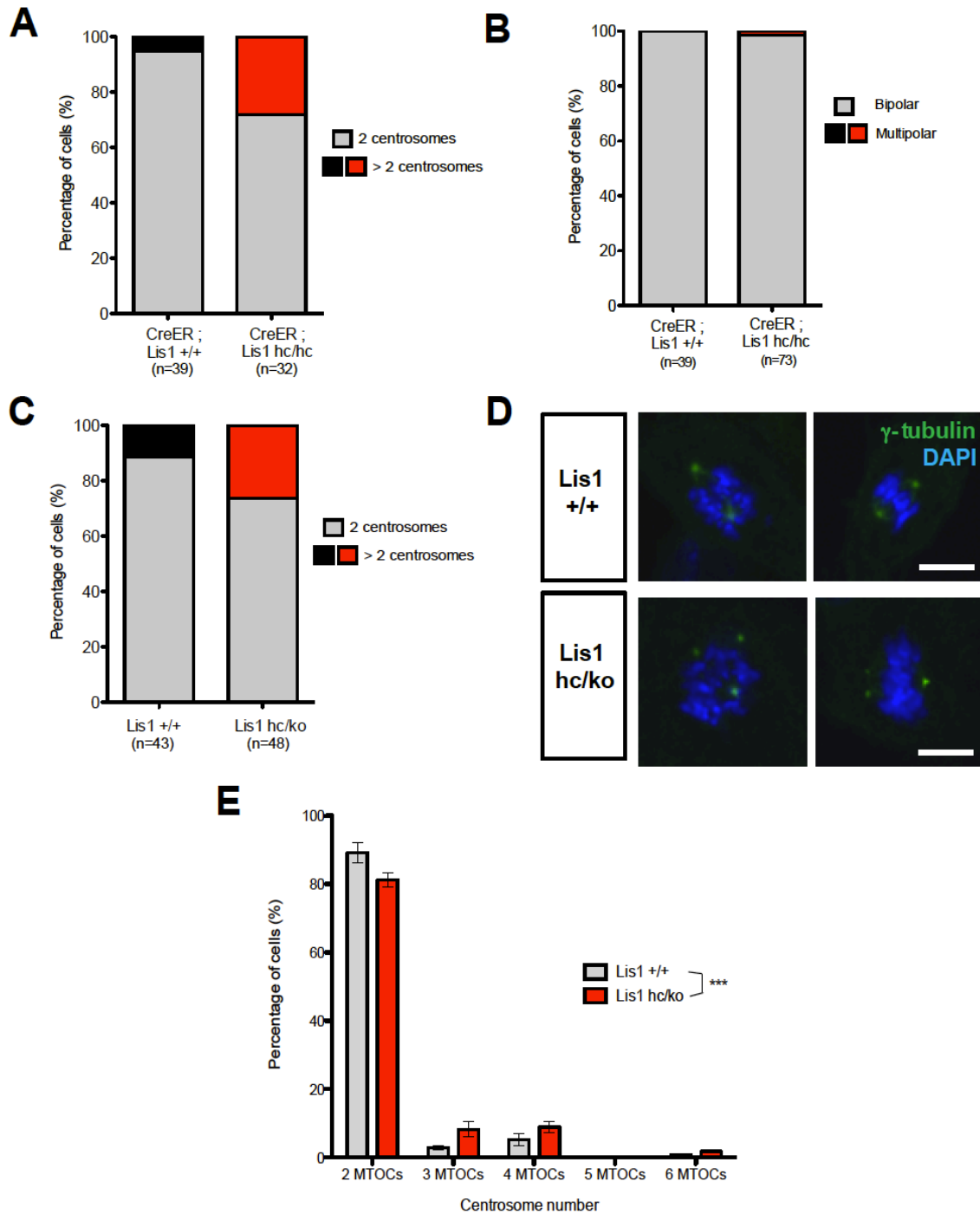


Figure 2-3. Loss of LIS1 leads to extra centrosomes formation and centrosome number abnormality. (A) Time-lapse live imaging analysis reveals the centrosome number abnormality in *Lis1*-CKO-Cre MEFs compared to WT-Cre. (B) Multipolar division was found in time-lapse live imaging of *Lis1*-CKO-Cre MEFs (1/73). (C) Fixed sample analysis of centrosome number from WT and *Lis1^{hc/ko}* MEFs. (D) WT MEFs with normal two centrosomes and *Lis1^{hc/ko}* MEFs with extra centrosomes. MEFs were stained with γ -tubulin (green) and DAPI (blue). Scale bars: 10 μ m. (E) Centrosome number distributions in WT and *Lis1^{hc/ko}* MEFs. Microtubule-organizing centers (MTOCs). More than 3 slides were analyzed, n > 250 cells from each genotype. Bars: mean \pm s.e.m., Asterisk: ***p < 0.001 by two-way ANOVA test.

co-localization of NDEL1 and MT staining in M phase of WT MEFs (Fig. 2-4 B). In addition, the number of cell cortex-associated NDEL1 puncta was significantly reduced in metaphase of *Lis1^{hc/ko}* MEFs, which indicates impaired NDEL1 targeting to the cortical membrane (Fig. 2-4 B). Together, these findings are consistent with a necessary cooperation between LIS1 and NDEL1 for MT plus-end targeting of these proteins each other to stabilize cortical MTs (Coquelle et al., 2002; Yingling et al., 2008).

Next, we examined pericentrin immunostaining and found that the size and shape of centriolar material in *Lis1^{hc/ko}* MEFs were disrupted compared to WT. Even in cells undergoing bipolar division with two distinguished centrosomes, *Lis1^{hc/ko}* MEFs frequently had enlarged spindle poles with larger amounts of centriolar material than WT. This generated asymmetry of the two spindle poles in *Lis1^{hc/ko}* MEFs, while symmetric bipolar spindles were maintained in WT MEFs (Fig. 2-4 C). In addition to asymmetric spindles, *Lis1^{hc/ko}* MEFs displayed an elongated, cylindrical shape of centriolar material rather than a normal sphere shape (Fig. 2-4 E), suggesting that LIS1 is required for maintaining proper centrosome integrity and assembly.

We assessed whether LIS1 may be necessary for the regulation centrosome organization or centrosome maturation by co-immunostaining with centrosome or centriole markers and several centrosome maturation markers that are associated with centriole distal/subdistal appendages. Mature centriole appendage proteins such as cennexin/ODF2 (Nakagawa et al., 2001), ninein (Mogensen et al., 2000) and Cep164, another mother centriole marker (Graser et al., 2007), displayed intact localization at the centrosomes in *Lis1^{hc/ko}* MEFs (Fig. 2-4 E, F and G). Only one centrin-positive centriole among a centriole pair had cennexin/ODF2 or ninein-immunoreactivity, suggesting that centrosomes in *Lis1^{hc/ko}* MEFs undergo normal centrosome maturation. However, a significant fraction of *Lis1^{hc/ko}* MEFs with bipolar spindles displayed a ‘centrosome clustering’ phenotype (with more than two pairs of centrioles with normal configuration in one pole), a phenotype reported in the cells with extra centrosomes (Kwon et al., 2008; Quintyne et al., 2005).

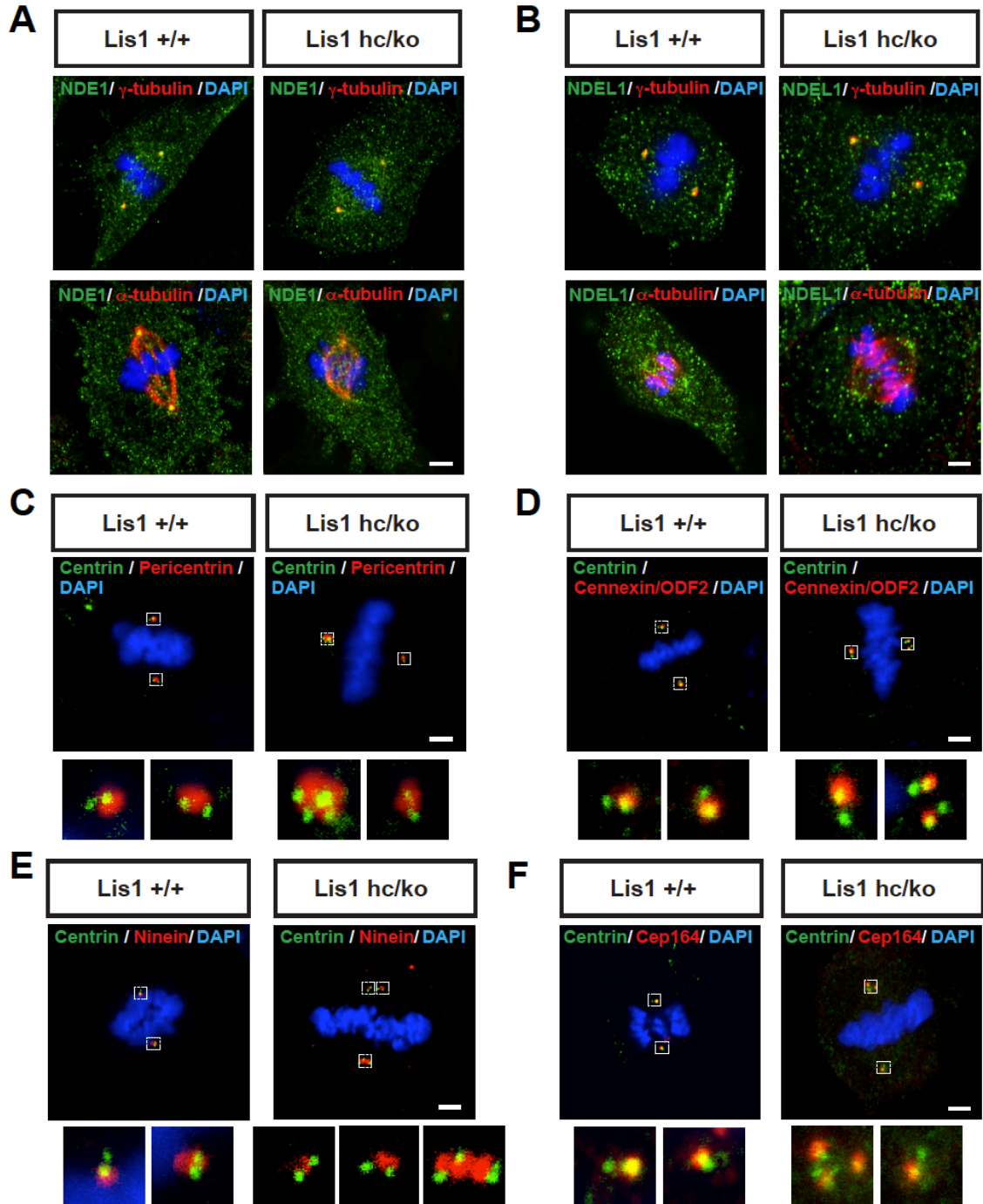


Figure 2-4. *Lis1* mutant MEFs exhibit centrosome clustering phenotype during mitosis. (A) Localization of NDE1 (green) and (B) NDEL1 (green) in *Lis1^{hc/ko}* MEFs and WT. Co-staining images in (A, B) with γ -tubulin (upper panel, red) or α -tubulin (lower panel, red) and DAPI (blue). (C-F) Centrosome clustering phenotype with normal centrosome maturation in *Lis1^{hc/ko}* MEFs. (C) Co-staining with pericentrin (pericentriolar material marker) and centrin (each centriole). Co-staining with centrin and several mature centriole markers: (D) cennexin/ODF2, (E) ninein, (F) Cep164, respectively. Insets in (C-F): High magnification images of centrosomes. Scale bars: 5 μ m.

Clustered spindle poles displayed a large amount of pericentrin-positive pericentriolar material (Fig. 2-4 C-F).

The cennexin/ODF2-positive mother centriole functions as a basal body, an anchor of non-motile primary cilium originating in interphase (Ishikawa et al., 2005). We hypothesized that the frequent appearance of extra centrosomes in *Lis1^{hc/ko}* MEFs may result in multiple primary cilia formation in these cells. In serum-starvation conditions, *Lis1^{hc/ko}* MEFs produced multiple cilia from amplified centrosomes, as measured by immunostaining of acetylated- α -tubulin and pericentrin, a primary cilia marker and a basal body marker, respectively (Fig. 2-5 A). There was a 3-fold increase in the percentage of cells with multiple cilia from *Lis1^{hc/ko}* MEFs ($5.1 \pm 1.4\%$) compared to WT MEFs ($1.7 \pm 0.5\%$) (Fig. 2-5 B). Given the 2-fold increase in incidence of extra centrosomes in *Lis1^{hc/ko}* vs. WT MEFs, we concluded that multiple centrosome formation in M phase of *Lis1^{hc/ko}* MEFs ultimately leads to ectopic primary cilia formation, suggesting amplified extra centrosomes in *Lis1* mutant MEFs are fully functional in interphase.

Chromosome missegregation and recruitment defects of kinetochore proteins in *Lis1* mutant MEFs

Time-lapse live imaging revealed congression of chromosomes at the metaphase plate in WT and *Lis1*-CKO-Cre MEFs, but metaphase plates were less compact and displayed distorted morphology in *Lis1*-CKO-Cre MEFs compared with those of WT-Cre MEFs (Fig. 2-6 A). We also observed several misaligned and unattached chromosomes scattered away from the metaphase plate in *Lis1*-CKO-Cre MEFs. *Lis1*-CKO-Cre MEFs displayed a 2-fold increase of lagging chromosomes in anaphase (Fig. 2-6 B) compared to WT-Cre (Fig. 2-6 D). We categorized the occurrence of lagging chromosomes into three groups: no, few, and numerous lagging chromosomes. Numerous lagging chromosomes were observed in very high frequency (76.7%) in *Lis1*-CKO-Cre MEFs compared to WT-Cre MEFs (Fig. 2-6 C). In addition, other types of severe chromosome segregation defects were also found in *Lis1*-CKO-Cre MEFs. There

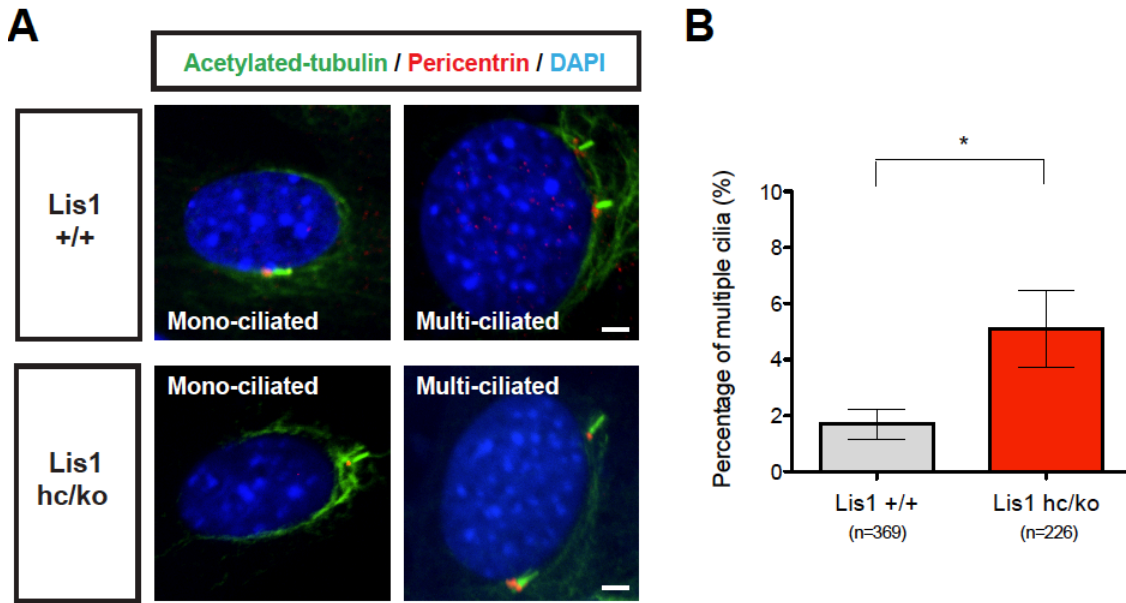


Figure 2-5. Loss of LIS1 causes frequent multiple cilia formation in interphase

(A) Primary cilia formation from serum-starved *Lis1^{hc/ko}* MEFs and WT. Primary cilia were identified with acetylated-tubulin (green) staining. Basal body and chromosomes were stained with pericentrin (red) and DAPI (blue), respectively. 1 cilium: Mono-ciliated, More than 2 cilia: Multi-ciliated. (B) Quantification of multiple cilia formation. Asterisk: * $p < 0.05$ by student's *t*-test. Scale bars: 5 μ m.

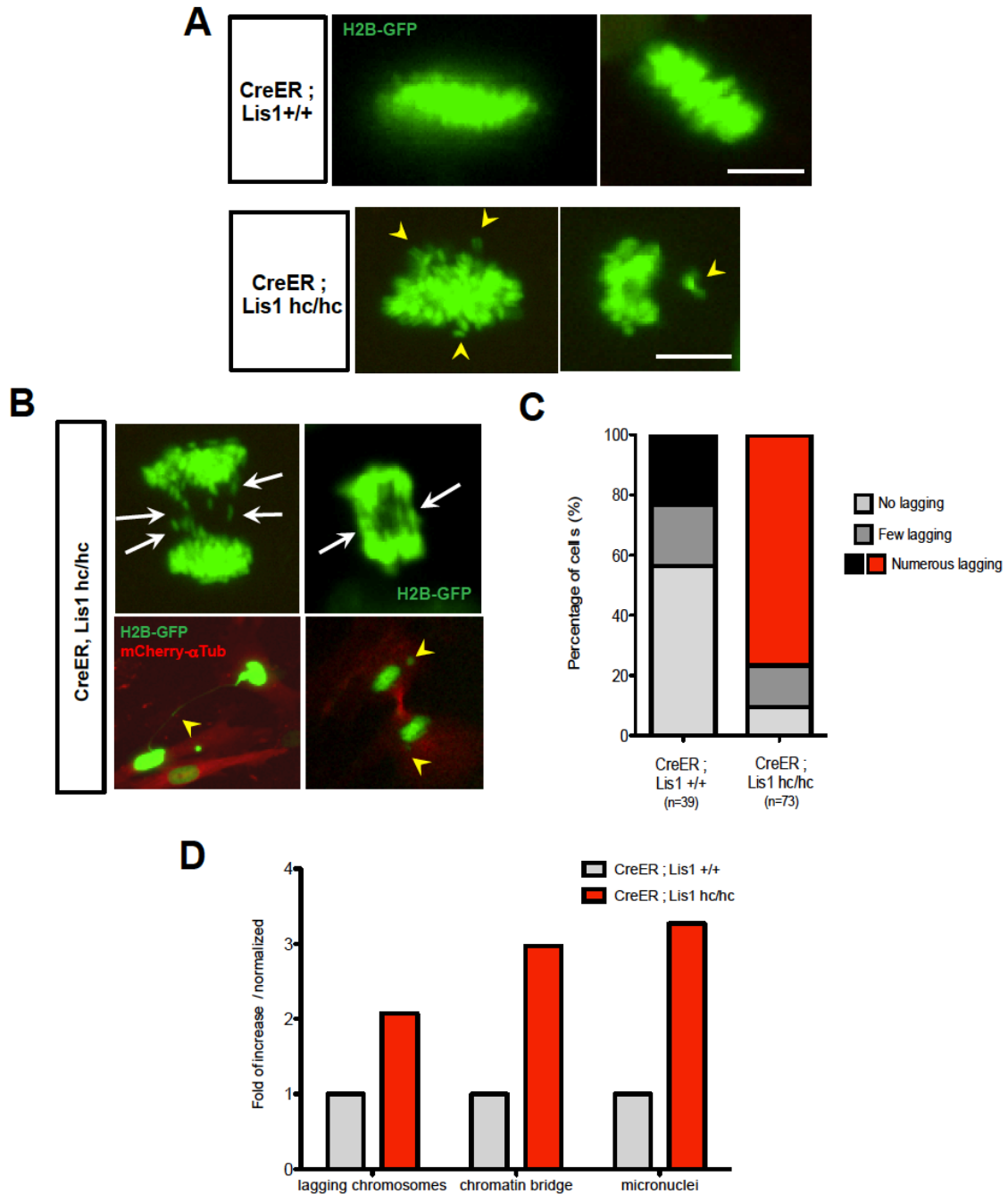


Figure 2-6. Loss of LIS1 induces chromosome misalignment in metaphase and chromosome missegregation in anaphase during mitosis. (A) Time-lapse live imaging analysis of chromosomal behavior (labeled with H2B-GFP, green) from *Lis1*-CKO-Cre MEFs and WT-Cre MEFs. Arrowhead: misaligned chromosomes in *Lis1*-CKO-Cre MEFs. Scale bars: 5 μ m. (B) Chromosome missegregation phenotypes in mitosis of *Lis1*-CKO-Cre MEFs. Arrow: numerous lagging chromosomes, Arrowhead: (left) the chromosomes stuck in intercellular chromatin bridge, (right) micronuclei formation in telophase. Microtubule networks were visualized by mCherry- α -tubulin (red). Scale bars: 5 μ m. (C) Quantification of lagging chromosome appearance in time-lapse live imaging of *Lis1*-CKO-Cre MEFs and WT-Cre MEFs. Numbers of lagging chromosomes - No lagging: 0, Few lagging: 1~3, Numerous lagging: > 4. (D) Increased incidence of various chromosome segregation defects *Lis1*-CKO-Cre MEFs compared to WT-Cre MEFs.

was a 3-fold increase in intracellular chromatin bridges and a 3-fold increase in micronuclei found in daughter cells derived from mitosis of *Lis1*-CKO-Cre compared to WT-Cre (Fig. 2-6 D).

We reasoned that these chromosome congression and separation defects in *Lis1*-deficiency might be caused by misregulation of protein targeting to kinetochores, since LIS1 is a known kinetochore-binding protein in prophase and prometaphase (Faulkner et al., 2000). Targeting of LIS1 to kinetochores (identified with CREST staining) was reduced to 50% in *Lis1^{hc/ko}* MEFs, as expected due to overall 35% reduction of LIS1 protein in these cells compared to WT (Fig. S3 A). In addition, there was an overall reduction in kinetochore recruitment of dynein subunits, including the dynein intermediate chain (DIC70.1) and the dynactin subunit p150^{Glued}, to 40% and 50%, respectively, compared to WT (Fig. 2-7 A and B). Targeting of CLIP170 to kinetochores was also significantly reduced in *Lis1^{hc/ko}* MEFs to 30% of WT levels (Fig. 2-7 C). Next, we determined interkinetochore distances that reflect the strength of the tension from kinetochore-bound MTs to the spindle poles. *Lis1^{hc/ko}* MEFs displayed a decrease in interkinetochore distance (*Lis1^{hc/ko}*: $0.65 \pm 0.17 \mu\text{m}$ vs. WT: $0.48 \pm 0.01 \mu\text{m}$) (Fig. 2-7 D). These data suggest that aberrant and/or unstable MT attachments to kinetochores in *Lis1^{hc/ko}* MEFs may result from a depletion of kinetochore-targeted proteins such as LIS1, the dynein/dynactin complex and CLIP170.

Impairment of mitotic spindle formation and spindle misorientation in *Lis1* mutant MEFs

Previously, it was shown that LIS1 overexpression results in spindle misorientation in MDCK cells (Faulkner et al., 2000), and that *Drosophila Dlis1* mutants as well as mouse *Lis1* mutants display mitotic spindle defects in NP division (Siller et al., 2005; Yingling et al., 2008).

Consistent with these findings, we uncovered defects in spindle formation and positioning from time-lapse live imaging of *Lis1*-CKO-Cre MEFs (Fig. 2-1 A). To determine mitotic spindle orientation parallel to the cell-substrate adhesion plane, which occurs in adherent cells

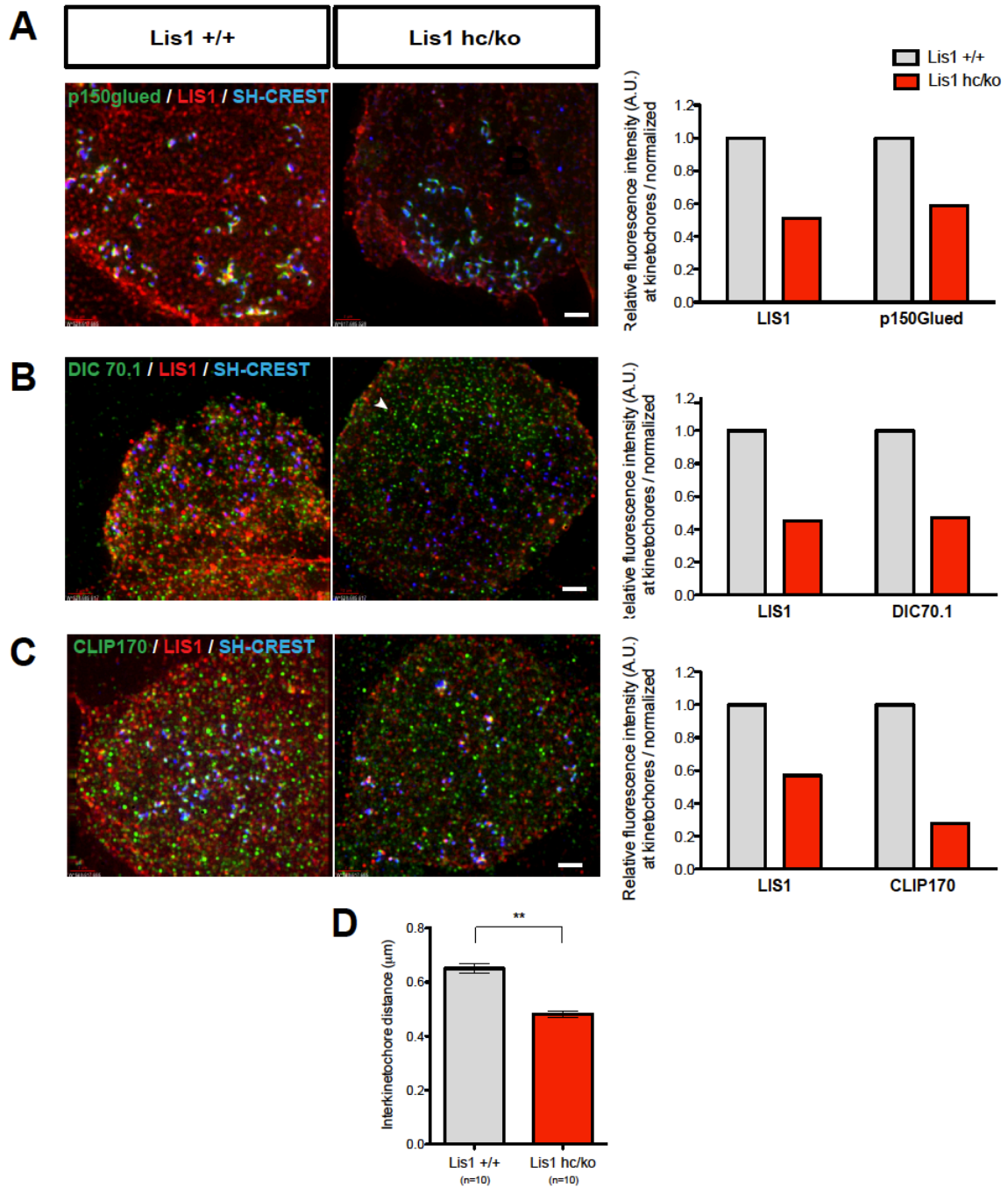


Figure 2-7. Loss of LIS1 causes less recruitment of kinetochore proteins to kinetochores on the chromosomes during mitosis. (A) Relative intensity of dynein intermediate chain (DIC70.1) signal at kinetochores, normalized to CREST staining of kinetochores. (B) A subunit of dynein complex, p150^{Glued} signal at kinetochores. (C) CLIP170 at kinetochores. (D) Average interkinetochore distance was reduced in *Lis1*^{hc/ko} MEFs compared to WT. Bars: mean \pm s.e.m., 10 kinetochores in 10 cells. Asterisk: **p < 0.01 by student's *t*-test. A.U.: arbitrary unit.

(Toyoshima and Nishida, 2007), we arrested MEFs in metaphase by MG132 treatment. The spindle poles were identified with pericentrin, a pericentriolar marker of centrosomes (Zimmerman et al., 2004). Confocal images from WT MEFs displayed a relatively narrow centrosomal distribution in the same or adjacent confocal planes along the cell axis. By contrast, *Lis1^{hc/ko}* MEFs exhibited a high degree of spindle tilting compared to the substrate plane (Fig. 2-8 A). Spindle angle (α° , measured by an amplitude of angle between centrosomes and the plane of cell-substrate) (shown in Fig. 2-8 B) was significantly increased in *Lis1^{hc/ko}* MEFs. The average spindle angle in *Lis1^{hc/ko}* MEFs ($\alpha^\circ = 16.9 \pm 1.5$) was increased about 2-fold compared with WT ($\alpha^\circ = 10.0 \pm 1.2$) (Fig. 2-8 C). Since *Drosophila Dlis1* mutant displayed defects in centrosome separation during mitosis of NPs (Siller et al., 2005), we expected that the distance between the two spindle poles may be impaired in *Lis1^{hc/ko}* MEFs. *Lis1^{hc/ko}* MEFs displayed a moderate change in pole distance ($8.8 \pm 0.2 \mu\text{m}$) compared with WT ($7.9 \pm 0.2 \mu\text{m}$), reflecting alteration in pulling forces on two spindle poles (Fig. 2-8 D).

To determine whether spindle misorientation in *Lis1^{hc/ko}* MEFs results from cell shape changes in these cells, we determined the cell height and the longest cell axis of the metaphase cells from *Lis1^{hc/ko}* MEFs and WT MEFs. Neither were significantly altered in *Lis1^{hc/ko}* MEFs compared with WT MEFs (cell height *Lis1^{hc/ko}*: $12.7 \pm 0.6 \mu\text{m}$ vs. WT: $13.7 \pm 0.4 \mu\text{m}$, and long axis *Lis1^{hc/ko}*: $17.9 \pm 0.9 \mu\text{m}$ vs. WT: $17.5 \pm 0.7 \mu\text{m}$) (Fig. 2-9 A and B).

Reduced cortical dynein/dynactin complexes in *Lis1* mutant MEFs during mitosis

To examine cortically located dynein/dynactin complex in *Lis1^{hc/ko}* MEFs, we performed immunostaining with the p150^{Glued} subunit of dynactin and found reduced staining in *Lis1^{hc/ko}* MEFs compared to WT MEFs during M phase (Fig. 2-10 A), especially at the polar cortex. Astral MT-associated p150^{Glued} signals were prominent in WT MEFs, however, they were severely reduced in *Lis1^{hc/ko}* MEFs. To examine dynein complex localization, we performed DIC subunit

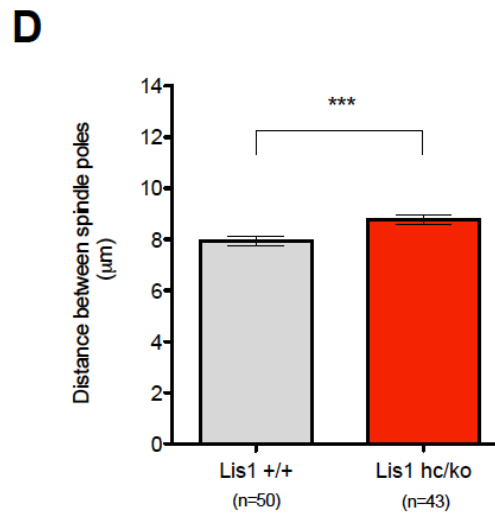
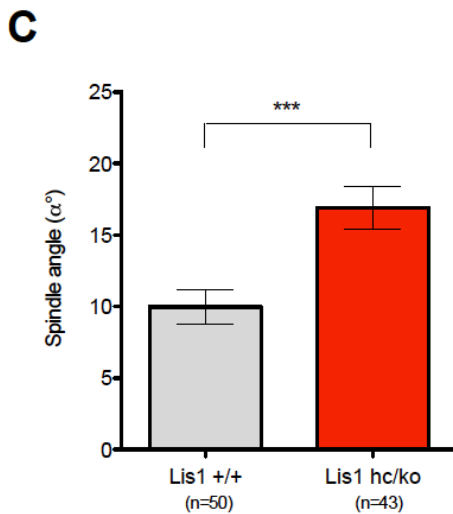
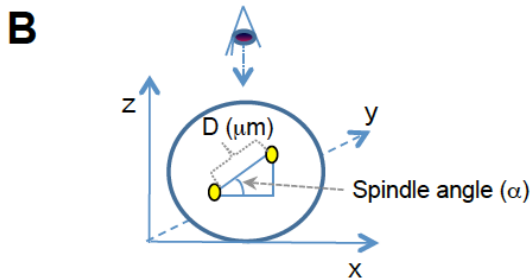
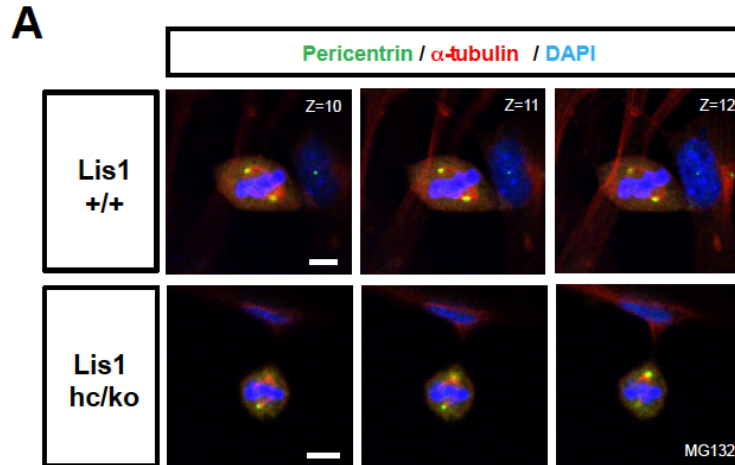


Figure 2-8. Loss of LIS1 impairs spindle orientation during mitosis of MEFs. (A) Confocal Z-stack image series of mitotic spindles stained with pericentrin (centrosomal marker, green), α -tubulin (mitotic spindle, red), and DAPI (blue). MEFs were arrested in metaphase with MG132 treatment for 2 h. Scale bars: 5 μm . (B) Schematic representation of spindle orientation in mitotic cells. Spindle angle (α°) and distance between spindle poles (D, μm) were measured by taking Z-stack confocal images from 0.5 μm thick sections. Centrosomes were identified with co-localization of pericentrin and α -tubulin (marked in yellow). (C) Average spindle angles of *Lis1*^{hc/ko} MEFs and WT. (D) Average distance between spindle poles. Bars in (C, D): mean \pm s.e.m., Asterisks in (C, D): **p < 0.01 by student's *t*-test. ns: not significant.

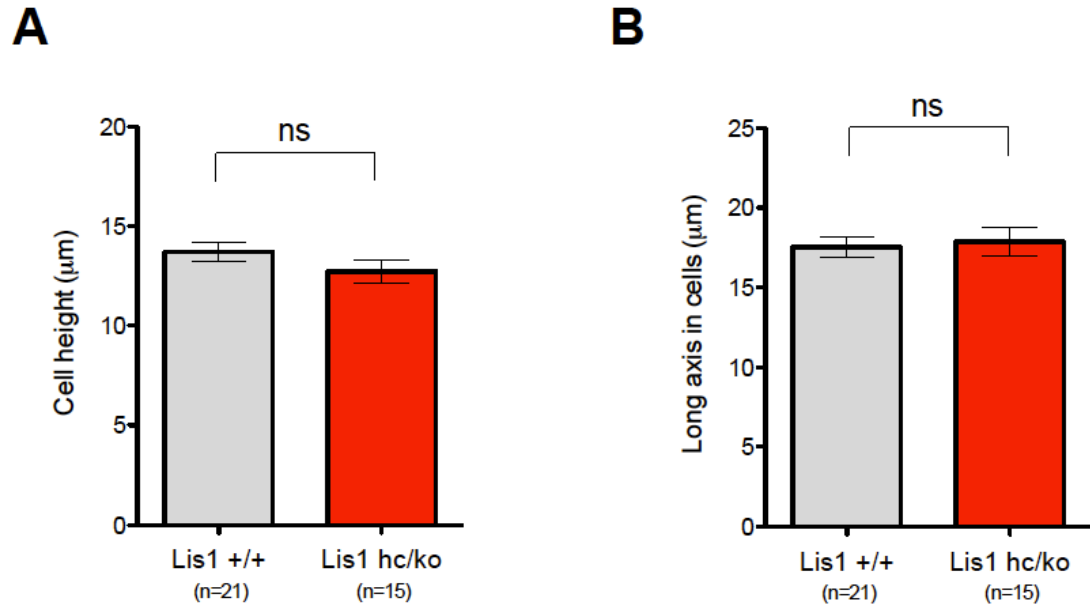


Figure 2-9. Normal cell shape and morphology in metaphase of *Lis1* mutant MEFs. (A) No change in cell height measured by DHCC (lipophilic dye) (B) No change in long axis from metaphase cells of *Lis1^{hc/ko}* MEFs compared to WT. Bars in (A, B): mean \pm s.e.m., ns: not significant by student's *t*-test.

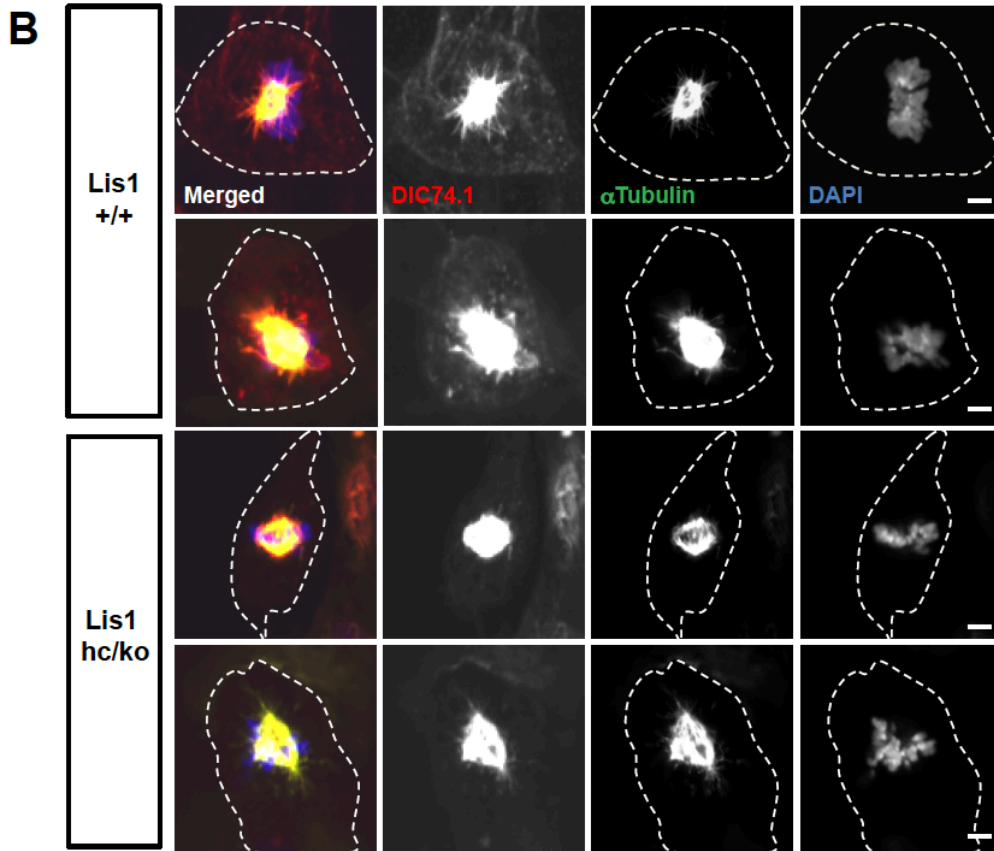
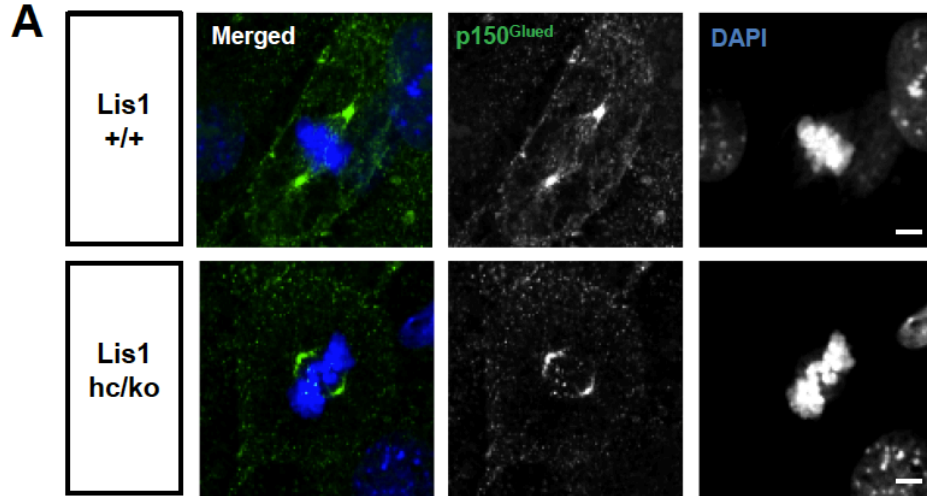


Figure 2-10. Loss of LIS1 results in less cortical dynein/dynactin complex recruitment to the cell cortex during mitosis. (A) Distribution of a dynactin subunit, p150^{Glued} (green) in mitosis of *Lis1*^{hc/ko} MEFs and WT. Chromosomes were stained with DAPI (blue). (B) Distribution of a dynein complex subunit, DIC74.1 (red) in mitosis of *Lis1*^{hc/ko} MEFs and WT. Co-staining with α -tubulin (green) and DAPI (blue). White dashed lines illustrate cell membranes. Scale bars: 5 μ m.

immunostaining. DIC74.1-immunoreactive puncta were detected near the cortical membrane in M phase of WT MEFs, but the number of these cortical puncta was diminished in *Lis1^{hc/ko}* MEFs (Fig. 2-10 B). Reduced localization of cortical dynein/dynactin complex in M phase may ultimately result in spindle misorientation in *Lis1^{hc/ko}* MEFs. These findings suggest that LIS1 mediates dynein/dynactin targeting to the cell cortex in this cell cycle, contributing to spindle orientation and positioning to ensure proper cell division.

Abnormal interaction between plus-ends of astral MTs and the cell cortex in *Lis1* mutant MEFs

Previous studies (Faulkner et al., 2000; Yingling et al., 2008) and the dynein studies described above (Fig. 2-10) suggested that astral MTs may be reduced in *Lis1^{hc/ko}* cells, so we examined astral MTs in great detail. We found that WT MEFs in early anaphase displayed clear astral MTs-cortex interaction and they maintained a wide angle compared to lateral surface of cell cortex (end-on interaction) (Gusnowski and Srayko, 2011) (Fig. 2-11 A, B). Each lobe of the polar cortex was filled with straightened astral MT tips, suggesting pulling force between spindle poles and the cell cortex. By contrast, the radial arrays of astral MTs were reduced in *Lis1^{hc/ko}* MEFs. These astral MTs were often curled and contacted the cell cortex laterally with a shallow angle (lateral or side-on interaction, MT sliding) (Gusnowski and Srayko, 2011), suggesting that these astral MTs were not under strong tension (Fig. 2-11 A, B). The angle between astral MT tips and cortical membrane was measured (θ°). The lateral interaction ($\theta^\circ < 60$) of astral MTs to the polar cortex was significantly increased in *Lis1^{hc/ko}* MEFs (*Lis1^{hc/ko}* : 29.6% vs. WT 69.2%) (Fig. 2-11 B, C). In addition, astral MTs in WT MEFs never crossed the equatorial region where the cleavage furrow forms, but in the case of *Lis1^{hc/ko}* MEFs with extra centrosomes, a fraction of astral MTs connected to the opposite polar cortex far from the closer pole (Fig. 2-11 A, right).

The dynein/dynactin complex is targeted to MT plus-end tips by EB1, a MT plus-end binding protein (Mimori-Kiyosue et al., 2000; Schuyler and Pellman, 2001), and is necessary for

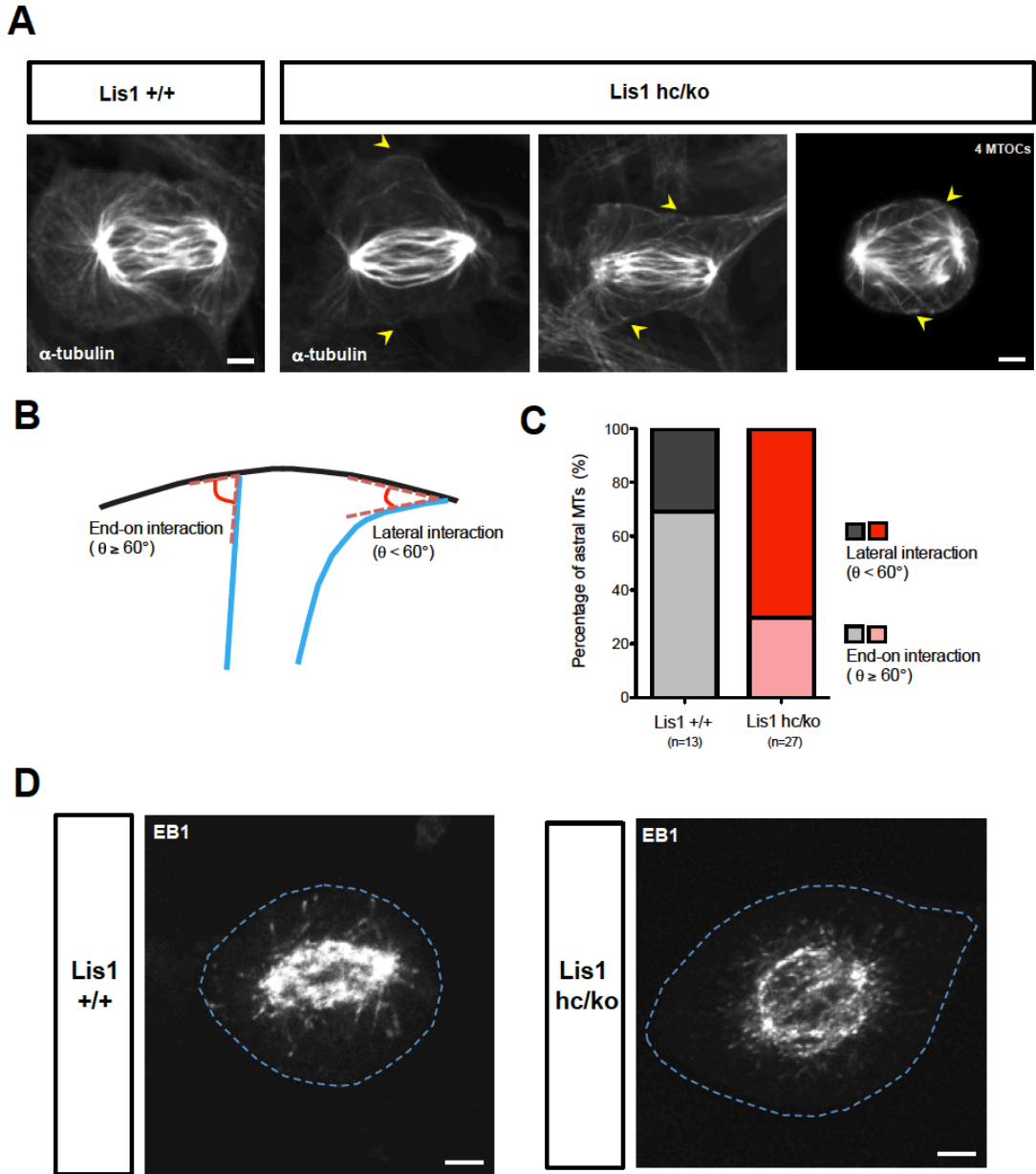


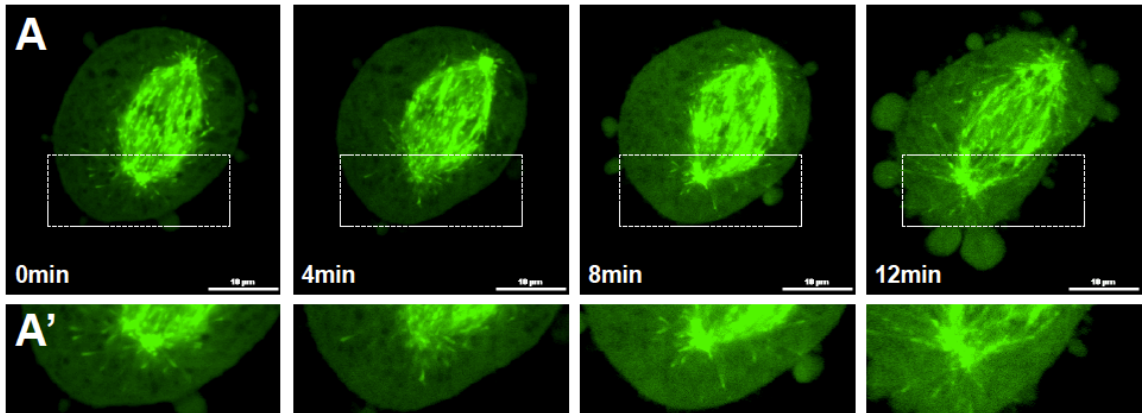
Figure 2-11. Loss of LIS1 causes aberrant interactions between astral microtubule plus ends and the cell cortex. (A) The astral microtubules in early anaphase from *Lis1^{hc/ko}* MEFs and WT stained with α -tubulin after glutaldehyde fixation. Arrow: aberrant astral microtubule tips in *Lis1^{hc/ko}* MEFs. (right panel): Misattachment of astral microtubules to the opposite polar cortex in *Lis1^{hc/ko}* MEFs harboring extra centrosomes (4 MTOCs). (B) Schematic representation of interaction between astral MTs and the cell cortex – End-on interaction ($\theta^\circ \geq 60$) vs. Lateral interaction ($\theta^\circ < 60$). (C) Quantification of types of astral MT interaction with the cell cortex in MEFs (D) Localization of microtubule plus ends stained with EB1 (microtubule plus-end binding protein) in metaphase of *Lis1^{hc/ko}* MEFs and WT. Blue dashed lines indicate cell membranes. Scale bars: 5 μ m.

establishment of astral MTs and appropriate spindle orientation in M phase (Toyoshima and Nishida, 2007). To investigate the interaction between MT plus-end tips and the cell cortex, we examined EB1 localization and distribution in WT and *Lis1*^{hc/ko} MEFs. In metaphase, WT MEFs displayed many discrete EB1-labeled MT plus-end tips nearly touching the cell cortex (Fig. 2-11 D), whereas fewer MT plus-end tips was found in the vicinity of the cell cortex and the length of each astral MT strand was reduced in *Lis1*^{hc/ko} MEFs (Fig. 2-11 D). Together, these data support the notion of reduced anaphase spindle pulling forces in *Lis1*^{hc/ko} MEFs.

Reduced frequency of cortical targeting of astral MT plus-ends in *Lis1* mutant MEFs

To further investigate how LIS1 affects the dynamics of MT plus-end movements, we performed time-lapse live-imaging experiments in EB1-GFP expressing MEFs undergoing M phase and traced MT plus-end comet movements by confocal microscopy. In WT MEFs, the growing MT plus-end comets (EB1-GFP) were generated mainly from the centrosomes and EB1 comets established very transient contacts to the cell cortex in metaphase. (Fig. 2-12 A) The frequency of EB1 comets-cell cortex contacts was further increased at the onset of anaphase with spindle pole elongation, suggesting that pulling forces were generated from this MT-cortex interaction. However, *Lis1*^{hc/ko} MEFs displayed significantly decreased numbers of MT asters with EB1 comets, and the frequency of transient interactions of MT plus-end tips with the cell cortex was also reduced (Fig. 2-12 B). These findings demonstrate that cortical interactions of MT asters were significantly impaired in *Lis1*-deficient mitosis

Lis1 +/+, EB1-GFP



Lis1 hc/ko, EB1-GFP

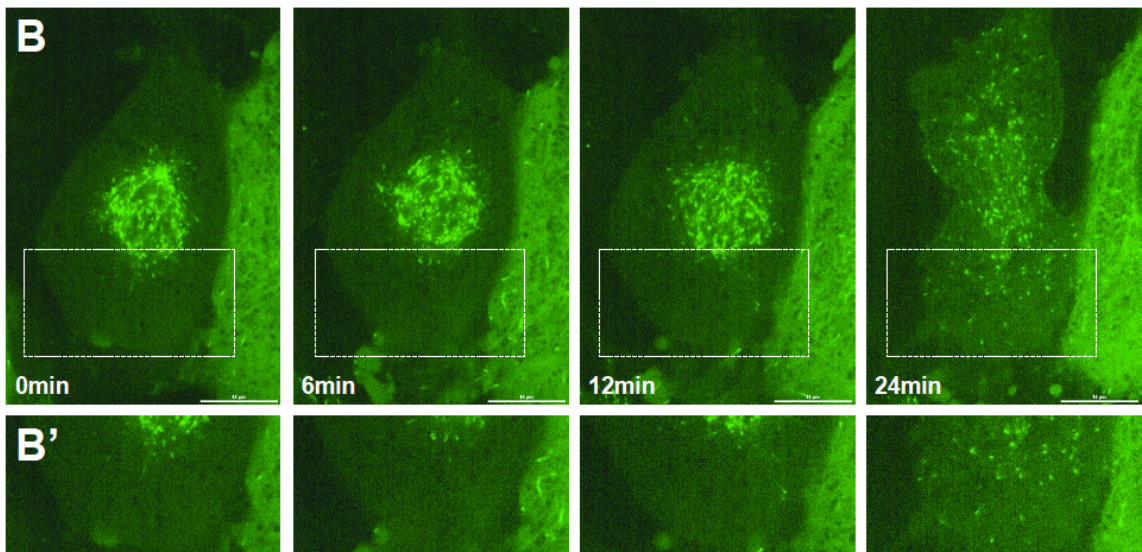


Figure 2-12. Reduced frequency of movement of EB1-labeled astral MT plus-ends near the cell cortex. (A) Frame series of time-lapse live imaging movies from WT MEF infected with EB-GFP adenovirus. (B) from *Lis1^{hc/ko}* MEF. (A', B') High magnification images from insets in (C, D). Scale bars: 10 μ m. These montages are generated from the representative movies of dividing MEFs from each genotype (more than 10 cells were imaged for live imaging).

Spindle misorientation and centrosome clustering phenotypes in *Lis1* mutant MEFs are rescued by MT stabilization, as well as LIS, NDE1, NDEL1, and dynein overexpression

We first hypothesized that spindle misorientation may be a result from misregulation of MTs in *Lis1^{hc/ko}* MEFs. To test this possibility, we treated WT MEFs and *Lis1^{hc/ko}* MEFs with taxol, a MT stabilizing reagent, and then analyzed spindle orientation in metaphase cells. DMSO-treated *Lis1^{hc/ko}* MEFs displayed significant spindle misorientation compared to DMSO-treated WT control MEFs (*Lis1^{hc/ko}*: $\alpha^\circ = 20.5 \pm 2.9$ vs. WT: $\alpha^\circ = 11.1 \pm 1.4$) (Fig. 2-13 A). In previous study, 1 μ M taxol treatment had been used to restore astral MTs by MT stabilization (Thoma et al., 2009). Notably, 1 μ M taxol treatment in *Lis1^{hc/ko}* MEFs led to astral MT enrichment (based on EB1 staining, data not shown). Importantly, taxol rescued spindle misorientation, and average angle of spindle orientation from taxol-treated *Lis1^{hc/ko}* MEFs was similar to those of untreated or taxol-treated WT MEFs (taxol-treated *Lis1^{hc/ko}*: $\alpha^\circ = 11.2 \pm 1.6$ vs. taxol-treated WT: $\alpha^\circ = 11.3 \pm 1.7$) (Fig. 2-13 A). These results suggest that taxol treatment can restore reduced MT plus end movements near the cell cortex by stabilizing MTs in *Lis1^{hc/ko}* MEFs.

Since LIS1 and its binding partner proteins, NDE1, NDEL1 and cytoplasmic dynein are all localized close to the cell cortex in WT MEFs, we hypothesized that ectopic overexpression of these proteins may rescue spindle orientation defects of *Lis1^{hc/ko}* MEFs during mitosis by sequestering the remaining LIS1 to help transport it to the critical sites such as the cell cortex. We generated a series of retroviruses encoding GFP, GFP-LIS1, GFP-NDEL1, GFP-NDE1, and GFP-DIC1. MEFs were transduced with each virus and spindle orientation was measured from metaphase-arrested GFP-positive cells. As expected, spindles were severely misoriented in GFP-infected *Lis1^{hc/ko}* MEFs (*Lis1^{hc/ko}* + GFP, control) (Fig. 2-13 B). Overexpression of ectopic LIS1 in WT MEFs resulted in severe spindle misorientation (Fig. 2-13 B), suggesting that precise levels of LIS1 are critical for normal spindle orientation. However, spindle orientation in *Lis1^{hc/ko}* MEFs was improved by GFP-LIS1, suggesting ectopic overexpression of LIS1 may restore the cortical

factors on the cell cortex and form appropriate spindle angle. Interestingly, *Lis1^{hc/ko}* MEFs infected with GFP-NDEL1, GFP-NDE1 and GFP-DIC1 also displayed reduced spindle angle compared to GFP-infected *Lis1^{hc/ko}* MEFs (Fig. 2-13 B). These results support the interpretation that LIS1 acts cooperatively with NDE1/NDEL1 and dynein to regulate precise spindle orientation via a LIS1-NDEL/NDE1-dynein complex to regulate MTs.

To test whether these components in the LIS1 protein complex also contribute to centrosome amplification and clustering in *Lis1^{hc/ko}* MEFs, we analyzed GFP-positive cells overexpressing each transgene. Similar to spindle orientation, overexpression of ectopic LIS1 in WT MEFs results in a dramatic increase in the percentage of cells displaying centrosome clustering (Fig. 2-13 C), further suggesting that precise levels of LIS1 are critical for normal centrosomal organization. The percentage of cells that displayed centrosome clustering phenotype was reduced in GFP-LIS1 and GFP-NDE1 expressing *Lis1^{hc/ko}* MEFs to nearly levels found in WT MEFs (Fig. 2-13 C). However, GFP-NDEL1- or GFP-DIC1-overexpressing MEFs demonstrated a lesser and relatively partial rescue of centrosome clustering phenotype compared to GFP-LIS1 and GFP-NDE1 (Fig. 2-13 C).

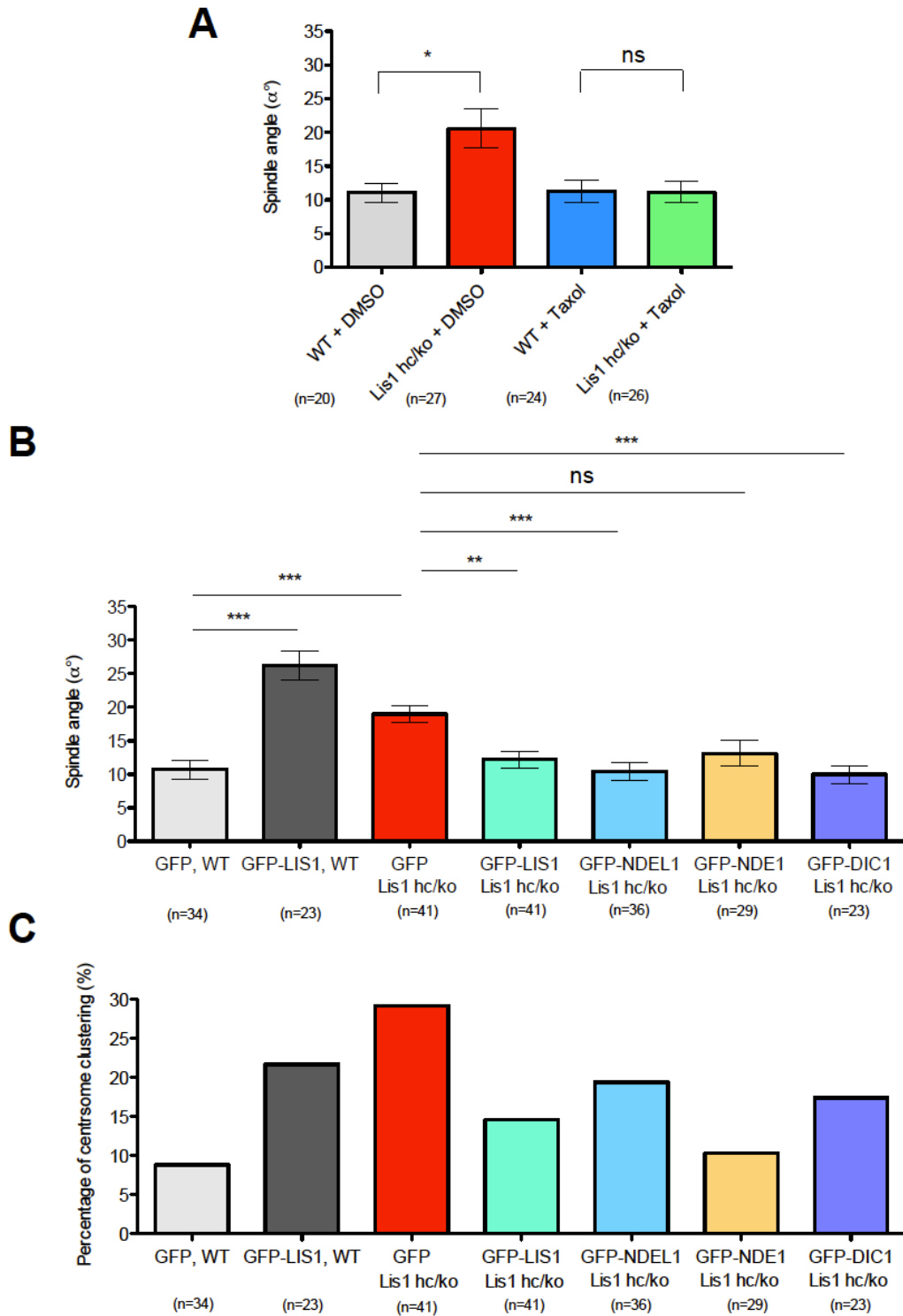
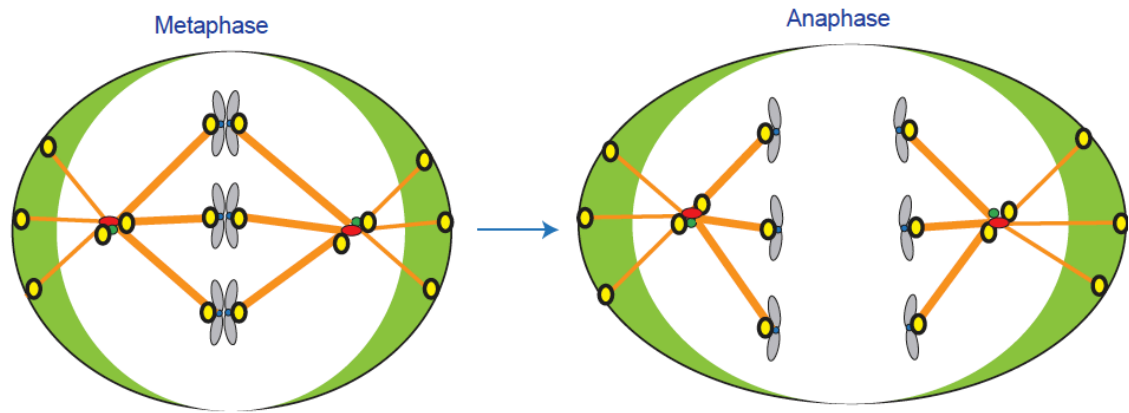


Figure 2-13. Spindle misorientation and centrosome clustering phenotype in *Lis1* mutant MEFs are restored by overexpression of several components of LIS1-NDEL1/NDE1-dynein complex. (A) Average spindle angles in WT and *Lis1*^{hc/ko} MEFs treated with DMSO and taxol. (B) MEFs infected with retroviruses encoding GFP, GFP-LIS1, GFP-NDEL1, GFP-NDE1, and GFP-DIC1. (C) Occurrence of centrosome clustering phenotype. Bars in (A, B): mean ± s.e.m., Asterisks in (A): *p < 0.05 by student's *t*-test. (B): **p < 0.01, ***p < 0.001 by ANOVA with Bonferroni's posthoc test. ns: not significant.

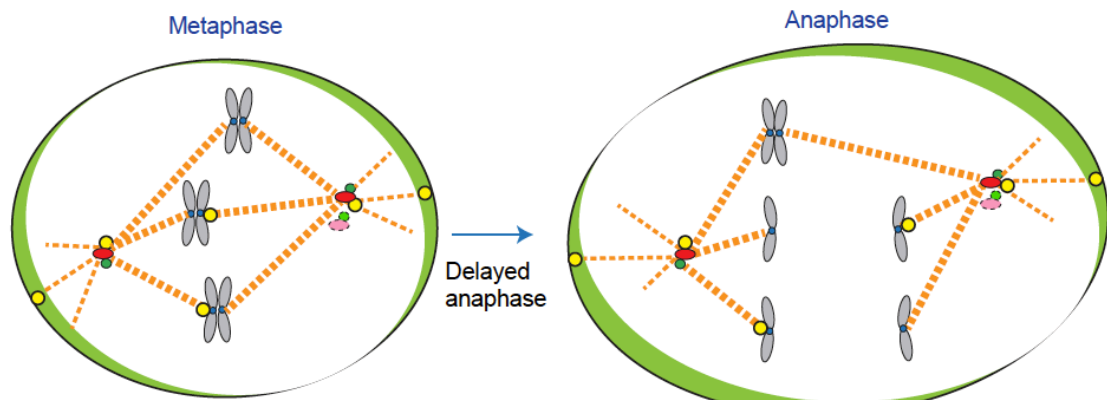
Discussion

Heterozygous loss-of-function of LIS1 in humans results in the neurodevelopmental brain malformation disorder - lissencephaly, a neuronal migration disorder. We and others demonstrated that LIS1 plays important roles during mitosis in mammalian cells (Faulkner et al., 2000; Tai et al., 2002; Tsai et al., 2005; Yingling et al., 2008). Using *Lis1* mutant mice, we previously showed that *Lis1* deficiency causes growth defects of MEFs and cell death of self-renewing NPs (Yingling et al., 2008; Wynshaw-Boris et al., 2010). However, the exact cellular mechanisms regulated by LIS1 during cell division are not well understood. Due to severe prometaphase arrest phenotype resulted from complete loss-of-function by siRNA-mediated knockdown or antibody injection against LIS1 (Faulkner et al., 2000; Tai et al., 2002; Tsai et al., 2005), the dose-dependent mitotic functions of LIS1 have not been determined previously. Here, we studied the detailed mitotic processes regulated by LIS1 in mouse primary MEF culture. We took advantage of various *Lis1* genetic allelic series to finely control LIS1 protein level by using *Lis1* mutant MEFs, employing both tamoxifen-inducible acute conditional knock-out (*CreER*, *Lis1^{hc/hc}* + TM) and conventional knock-out (*Lis1^{hc/ko}*) with 35% LIS1 protein compared to WT. We found that mouse LIS1 is essential for maintaining normal centrosome number and preserving centrosomal integrity in each mitotic cycle (Fig. 2-14). LIS1 has kinetochore-specific functions to complete chromosome congression by recruiting several kinetochore proteins to ensure anaphase progression with accurate chromosome segregation. Most importantly, time-lapse live cell imaging of MEFs undergoing mitotic cell phases revealed that LIS1 is the crucial for mitotic spindle formation to determine its positioning and orientation during mitosis. We also found that LIS1 is an important regulator of LIS1-NDE1/NDEL1-dynein complex to enhance astral MT plus ends dynamics and to mediate offloading of dynein/dynactin on the cell cortex, which contributes to MT-cortex interaction during mitosis (Fig. 2-14). Proposed cellular

Normal mitosis in *Lis1*^{+/+} (or) WT-Cre MEFs



Abnormal mitosis in *Lis1*^{hc/ko} (or) *Lis1*-CKO-Cre MEFs



Incomplete chromosome congression
Multiple clustered centrosomes
Less contacts between astral MT and cortex
Spindle misorientation

Chromosome missegregation



Figure 2-14. Proposed working model of LIS1 function in mitotic cell divisions. See text in discussion.

functions of LIS1 during mitosis of MEFs in the present study are consistent with the roles of *Pac1*, yeast *Lis1* homolog, in dynein offloading to the cell cortex from the plus-ends of astral MTs by increasing the frequency of cortical targeting of dynein/dynactin complex (Lee et al., 2005; Markus et al., 2011; Markus et al., 2009). Here we propose that LIS1 is a key protein to integrate signals from the cell cortex to transmit to mitotic spindles through astral MT regulation during mitosis.

Centrosome amplification at MT minus-ends in *Lis1*-deficient mitosis

Lis1 CKO MEFs frequently displayed aberrant centrosome numbers (3 or 4 MTOCs), suggesting that LIS1 is indispensable for centrosome number maintenance during mitotic cell division. The extra centrosomes in *Lis1^{hc/ko}* MEFs transiently clustered into two distinct opposite poles as multiple centriole pairs to form a pseudo-bipolar spindle. This result is consistent with the finding of multiple centrosomes in approximately 5% of *Drosophila DLis1*^{-/-} mutant NPs compared to 0% in WT NPs (Siller et al., 2005). Since the presence of extra centrosomes delays mitotic progression (Yang et al., 2008), LIS1 may be involved in mitotic checkpoint control by maintaining a consistent centrosome number during mitotic cell cycle. Three possible mechanisms can cause abnormal centrosome numbers: (1) misregulation of centrosome assembly, (2) failure of cytokinesis, and (3) dysfunction of the centrosome duplication cycle (Kramer et al., 2011; Nigg, 2002). Centrosome morphology was abnormal and enlarged in a majority of *Lis1^{hc/ko}* MEFs because of this centrosomal clustering, suggesting that there are minor defects in centrosome assembly in *Lis1^{hc/ko}* MEFs. However, the configuration of centrosomes as a mother-daughter centriole pair and centrosome maturation were normal in *Lis1^{hc/ko}* MEFs as indicated by mother centriole-specific proteins such as cennexin/ODF2, ninein, and Cep164, even at amplified centrosomes. Since the frequency of centrosome amplification was increased, the over-production of multiple mother centrioles in M phase led to the formation of multiple primary cilia during interphase, which means they are functional. Intriguingly, we have found defects in cytokinesis in

Lis1^{hc/ko} MEFs (unpublished data), which may partially contribute to centrosome number abnormality in *Lis1*-deficiency. Finally, dysregulation of the centrosome over-duplication cycle may be evoked by loss of LIS1 by misregulating a signaling pathway. We found that LIS1 and NDE1 overexpression in *Lis1^{hc/ko}* MEFs rescued centrosome amplification phenotype, suggesting NDE1 converges into LIS1-dependent centrosome number regulation pathway. For example, aberrant activation of Rho GTPases (RhoA, RhoC) enhances ROCK2 kinase activity and ultimately promotes centrosome amplification in other mammalian cells (Fukasawa, 2011; Kanai et al., 2010; Ma et al., 2006). Intriguingly, *Lis1* heterozygous MEFs (*Lis1^{ko/+}*) displayed elevated RhoA GTPase activity compared with WT MEFs (Kholmanskikh et al., 2006), suggesting that a high level of LIS1 protein expression is required for inhibiting RhoA GTPase. Therefore, misregulated RhoA signaling pathway in *Lis1^{hc/ko}* MEFs may cause ROCK activation to induce centrosome over-duplication.

Missegregation of chromosomes and fate determinants in *Lis1*-deficient mitosis

Appropriate levels of LIS1 protein are required for spindle assembly checkpoint control to inhibit improper chromosome kinetochore-MT attachments and ensure accurate chromosome segregation and inheritance to two daughter cells. *Lis1^{hc/ko}* MEFs displayed reduced targeting of kinetochore proteins such as dynein/dynactin and CLIP170. The dramatic increase of extra centrosomes in *Lis1^{hc/ko}* MEFs may lead to merotelic kinetochore-chromosome attachments by interfering with kinetochore-MT capture (Ganem et al., 2009). Improper kinetochore-MT attachments and extra centrosomes promote genomic instability by generating aneuploid daughters after mitosis. The frequent formation of chromatin bridges and micronuclei in *Lis1*-deficient mitosis reflects severe chromosome segregation defects. Consistent with a genomic stability function for LIS1, a particular human hepatocellular carcinoma cell type displays downregulation of *LIS1* mRNA and protein, and the severity of tumor formation is strongly correlated with *LIS1* downregulation (Xing et al., 2011). Human cells injected into nude mice

after *LIS1* knockdown display increased tumor formation compared with control cell-injection, suggesting that LIS1 may act as a tumor suppressor under certain conditions. Together, these results suggest that proper level of LIS1 expression is required for genomic stability to prevent detrimental loss of chromosomes during mitosis.

LIS1-dependent centrosome number maintenance may play critical roles in the maintenance of genomic stability and this may be important for the regulation of asymmetric NP division during development. In *Drosophila*, PLK4 homologue mutants induce the formation of extra centrosomes and defects of alignment of apically distributed cell fate determinants during NP divisions (Basto et al., 2008). Multiple MTOC-harboring NPs were unable to properly orient the mitotic spindle and the relationship between mitotic spindles and apical markers was disrupted. We also frequently observed three centrosomes (3 MTOCs) in apical NPs in the developing brain from *Lis1* mutant mice (unpublished data), suggesting that mammalian NP cells may employ similar mechanisms.

Spindle misorientation and reduced interaction between astral MT plus-ends and the cell cortex during mitosis in *Lis1* mutant MEFs

Spindle orientation and positioning are critical for the proper segregation of chromosomes and fate determinants to the daughter cells. Here we demonstrated that *Lis1*-deficiency in MEFs results in spindle misorientation with a high degree of spindle tilting compared with a plane of adhesion substrate. We found spindle orientation defects in NPs from *Lis1* mutant mice (Yingling et al., 2008). NDEL1- (Pramparo et al., 2010) and NDE1-depleted NPs (Feng and Walsh, 2004) also displayed severe spindle misorientation. In the present study, we demonstrated that *Lis1*-deficiency results in reduced cortical dynein in dividing MEFs. The number of astral MTs and the frequency of movements of EB1-labeled MT plus-ends reaching to the cortex were significantly reduced in *Lis1*^{hc/ko} MEFs compared to WT MEFs, leading to a lack of tension from the cell cortex to the spindle poles. Since LIS1-NDE1/NDEL1-dynein/dynactin complex is found in close

proximity to the cell cortex, it is likely that this protein complex may play a key role in mediating contacts between astral MTs and cortical factors. Due to the loss of LIS1, a key component of this complex, the LIS1-NDE1/NDEL1-dynein/dynactin complex may become destabilized at the cell cortex. Reduction of these cortical dynein complex (LIS1-NDE1/NDEL1-dynein)-driven pulling forces may be the cause of these spindle and astral MT defects in *Lis1* mutant MEFs and NPs. Several dynein/dynactin subunits displayed reduced localization to cortical sites during mitosis of *Lis1^{hc/ko}* MEFs. Most recently, it was shown that barrier- or bead-attached dynein controls the dynamics of MT plus-ends *in vitro* (Hendricks et al., 2012; Laan et al., 2012), indicating that cortical dynein is the key component to mediate interactions between astral MT plus-ends and the cell cortex. The amount of cortical dynein at the cell cortex may be proportional to the ability to induce MT end-on interaction (perpendicular to the cell cortex), and/or to inhibit MT lateral interaction (parallel to the cell cortex) (Gusnowski and Srayko, 2011).

In addition to LIS1-NDE1/NDEL1-dynein complex-mediated function near the cell cortex to control MT dynamics during the formation of the mitotic spindles, other cytoskeletal components may contribute to this mitotic function of LIS1. Subcortical actin cytoskeletal components as well as actin retraction fibers at adhesion sites have been implicated in spindle formation during mitosis (Fink et al., 2011; They et al., 2007). Interestingly, *Lis1* heterozygous mutant neurons (*Lis1^{ko/+}*) displayed misregulated actin stress fiber formation at leading edges during cell migration (Kholmanskikh et al., 2003). This finding raises the possibility that dysfunction of the actin cytoskeleton affected by reduced LIS1 protein levels has at least an indirect impact on actin-dependent mitotic spindle regulation during cell division. The cell cortex is a critically important site for vigorous crosstalk and interaction between MTs and the actin cytoskeleton to integrate intrinsic and extrinsic signal cues and transmit those signals into mitotic spindle regulatory pathway. We can conclude that LIS1, as a central component of LIS1-NDE1/NDEL1-dynein complex, participates in the regulation of MT plus-ends dynamics on astral MTs near the cell cortex to ensure mitotic spindle positioning and orientation, but in the future, it will be important

to determine whether LIS1 directly regulates the actin cytoskeleton as well to promote proper actin fiber assembly at the cortical adhesion-binding sites during cell division.

Implication of mitotic defects caused by loss of LIS1 protein

There are still important questions remain to be unanswered regarding severe mitotic phenotype seen in *Lis1* mutant MEFs. The most obvious phenotype displayed in *Lis1* mutant mice has been detected in developing mouse brain, especially in NP mitosis, not in other tissues. Although we found possible common regulatory mechanisms of mitotic spindle positioning and its orientation governed by LIS1 in MEFs and NPs, astral MT interaction with the cell cortex in polarized NPs (along the apical-basal axis) may be much more complex than MEFs. Mouse NPs also undergo symmetric and asymmetric division to generate different daughter cells, the determining these types of divisions and the daughter cells fate can be potentially influenced by LIS1 protein level. Presumably, it is possible that mitotic defects in NPs are much more sensitive to LIS1 expression levels than any other tissue and cell types. It also has been accounted for the discrepancy between *in vivo* and *in vitro* effects of *Lis1*-deficiency. Primary culture condition of MEFs may exaggerate the changes of LIS1 effects on mitosis *in vitro*.

Chapter 3. Function of LIS1 in Cytokinesis

3.3 Introduction

Cytokinesis is a critical final step of cell division required for correct partitioning of the cytoplasm and chromosomes to the daughter cells through dramatic cytoskeletal reorganization initiated from anaphase C phase (cytokinesis phase) (Canman et al., 2000) to telophase (Eggert et al., 2006; Piekny et al., 2005). Incomplete cytokinesis results in aneuploidy with missegregated chromosomes. Furthermore, cytokinetic failure increases binucleated daughter cells with tetraploidy.

Notably, microtubules (MTs) play important instructive roles to provide positional cues of cleavage furrow at the equatorial cortex by inducing assembly of antiparallel MT bundles at the spindle midzone, called the central spindle. Central spindle activity stimulates the formation of the cleavage furrow at the equatorial cortex, termed “equatorial stimulation” (Bement et al., 2005; von Dassow, 2009; Werner et al., 2007). At the polar cortex, dynamic crosstalk between astral MTs and cortical actin patches generates inhibitory signals near the polar cortex, which ultimately helps restrict cleavage furrow positioning to the equatorial cortex, termed “polar relaxation” (Canman et al., 2003; Foe and von Dassow, 2008; Murthy and Wadsworth, 2008). The combination of these actions between stimulatory signals at the equatorial cortex and inhibitory signals at the polar cortex is a prerequisite for proper cleavage furrow positioning at the cell equator. At the molecular level, division plane specification is mainly mediated by a small GTPase RhoA-active zone (Bement et al., 2005; Nishimura and Yonemura, 2006), followed by the recruitment of contractile ring components to the equatorial cortex that includes the scaffold protein anillin (D'Avino et al., 2008; Gregory et al., 2008; Oegema et al., 2000; Piekny and Glotzer, 2008) and filamentous septin (Kinoshita et al., 2002; Maddox et al., 2007; Oegema et al.,

2000). Myosin-II is also recruited to the equatorial cortex and serves as a force generator to promote furrow ingression and membrane constriction by activating cortical contractility through crosslinking filamentous actin (F-actin) (Glotzer, 2005; Straight et al., 2003; Zhou and Wang, 2008). The RhoA-downstream effectors ROCK (Rho-kinase) and citron kinase phosphorylate the specific sites in myosin light chain that are important for its motor activity (Kosako et al., 2000; Yamashiro et al., 2003).

Interestingly, fewer or elongated astral MTs destabilize the cleavage furrow leading to the misregulation of polar actomyosin contractility, mislocalization of the cleavage furrow, cell shape oscillation, and cytokinetic failure (Canman et al., 2003; Murthy and Wadsworth, 2008; Rankin and Wordeman, 2010). Vigorous cell shape oscillation and spindle rocking have been found during cytokinesis in anillin-depleted cells (Echard et al., 2004; Kechad et al., 2012; Piekny and Glotzer, 2008; Straight et al., 2003; Zhao and Fang, 2005). The formation of ectopic membrane bulges and large size of membrane blebbing from abnormal membrane contractility (hyper-cortical contractility) is another key feature of these oscillated movement in cytokinesis, suggesting that rapid actomyosin turnover at the cell membrane is tightly controlled to retain cleavage furrow positioning at the cell equator (Sedzinski et al., 2011). Impairment of cortical contractility is accompanied by dispersed F-actin focusing and aberrant RhoA localization at the contraction sites, which ultimately leads to mislocalization of the cleavage furrow and cytokinetic failure (Watanabe et al., 2008).

Dynamic astral MTs have been implicated in the inhibition of actomyosin-based contraction. Therefore, MT depolymerization stimulates certain pools of the actomyosin cytoskeleton at the cell cortex (Mandato et al., 2000). Several studies support the idea that the entire cell cortex relieved from the proper contacts of MTs has ability to be competent for the formation of cleavage furrow contraction during cytokinesis (Canman et al., 2003; Murthy and Wadsworth 2008; Rankin and Wordeman, 2010).

During early cell division of the sea urchin egg, two important MT-binding proteins have critical roles in cytokinesis: EB1, MT plus-end binding protein; and the dynein motor. Injection of antibodies against EB1 and p150^{glued} or p50 dynamitin overexpression disrupted and delayed normal cytokinesis of these cells (Strickland et al., 2005), suggesting that dynein (the MT minus-end directed motor) and MT plus-end binding proteins may play important roles in the crosstalk between MT-regulated spindles and actomyosin-regulated cell cortex.

In this aspect, LIS1 is an important regulator of dynein as well as a MT-binding protein, and is a good candidate to link molecularly the MT and actin cytoskeletons during cell division including cytokinesis. Human *LIS1* haploinsufficiency causes lissencephaly (smooth brain), a neuronal migration disorder and severe brain malformation during early development (Dobyns et al., 1993; Hattori et al., 1994). LIS1 directly interacts with evolutionarily conserved nuclear distribution proteins such as NDEL1, NDE1 (both NudE homologues) (Feng et al., 2000; Niethammer et al., 2000; Sasaki et al., 2000) and NUDC (Morris et al., 1998). Importantly, NUDC has been implicated in cytokinesis (Aumais et al., 2003) as a substrate of Plk1 kinase (Zhang et al., 2002; Zhou et al., 2003). Mouse *Lis1* deficiency or *Lis1* heterozygosity leads to misregulation of F-actin during migration of post-mitotic neurons by elevating RhoA GTPase activity and antagonistically inactivating other family members of small GTPases Rac1/Cdc42 (Kholmanskikh et al., 2003; Kholmanskikh et al., 2006). Cytokinetic delay and incomplete cytokinesis was described after knockdown of dynein subunits (DLIC2, LC8) (Palmer et al., 2009), and a novel LIS1/DIC (dynein intermediate chain)/MT-binding partner, DCDC5 (doublecortin domain-containing protein 5) (Kaplan and Reiner, 2011), in HeLa cells. Thus, we hypothesized that LIS1 may be essential for normal cytokinesis in mouse cell division.

3.2 Results

Cytokinesis defects and increased binucleated cell numbers during cell division of *Lis1* mutant MEF

First, we examined the frequency of completion of cytokinesis in both WT (*Lis1*^{+/+}) MEFs and *Lis1* compound heterozygote (*Lis1*^{hc/ko}) mutant MEFs harboring 35% of LIS1 protein level compared to WT. Incomplete cytokinesis was detected as a failure to separate the intercellular bridge linking cytoplasm of two daughter cells analyzed from timelapse live-imaging of MEF cell division. Sequential events during the entire cell division were visualized by mCherry- α -tubulin, a fluorescently labeled MT marker and H2B-GFP, a chromosomal probe. Only 6.5% (6/93) of WT MEFs displayed incomplete cytokinesis, while in *Lis1*^{hc/ko} MEFs, the frequency of incomplete cytokinesis was dramatically increased to 38.9% (14/36) (Fig. 3-1 A).

To test whether acute loss of *Lis1* also caused similar effects on cytokinesis, we derived *Lis1* MEFs from tamoxifen (TM)-inducible conditional homozygous mutants (*CreER; Lis1*^{hc/hc}). We treated these cells with 12 h 4-hydroxy-TM and compared their phenotypes with those of control *Lis1* WT MEFs (*CreER; Lis1*^{+/+}). Similar to *Lis1*^{hc/ko} mutant MEFs, acute deletion of *Lis1* in tamoxifen treated *CreER; Lis1*^{hc/hc} MEFs also led to frequent cytokinetic failure and a high percentage of binucleation, 23.5% (4/17) compared to 3.7% (1/27) control *CreER; Lis1*^{+/+} MEFs, where duplicated chromosomal sets were either combined resulting in tetraploidy or when there was a bi-lobed shape to the nuclei inside of the fused cytosols of the two daughters (Fig. 3-1 B).

To assess whether the increased cytokinetic failure frequency ultimately affected cell survival or cell death, we performed cleaved-caspase 3 immunostaining as a measure of apoptotic cell death. *Lis1*^{hc/ko} MEFs displayed more than 2-fold increased cleaved-caspase 3 staining-positive cells compared with WT MEFs, suggesting *Lis1* deficiency induces elevated apoptosis of MEFs (Fig. 3-1 C).

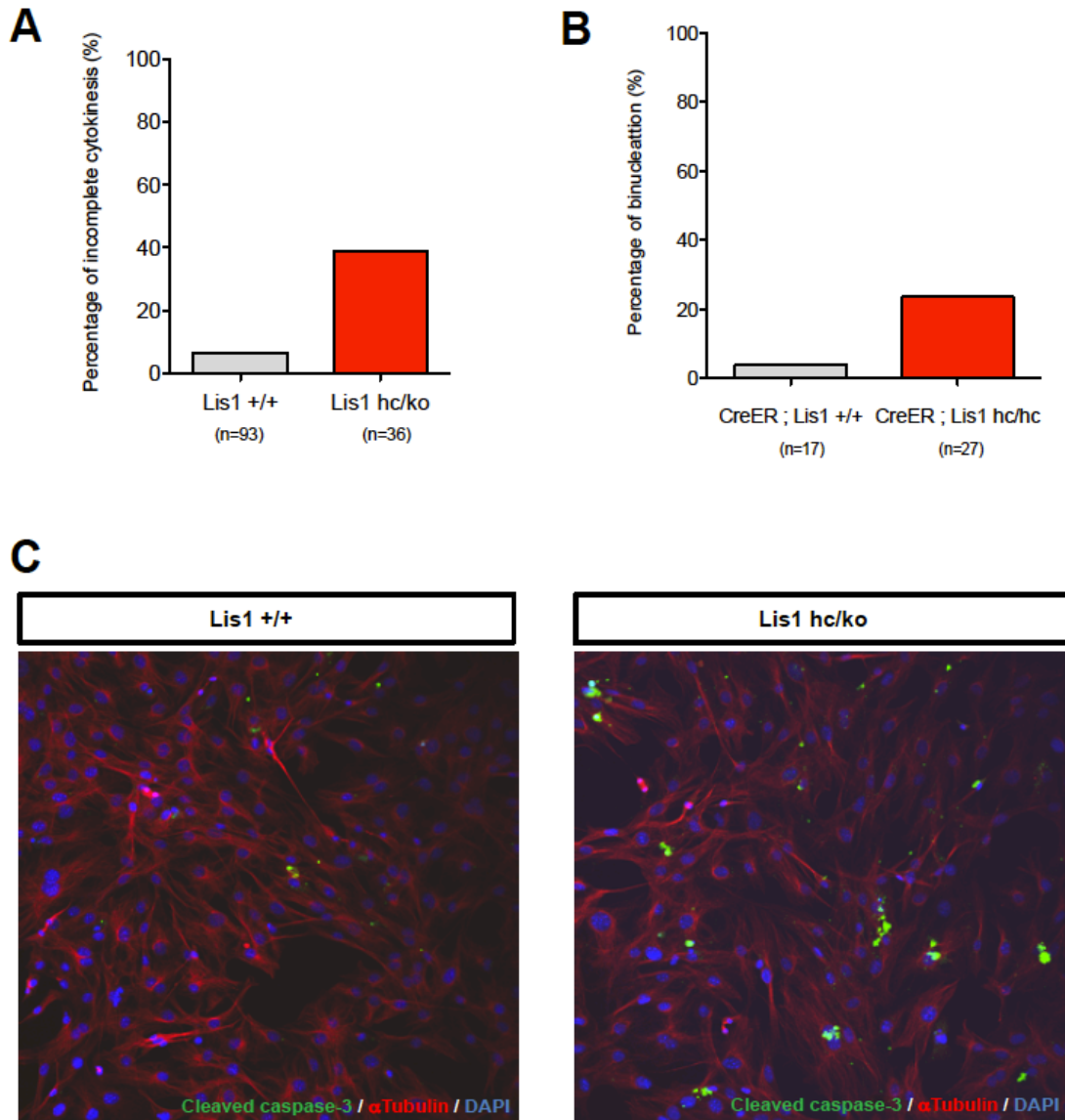


Figure 3-1. Loss of LIS1 disrupts normal cytokinesis and leads to increased formation of binucleated daughter cells.

(A) *Lis1*-deficient compound heterozygous mutant MEFs (*Lis1*^{hc/ko}) displaying frequent failure of cytokinesis compared to WT MEFs in timelapse live-imaging. (B) Increase in occurrence of binucleated daughter cells from MEFs with acutely deleted *Lis1*. (C) Increased apoptotic cell death from *Lis1*^{hc/ko} MEFs compared with WT MEFs (Green: Apoptotic cells identified by cleaved caspase-3 staining, red: α -tubulin, blue: DAPI).

Dramatic cell shape oscillation and spindle rocking during cytokinesis in *Lis1* mutant MEF cell division

To gain further insights into the cellular mechanisms responsible for the cytokinetic defects found in *Lis1* mutant MEFs, we monitored the detailed mitotic progression focusing on anaphase to telophase and cytokinesis onset timing. We analyzed the dynamic movements of MT-enriched midbody and cleavage furrow positioning throughout cell division. Acute-deletion of LIS1 in tamoxifen-treated (*CreER; Lis1^{hc/hc}, TM 12 h*) MEFs resulted in drastic oscillations in cell shape (Fig. 3-2 A), similar to the phenotype described in anillin-depleted cells (Echard et al., 2004; Kechad et al., 2012; Piekny and Glotzer, 2008; Straight et al., 2003; Zhao and Fang, 2005). At the beginning of anaphase onset in timelapse movies of *Lis1* mutant MEFs, the midbody was properly positioned in the central spindle zone. However, the position of the midbody was destabilized and oscillated between the cytoplasm of the two daughter cells. More surprisingly, the previously separated chromosome sets moved back and forth between two daughter cells and spindle rocking was prominent, reflecting mispositioning of unstable MT attachments between the cell cortex and the mitotic machinery. This phenotype was termed “hyper-contractility” in cells with depleted contractile ring components, and is usually caused by hyperactivity of the actomyosin cytoskeleton during cytokinesis. In the most severe case (shown in Fig. 3-2 B), one daughter inherited two-sets of chromosomes (tetraploidy) with binucleation, and the other daughter cell underwent immediate cell death.

We next examined the frequency of appearance of the hyper-contractility phenotype during cytokinesis. WT MEFs displayed this oscillated movements rarely, in only 4.3% of cell divisions (4/96). By contrast, more than a half of the cell divisions (55.6%, 20/36) in *Lis1^{hc/ko}* MEFs displayed hyper-contractility in some phases of cytokinesis (Fig. 3-2 C).

The significant formation of ectopic membrane bulges detected during cytokinesis in *Lis1* mutant MEFs led us to examine differential interference contrast (DIC) timelapse images to

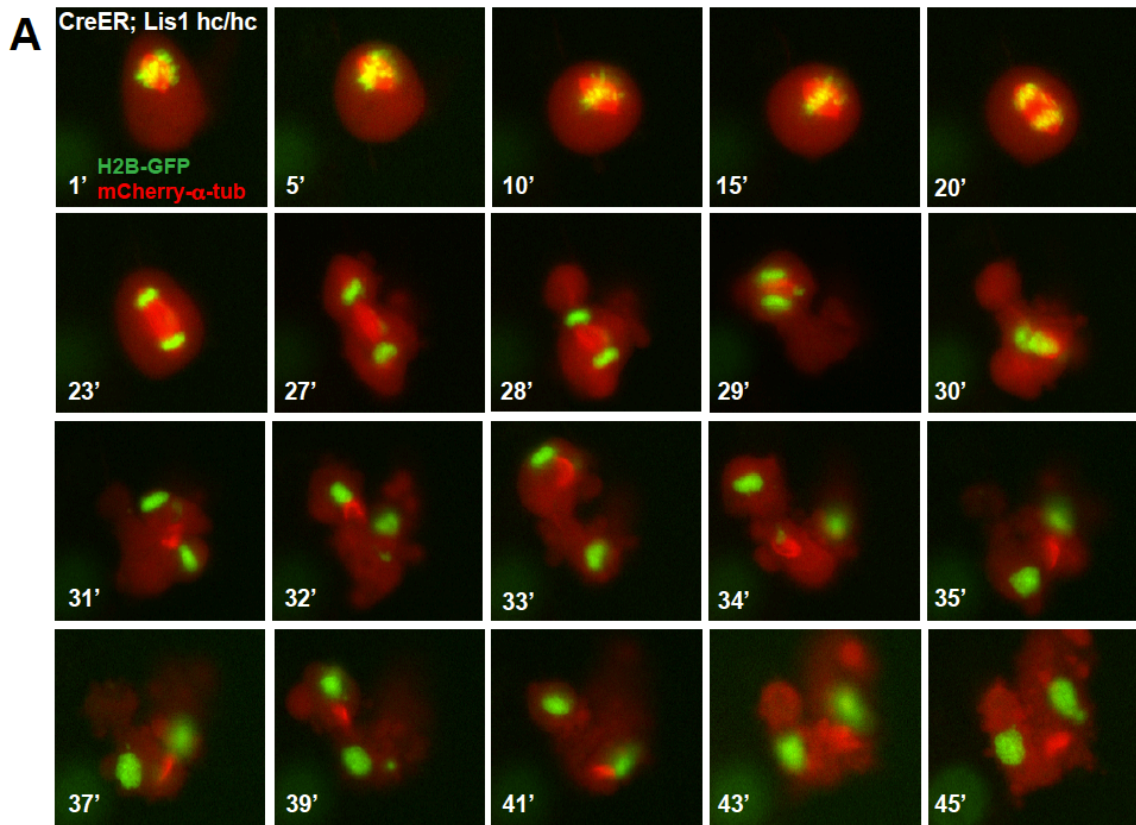


Figure 3-2. Loss of LIS1 results in cell shape oscillation and spindle rocking to cause cytokinetic failure with aberrant cleavage furrow positioning.
 (A) MEFs with acutely deleted *Lis1* showing severe defects during cytokinesis, the mitotic cell phase when cleavage furrow positioning is determined. Midbody (highly concentrated with red fluorescence: mCherry- α -tubulin) instability accompanied by vigorous cell shape oscillation and spindle rocking (visualized by green fluorescence: H2B-GFP).

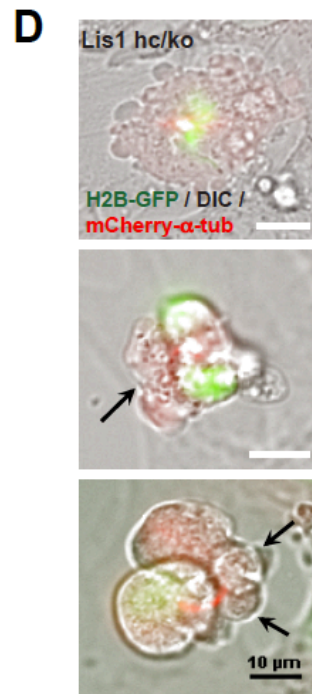
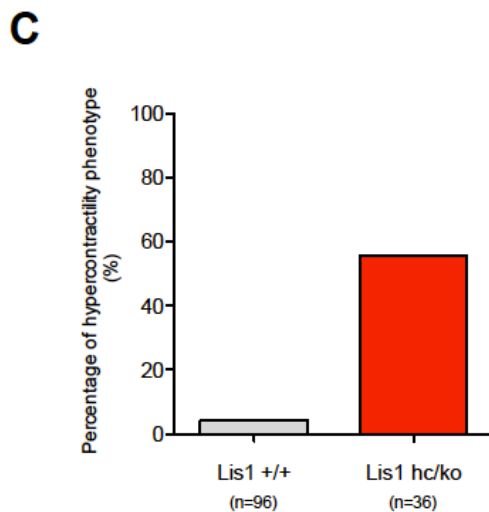
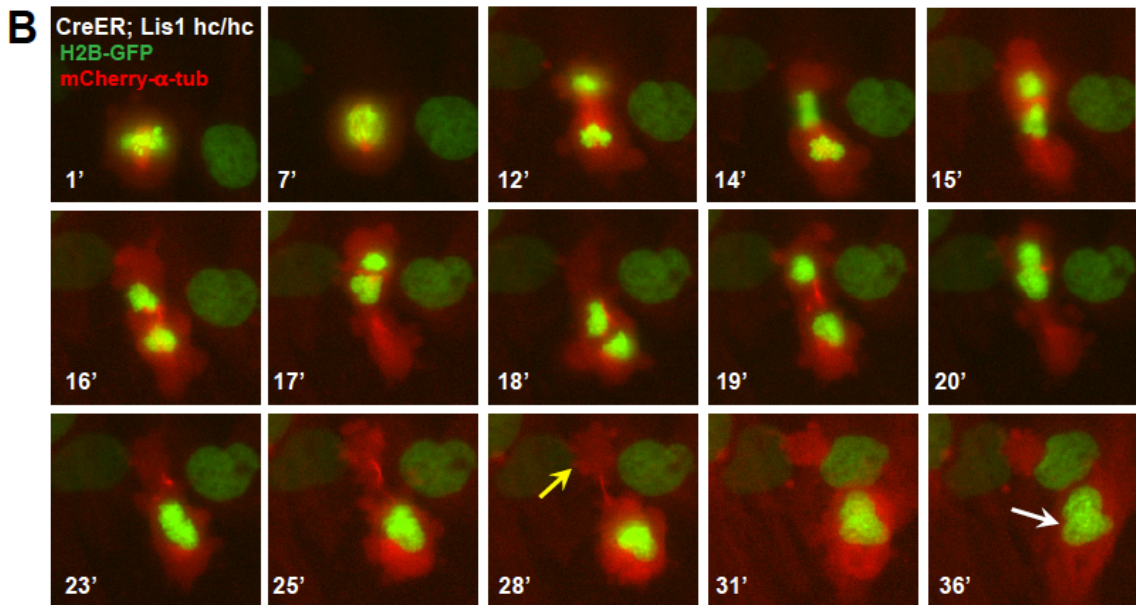


Figure 3-2. Loss of LIS1 results in cell shape oscillation and spindle rocking to cause cytokinetic failure with aberrant cleavage furrow positioning.

(B) MEFs with acutely deleted *Lis1* undergoing abnormal cell shape and chromosome oscillation between two daughter cells. Yellow arrow (28'): anucleated one daughter cell, White arrow (36'): binucleated and bi-lobed one daughter cell. (C) Increase in the frequency of hypercontractility phenotype in *Lis1*^{hc/ko} MEFs. (D) Single snapshots from the merged images with DIC (differential interference contrast) and fluorescence timelapse images (Green: H2B-GFP, red: mCherry- α -tubulin, grey: DIC) from timelapse movies (Black arrows: aberrant formation of huge membrane blebs). Scale bars: 10 μ m.

observe membrane dynamics in detail combined with other fluorescent signals (H2B-GFP, mCherry- α -tubulin). We found that *Lis1*^{hc/ko} MEFs exhibited vigorous membrane blebbing in anaphase onset and cytokinesis (Fig. 3-2 D). The frequency of occurrence of blebs was significantly increased in *Lis1*^{hc/ko} MEFs and the size of ectopic blebs was also much larger than in WT MEFs.

Mislocalization of contractile ring components and RhoA-actomyosin during cytokinesis of *Lis1* mutant MEFs

We next determined whether critical regulators of cytokinesis are involved in *Lis1*-dependent cytokinesis failure. RhoA is an evolutionarily conserved positive regulator of cytokinesis in many organisms, so we investigated RhoA localization in *Lis1* mutant MEFs from anaphase to cytokinesis. In order to dissect only cell membrane-bound and active GTP-bound form of RhoA, we fixed MEFs with 10% trichloroacetic acid (TCA) (Yonemura et al., 2004). In WT MEFs, active RhoA accumulated specifically at both sides of the equatorial cortex symmetrically in early anaphase and was further concentrated in the midbody in telophase and throughout cytokinesis (Fig. 3-3 A). In all cell cycle phases from anaphase to telophase, RhoA was colocalized with cell cortex-associated anillin, a key component of the contractile ring that defines the future cleavage furrow ingression site. By contrast, *Lis1*^{hc/ko} MEFs displayed frequent abnormalities during cytokinesis; approximately 60% of cells displayed abnormal cytokinesis patterns including mislocalization of the cleavage furrow and the formation of huge polar blebs in various cortical sites (Fig. 3-3 A). In early anaphase, the RhoA and anillin-positive zone near the equatorial cortex was much broader in *Lis1*^{hc/ko} MEFs than WT MEFs. In particular, the anillin-positive cell cortex (contractile ring) was not constricted and many abnormal anillin puncta were distributed along the central spindle zone, a default location when anillin is not associated with the equatorial cortex (data not shown). In late anaphase, an aberrant cleavage furrow was found at only one side of the cell cortex of *Lis1*^{hc/ko} MEFs, resulting in asymmetric mislocalization of RhoA and anillin,

although the chromosome sets were properly segregated into two daughter cells. The binucleated *Lis1^{hc/ko}* mutant MEFs had many protruding polar blebs in ectopic locations along the whole cell cortex. Intriguingly, RhoA decorated the membrane structure of all of these polar blebs, although anillin was not associated with these blebs, suggesting that the RhoA and actomyosin may be the primary signal to produce this aberrant polar membrane bulges.

Next, we examined the localization of myosin-II motors in *Lis1^{hc/ko}* MEFs compared to WT MEFs during cytokinesis. Myosin-II is one of main regulatory components of cortical contraction, working cooperatively with the actin cytoskeleton during cytokinesis (Piekny et al., 2005). In WT MEFs, the majority of non-muscle myosin heavy chain IIA (NMHCIIA) staining at the spindle midzone overlapped with focused phalloidin staining specific for F-actin, called the F-actin focusing zone (Fig. 3-3 B). However, we found that *Lis1^{hc/ko}* MEFs displayed less-focused and elongated NMHCIIA staining at the spindle midzone compared to WT MEFs (Fig. 3-3 B). Importantly, *Lis1^{hc/ko}* MEFs had a reduced F-actin focusing zone with less NMHCIIA accumulation at the spindle midzone. Furthermore, both NMHCIIA and F-actin were detected at the cortical patches in ectopically located membrane bulges in the polar cortex during cytokinesis. These findings suggest that cortical constriction at the equatorial cortex was abnormally regulated in *Lis1* mutant MEFs, leading to aberrant positioning of the cleavage furrow, and that this may be caused by hyper-contractility of the cell cortex from misregulation of actomyosin-mediated signaling provoked by *Lis1* deficiency.

Mislocalization of myosin-II in *Lis1* mutant MEFs during cytokinesis

To further explore the cellular basis of cytokinesis failure from *Lis1* mutant MEFs, we investigated actomyosin dynamics by performing timelapse live-imaging of myosin regulatory light chain1 (MRLC1)-GFP. MRLC1-GFP has been used a reliable probe to monitor myosin motor in live cells (Beach et al., 2011), especially during cytokinesis (Miyachi et al., 2006). We generated MRLC1-GFP and H2B-tdTomato retroviruses and infected MEFs to visualize myosin

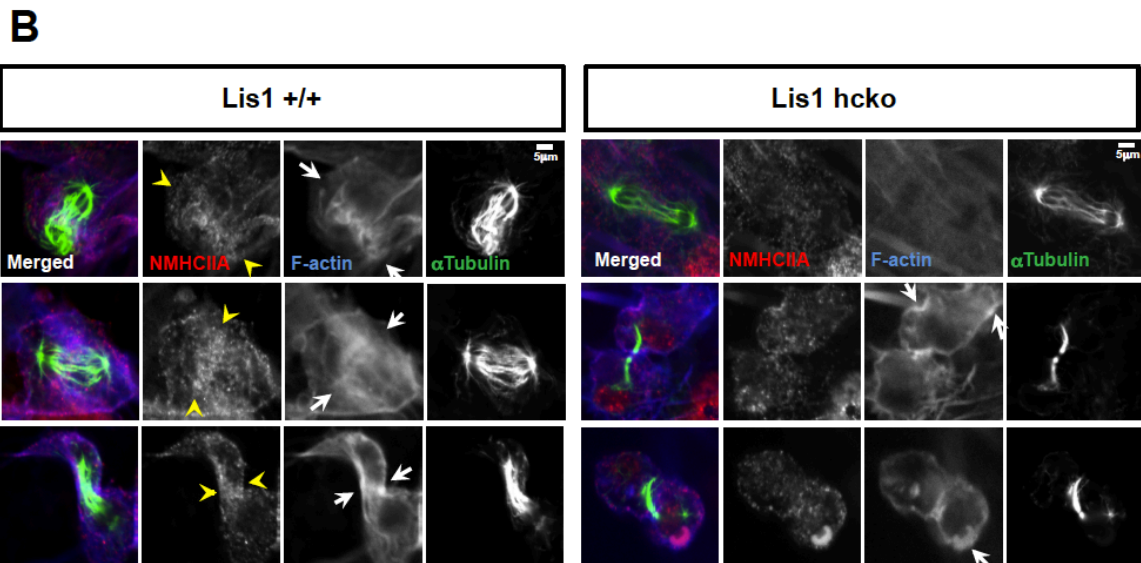
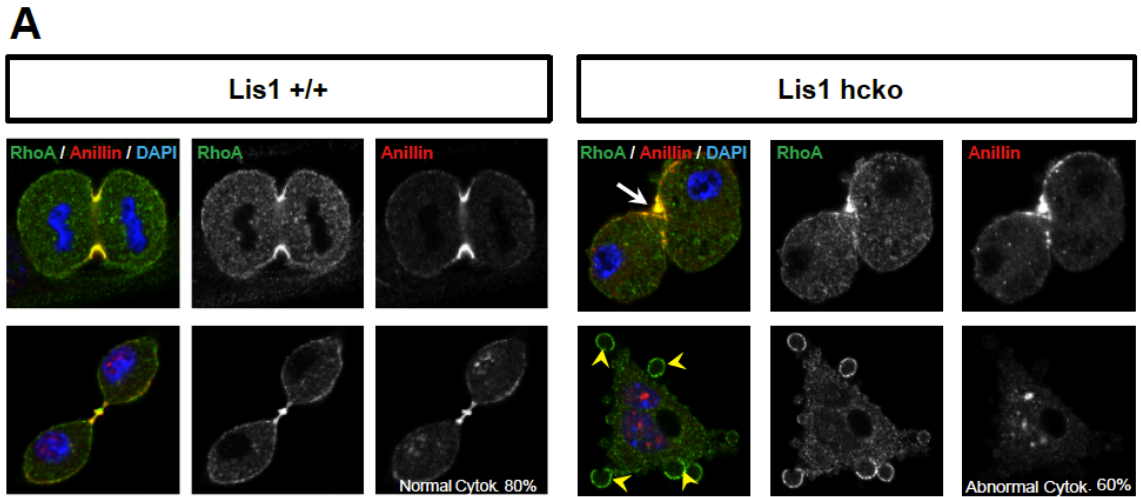


Figure 3-3. *Lis1* mutant MEFs display mislocalization of RhoA-actomyosin and contractile ring components.

(A) Left panels: WT MEFs showing normal cleavage furrow positioning labeled with TCA-fixed RhoA and anillin co-staining at the equatorial cortex from early anaphase to late telophase ; Right panels: *Lis1* mutant MEFs (*Lis1^{hc/ko}*) displaying mislocalization of RhoA and anillin, Top: asymmetric cleavage furrow formation, Bottom: binucleated cells with many RhoA-positive aberrant membrane blebbs (green: RhoA, red: anillin, blue: DAPI). (B) Left panels: WT MEFs with accumulation of non-muscle myosin heavy chain II-A (NMHCIIA) at the cell equator (yellow arrowheads). Colocalization of staining of NMHCIIA and F-actin (phalloidin)-focusing zone (white arrows) ; Right panels: *Lis1* mutant MEFs (*Lis1^{hc/ko}*) displaying dispersed and less-focused actomyosin at the cell equator. White arrows: aberrantly localized ectopic membrane bulges. (Green: α -tubulin, red: NMHCIIA, blue: F-actin). Scale bars: 5 μ m.

and chromosomes, respectively. In control MEFs (*CreER; Lis1^{+/+}, TM 24 h*), myosin accumulated at the equatorial cortex and the contractile ring constricted normally (Fig. 3-4 A). By contrast, Cre-inducible *Lis1* mutant MEFs (*CreER; Lis1^{hc/hc}, TM 24 h*) displayed unstable myosin movements (Fig. 3-4 B). Furrow ingression first progressed but regressed abnormally, which failed to restrict the cleavage furrow at the equatorial cortex and ultimately resulted in failure of cytokinesis. In the most severely affected occasions, *Lis1* mutant MEFs displayed an aberrant uncoupling between chromosome segregation and cytokinesis (Fig. 3-4 C). In normal cytokinesis, chromosome sets first separated into two daughters and was followed by equatorial constriction to initiate cytokinesis. However, this sequential regulation of cytokinesis was disrupted in *Lis1* mutant MEFs. Although chromosome sets did not segregate precisely into two daughters before the onset of mitotic spindle elongation in anaphase, actomyosin-mediated hyper-contractility of the cell cortex triggered cytokinesis progression, producing binucleated cells with tetraploidy (identified with no separation of two chromosome sets by H2B-tdTomato) and cytokinetic failure. Oscillated movements of myosin was observed as well, which also supports that aberrant cytoplasmic pushing forces were generated by ectopically-located myosin at the polar cortex during cytokinesis of *Lis1* mutant MEFs.

Failure to maintain contractile ring components at the equatorial cortex in *Lis1* mutant MEFs

To test whether the actomyosin abnormality in *Lis1* mutant MEFs resulted in deleterious effects on the recruitment of other contractile components to the equatorial cortex, we performed timelapse imaging of septin 6 (SEPT6)-GFP. SEPT6-GFP localizes at the cleavage furrow in T cell division (Gilden et al., 2012) and the septin complex is one of the important components of the contractile ring in a protein complex with anillin during cytokinesis. We infected MEFs with SEPT6-GFP and performed timelapse imaging of cytokinesis. In control MEFs, SEPT6 was enriched at the equatorial cortex in anaphase and was maintained at the cleavage furrow

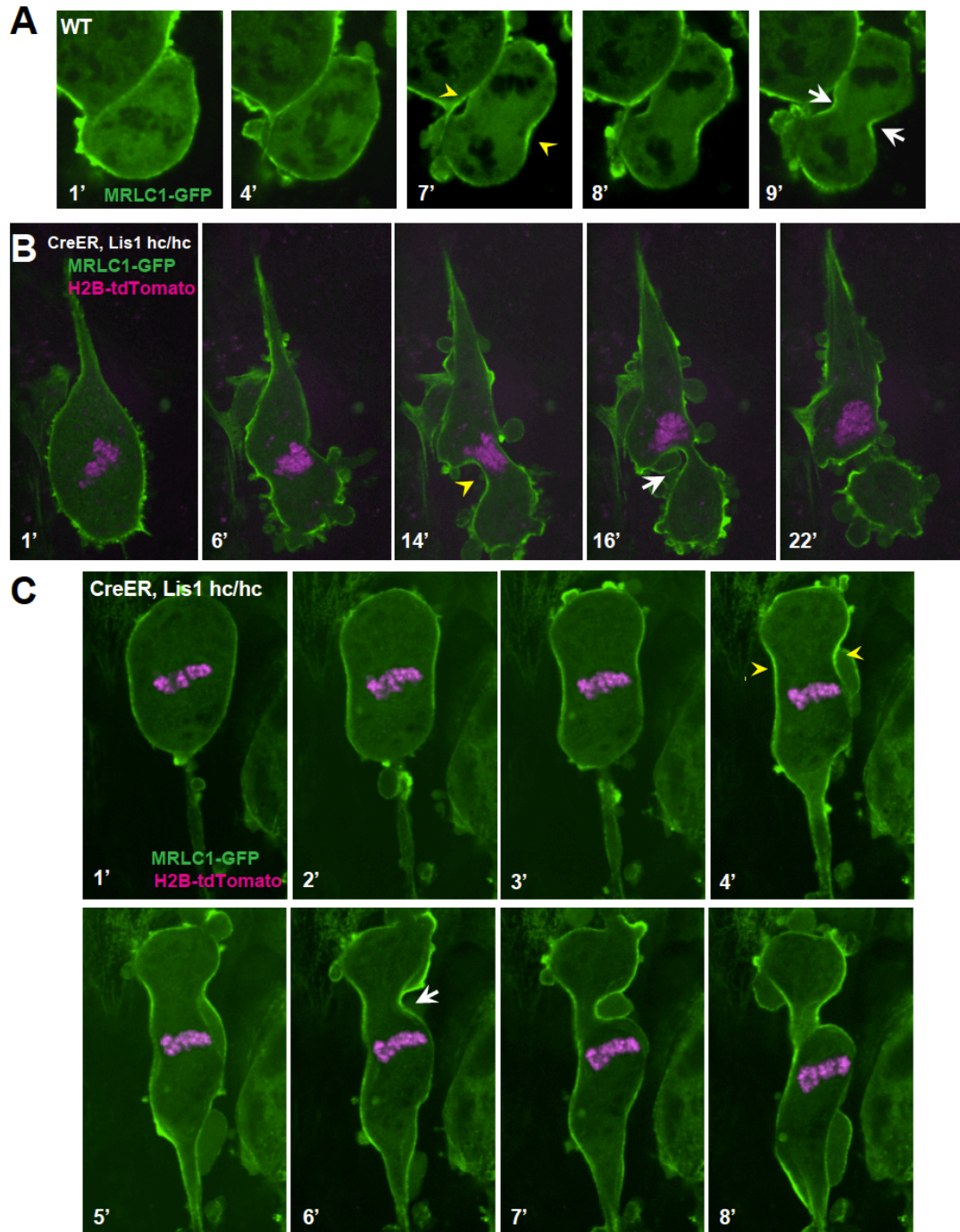


Figure 3-4. Myosin-II (MRLC1) was abnormally distributed in *Lis1* mutant MEFs during cytokinesis. (A) WT MEFs showing normal recruitment of myosin regulatory light chain 1 (MRLC, green) of Myosin-II subunit at the equatorial cortex during cytokinesis. Dark black spots inside of the cells indicating chromosome sets. (B) *Lis1* mutant MEFs (*CreER; Lis1 hc/hc + 24 h TM*) infected with MRLC1-GFP (green) and H2B-tdTomato (magenta), undergoing cytokinetic failure with asymmetrically mis-positioned cleavage furrow. (C) *Lis1* mutant MEFs clearly to show uncoupling between the chromosome separation (usually precedes before cytokinesis onset) and cleavage furrow ingression. *Lis1* mutant MEFs (4') still maintaining unsegregated tetraploid chromosomes to initiate furrow contraction from actomyosin ring. (Yellow arrowheads: initial accumulation of MRLC1, white arrows: final cleavage furrow positioning).

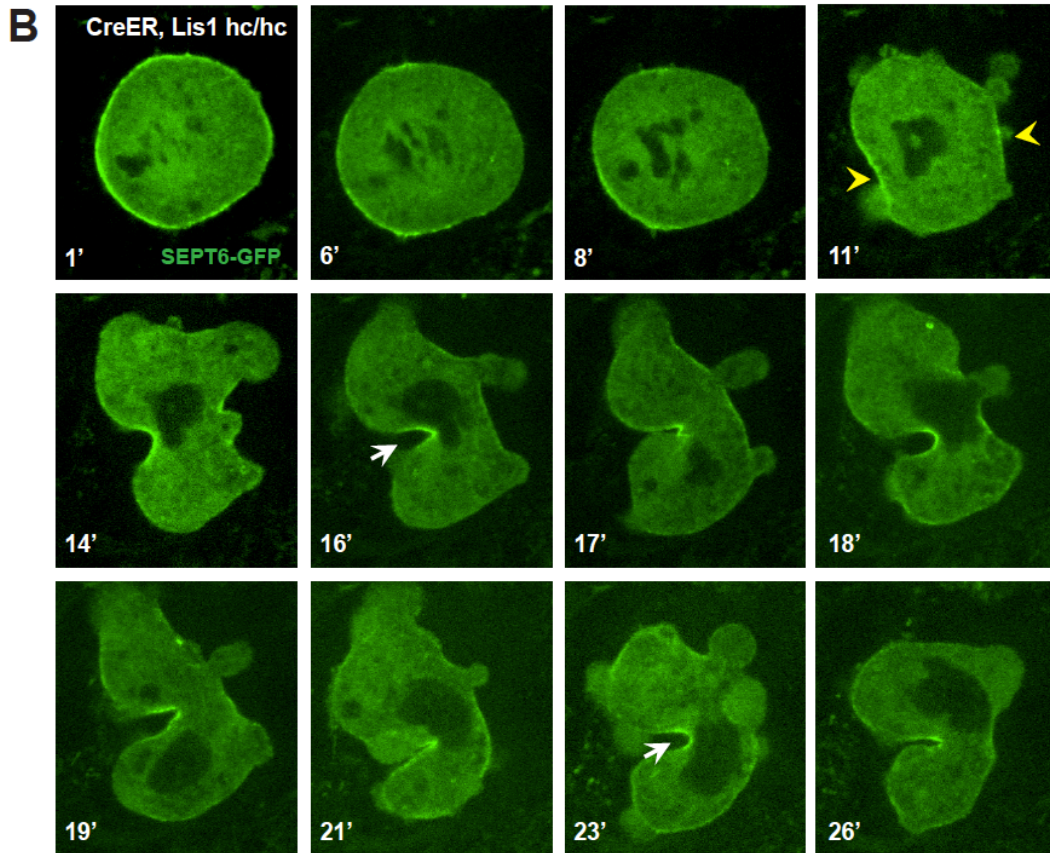
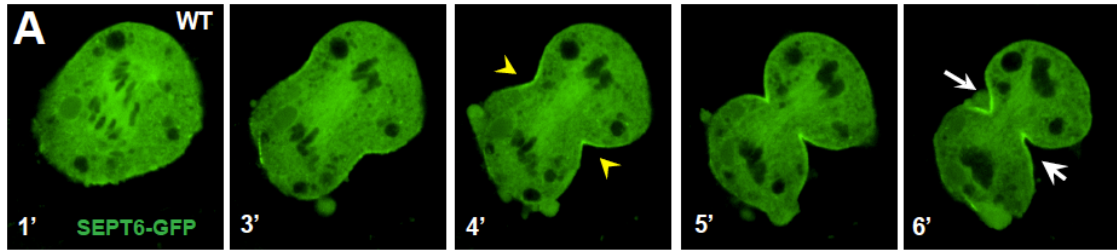


Figure 3-5. Contractile ring component (SEPT6) was not properly maintained at the equatorial cortex in *Lis1* mutant MEFs.

(A) WT MEFs showing normal recruitment of septin 6 (SEPT6-GFP, in green), an actomyosin-fiber crosslinking protein in contractile ring components, to the equatorial cortex. (B) *Lis1* mutant MEFs (*CreER; Lis1 hc/hc + 24 h TM*) undergoing vigorous cell shape oscillation with spindle/chromosome rocking. *Lis1* mutant MEFs displaying chromosome missegregation and failures in maintaining proper contractile ring contraction site. Dark black spots inside of the cells indicating chromosome sets. (Yellow arrowheads: initial accumulation of MRLC1, white arrows: final cleavage furrow positioning).

ingression site (Fig. 3-5 A). However, after acute deletion of *Lis1* in tamoxifen treated Cre-inducible *Lis1* mutant MEFs (*CreER; Lis1^{hc/hc}, TM 24 h*), SEPT6 was initially observed at the equatorial cortex at anaphase onset but then regressed away, and weak SEPT6 accumulation was observed at the cell equator accompanied by vigorous cortical deformation and chromosome oscillation/rocking (chromosomes were identified as darker spots in the SEPT6-GFP background) (Fig. 3-5 B). Taken together, these results indicate that the contractile ring components were not retained properly at the equatorial cortex, similar to actomyosin defects, resulting in cytokinetic failure in *Lis1*-depleted MEFs.

3.3 Discussion

LIS1, a novel regulatory factor in cytokinesis

In this study, we demonstrate that mouse LIS1 is essential for the precise separation of cytosolic components during cytokinesis and cell division. In mammalian cells, LIS1 has been implicated mitotic spindle regulation in the cell cycle from metaphase to anaphase (Faulkner et al., 2000; Yingling et al., 2008) and its function has been extensively studied in post-mitotic neurons during neuronal migration in neurodevelopment (Gambello et al., 2003; Hirotsune et al., 1998; Sasaki et al., 2000; Tsai et al., 2005). However, additional roles of LIS1 during cytokinesis have not been examined, when cooperative interaction between two cytoskeletal components – MTs and actomyosin – are crucial for the appropriate separation of two daughter cells. We found that *Lis1* mutant MEFs displayed a profound delay in cytokinesis and consequently displayed failure of cytokinesis, accompanied by binucleation of two chromosome sets in one cell and concomitant cell death in the other anucleated cell. The frequency of both incomplete cytokinesis and binucleation was significantly increased approximately 6-fold in *Lis1* mutant MEFs compared to WT MEFs, suggesting that LIS1 is essential for accurate cytokinesis.

We also observed cell shape oscillations and vigorous rocking of chromosomes /spindle phenotype in *Lis1* mutant MEFs from timelapse live-imaging analysis experiments, similar to those of anillin-depleted cells (Echard et al., 2004; Kechad et al., 2012; Piekny and Glotzer, 2008; Straight et al., 2003; Zhao and Fang, 2005). This implies that *Lis1* mutant MEFs have defective positioning of the cleavage furrow outside of the cell equator and failure in the recruitment of contractile ring components to the equatorial cortex. Intriguingly, severe cell shape oscillation and cytokinetic defects were also reported from nocodazole (MT-depolymerizing reagent)-treated cells (Canman et al., 2003), suggesting that misregulation of either MTs or the MT-actomyosin interface at the cell cortex in *Lis1* mutant MEFs may cause hyper-contractility to provoke abnormal cortical contraction (cell shape oscillation) in *Lis1* mutant MEFs.

LIS1 regulates RhoA-actomyosin signaling pathway and contractile ring components

To investigate the cellular mechanisms regulated by LIS1, we examined other key molecules known to act in cytokinesis such as RhoA and its downstream effectors, including contractile ring components and actomyosin. We found that RhoA and anillin, a contractile ring component, were mislocalized in *Lis1* mutant MEFs. RhoA was detected at the cell cortex of large membrane blebs at ectopic sites in the binucleated *Lis1* mutant MEFs. The myosin II-positive zone and F-actin (phalloiding staining) focusing zone were dispersed at the equatorial cortex or aberrantly located at the polar blebs in *Lis1* mutants. Taken together, these results support the requirement of LIS1 to restrict the cleavage furrow at the equatorial cortex and finely modulate the RhoA-anillin-actomyosin signaling pathway. By performing timelapse live-imaging of MRLC1, myosin subunit consisting of actomyosin fibers and SEPT6, a contractile ring component, we confirmed that LIS1 controls cleavage furrow positioning by regulating both actomyosin and contractile ring movements in the early phases of cytokinesis.

Previously, *Lis1* heterozygous neurons were found to display impairment of F-actin in the leading processes and perturbed GTPase activities of RhoA-Rac1-Cdc42, important regulators of

the actin cytoskeleton during early development. *Lis1*^{+/-} MEFs also displayed abnormal activation of GTPase activities; RhoA was hyperactivated about 3-fold increase in GTPase activity assays in *Lis1*^{+/-} MEFs compared to WT MEFs, while Rac1 and Cdc42 activities were suppressed about 2-fold (Kholmanskikh et al., 2003). Further, LIS1 interacts with a CLIP170/IQGAP/Cdc42 complex at the MT plus-end tips (Kholmanskikh et al., 2006). These results indicate that LIS1 may regulate not only MTs but F-actin dynamics in many cell types. Therefore, based on the severe cytokinetic defects in *Lis1* mutant MEFs, the loss of LIS1 protein may result in hyperactive RhoA signaling to transmit an abnormal signal to actomyosin to generate hyper-contractility forces on the ectopic polar cortex, which is not a normal site of cytokinetic furrow ingression.

LIS1-RhoA-actomyosin signaling pathway: implications for neural progenitor cell division and lissencephaly

Here we demonstrate that mouse LIS1 deficiency causes interference in actomyosin distribution, hyper-contractility from abnormal cortical constriction, and misplacement of the cleavage furrow outside of the cell equator. Furthermore, RhoA, a key regulator of cytokinesis was mislocalized at the ectopic membrane bulges and contractile components (anillin and septin) were not retained at the equatorial cortex in *Lis1*-deficient MEFs during cytokinesis. Collectively, these findings imply that LIS1 may participate in the RhoA-actomyosin-contractile ring signal transduction pathway crucial for completion of cytokinesis. In addition, the previous report of dysregulated RhoA GTPase activity in *Lis1* heterozygous neurons and MEFs is consistent with the idea that LIS1 may normally suppress RhoA GTPase activity and inhibit hyper-activation of actomyosin during cytokinesis for proper cell division.

Recently, several studies demonstrated that mouse RhoA GTPase plays diverse roles in early neurodevelopment by regulating neural progenitor zone integrity mainly through F-actin at adherens junction (Cappello et al., 2012; Herzog et al., 2011; Katayama et al., 2011). In chicken neural tube development, changes in RhoA activity and overexpression of a dominant negative

form of RhoA alter spindle orientation of chick neural progenitors (Roszko et al., 2006). These results suggest that the spatiotemporal control of active RhoA-GTP is critical for normal neural progenitor function and cell division during neurodevelopment. However, it is unknown whether RhoA-mediated actomyosin regulation contributes to specific mitotic cell division process such as cytokinesis when cytosolic cell separation occurs with segregation of the cell fate determinants. Since mouse LIS1 has been implicated proper spindle formation and cell survival of neural progenitors (Yingling et al., 2008), it would be important to test whether the LIS1-RhoA-actomyosin pathway critical for cytokinesis in this particular study also participates in neural progenitor behavior and maintenance during brain development.

Thus far, cleavage plane specification in mouse neural progenitor is largely unexplored. There have been only a few studies demonstrating the importance of the presence of contractile ring components during neural progenitor division. It appears that anillin-ring constriction from the basal to apical side determines the cleavage furrow ingression site in mouse neural progenitors (Kosodo et al., 2008). Colocalization of citron kinase and RhoA at the apical neural progenitor zone in developing rodent brain has been reported (Di Cunto et al., 2000; Sarkisian et al., 2002). LIS1, as an important mediator of RhoA-actomyosin-contractile ring components signaling, may be a novel regulator of cytokinesis during normal brain development. In addition, further extensive studies on lissencephaly-causing gene acting in actin-MT-regulatory pathway may help explain the versatile function of these genes, like LIS1, that have dual roles in actomyosin cytoskeletal regulation important for neural progenitor maintenance as well as cell division and cytokinesis.

Chapter 4. Conclusions

4-1. Cytoskeletal regulation of microtubules and actin by lissencephaly-causing genes.

During neocortical development, the extensive migratory movements of neurons from their place of birth to their final location are essential for the coordinated wiring of synaptic circuits and proper neurological function. Failure or delay in neuronal migration causes severe abnormalities in cortical layering, which consequently results in human lissencephaly ('smooth brain'), a neuronal migration disorder. The brains of lissencephaly patients have less-convoluted gyri in the cerebral cortex with impaired cortical lamination of neurons. Since microtubule (MT) and actin-associated proteins play important functions in regulating the dynamics of MT and actin cytoskeletons during neuronal migration, genetic mutations or deletions of crucial genes involved in cytoskeletal processes lead to lissencephaly in human and neuronal migration defects in mouse. During neuronal migration, MT organization and transport are controlled by platelet-activating factor acetylhydrolase isoform 1b regulatory subunit 1 (PAFAH1B1, formerly known as LIS1, Lissencephaly-1), doublecortin (DCX), YWHAE, and tubulin. Actin stress fibers are modulated by PAFAH1B1 (LIS1), DCX, RELN, and VLDLR (very low-density lipoprotein receptor)/LRP8 (low-density lipoprotein-related receptor 8, formerly known as APOER2). There are several important levels of crosstalk between these two cytoskeletal systems to establish accurate cortical patterning in development. The recent understanding of the protein networks that govern neuronal migration by regulating cytoskeletal dynamics, from human and mouse genetics as well as molecular and cellular analyses, provides new insights on neuronal migration disorders and may help us devise novel therapeutic strategies for such brain malformations.

4-2. Mouse LIS1 is required for maintaining normal centrosome number and proper mitotic spindle orientation during mitotic cell division.

Heterozygous *LIS1* mutations are responsible for the human neuronal migration disorder lissencephaly. Mitotic functions of LIS1 have been suggested from many organisms throughout evolution. However, the specific cellular processes regulated by LIS1 during mitotic cell division remain to be elucidated. Here we show that time-lapse live cell imaging of mitosis from *Lis1* mutant MEFs revealed that LIS1 is required for tight control of chromosome congression and segregation to ensure kinetochore-MT interactions and anaphase progression. LIS1 is also essential for the establishment of mitotic spindle pole integrity by maintaining normal centrosome number. LIS1 plays crucial roles in mitotic spindle positioning and orientation by inducing astral MT plus-end movements toward the cell cortex, which enhances cortical targeting of LIS1-NDE1/NDEL1-dynein complex. Thus, we demonstrate that mouse LIS1 is a key component of LIS1-NDE1/NDEL1-dynein protein complex that is required for mitotic spindle regulation to establish contacts of MTs between centrosomes and the cell cortex to ensure proper cell division.

4-3. LIS1 integrates RhoA-actomyosin-contractile ring component signaling to restrict the cleavage furrow positioning at the equatorial cortex during cytokinesis.

Cytokinesis, the final step of cell division, is critical for the ultimate accurate segregation of chromosomes and cytosolic proteins into two daughter cells. Inappropriate cytokinesis results in genetic instability by promoting chromosome missegregation and aberrant cell division from altered inheritance of cell fate determinants. We performed timelapse live-imaging of mitotic cell division of mouse embryonic fibroblasts (MEFs) and found that *Lis1* (*Lissencephaly-1*) mutant MEFs displayed a high frequency of cytokinesis failure compared to control wild-type (WT) MEFs. Specifically, *Lis1* deficiency induced binucleation of daughter cells and concomitant cell death. During cytokinesis of *Lis1* mutant MEFs, actomyosin components including filamentous actin (F-actin) and myosin-II were not concentrated at the spindle midzone and often mislocalized at ectopic membrane sites of blebbing, reflecting hyper-contractility at the cell cortex. *Lis1* mutant MEFs displayed misregulation of the RhoA-actomyosin-contractile ring signaling

pathway that restricts the cleavage furrow ingression site at the equatorial cortex at the cell equator between two daughter cells. We demonstrate that mouse LIS1 is an important regulator functioning in RhoA-actomyosin-contractile ring component regulatory pathway to finely control cytokinesis during cell division.

4-4. Conclusions

In summary, we concluded that various proteins acting in MT-actin cytoskeletal regulatory pathways execute key functions in migratory cellular processes during neuronal migration in early development. Post-mitotic neurons have an extended leading process enriched with F-actin and MT bundles undergoing dynamic contacts with the migrating substrate (glial fiber or cell adhesion sites). During migration, the nuclei of these cells undergo extensive nucleokinesis (N-C coupling) driven by pulling and pushing forces from MT networks and F-actin fibers. Complicated protein networks participate in controlling dynamics of MTs and F-actin in neuronal migration. Thus, deleterious mutation or deletion of these genes has drastic effects on normal brain development, consequently leading to lissencephaly.

Among lissencephaly-causing genes, *LIS1* is the first human gene known to be responsible for the Type-1 lissencephaly and ILS. LIS1 has been identified as an important dynein-MT regulator to modulate primarily MT dynamics. In this study, we uncovered molecular mechanisms of LIS1 protein complex (with dynein/NDE1/NDEL1) to regulate dynein-MT-mediated link between astral MTs and the cell cortex during mitotic division. Spatiotemporal control of mitotic spindle by LIS1 is essential for mitotic cell cycle progression and cell separation.

Furthermore, we also proposed that LIS1 is indispensable for cytokinesis completion during the later stages of cell division. Since mouse LIS1 heterozygosity has been reported to result in misregulation of RhoA GTPase signaling pathway (with accumulation of hyperactive form of RhoA-GTP), the downstream effectors including actomyosin cytoskeleton and contractile ring components were mislocalized in genetic constitutive and acutely-deleted *Lis1* mutants. It

misleads to cytokinetic failure and impairment of cortical contractility with abnormal formation of ectopic blebs. It suggests that LIS1 is crucial for precise positioning of the cleavage furrow at the cell equatorial cortex during cytokinesis.

4-5. Implications

Many unanswered questions remain to understand the exact functions of LIS1 in neural progenitor (NP) cell division. The most obvious phenotype from LIS1 deficiency in human and mouse was reported in forebrain CNS development. Similarly, we previously demonstrated that the dividing NPs in the developing mouse from *Lis1* mutants displayed significant increases in both apoptotic cell death and mitotic spindle misorientation (Yingling et al., 2008). Although we found novel functions of LIS1 in mitotic spindle and centrosome regulation in MEFs, it is unknown whether the same mechanisms are responsible for the cell death of NPs during neurodevelopment. For example, loss-of-function of LGN (Leu-Gly-Asn-enriched protein) with knockdown and LGN-C terminal overexpression studies demonstrated severe mitotic spindle misregulation phenotypes in NPs without affecting cell survival of NPs in rodent brain development (Konno et al., 2008). This raises the question that mitotic spindle alteration by LIS1 may not be the only factor leading the failure of NP maintenance in the developing brain. A combined effect of loss of LIS1 on mitotic spindle misorientation and cytokinesis may together explain this severe NP phenotype. Conversely, LIS1 (or the LIS1 complex with NDE1/NDEL1/dynein) may specifically modulate additional pathways which LGN protein may not be involved in. It is possible that the actomyosin cytoskeleton under RhoA regulation (based on LIS1-dependent cytokinesis) may be an important part of the undiscovered pathways regulated by LIS1 in dividing NPs. In the future, it will be necessary to assess whether RhoA-actomyosin signaling is abnormally hyperactive by performing GTPase activity assay of RhoA from *Lis1* mutant NP pools. Since the downstream actomyosin signaling has not been carefully examined in *Lis1* mutant NPs, informative follow-up studies on LIS1-actomyosin regulations in NP cell

division could be suggested: (1) experiments that determine quantitatively F-actin content in NPs; (2) investigation of phosphorylated form of active myosin regulatory light chain (p-MRLC), an indicator of myosin constriction and elevation of RhoA-F-actin dynamics at the equatorial cortex (Matsumura et al., 2008); (3) modulation of RhoA-actomyosin pathway by introducing either dominant-negative forms of RhoA or constitutively-active form of antagonistically-acting Rac1/Cdc42 (Kholmanskikh et al., 2006) to rescue cytokinetic defects caused by LIS1 deficiency; (4) treatment with several potent inhibitors acting in RhoA-ROCK signaling pathway or myosin-II inhibitors (Kholmanskikh et al., 2003; Straight et al., 2003) to suppress hyperactive RhoA-actomyosin pathways if they cause cytokinetic failure of NPs.

On the other hand, it is also unclear whether dynein-dependent mechanisms play a role in LIS1-mediated cytokinesis in NPs. To test this possibility, it will be important to determine whether dynein inhibition by either overexpression of P50 dynamitin, a subunit of dynactin complex (Echeverri et al., 1996) or dynein knockdown mimics cytokinetic defects seen in *Lis1* mutant NPs. To distinguish whether LGN-dependent pathway contributes to LIS1-dynein-mediated cytokinetic phenotype, rescue experiments with overexpression of LGN in *Lis1* mutant NPs may be performed in the future.

The novel important findings from *in vivo* mouse *Lis1* mutants will provide a new avenue to identify the molecular networks (both *in vivo* and *in vitro*) functioning in actomyosin-cytokinesis pathways essential for NP survival and maintenance regulated potentially by other lissencephaly-causing genes.

Materials and Methods

Mice

Lis1 null (*Lis1*^{ko}, formerly referred as *Pafah1b1*^{tm1Awb}) and hypomorphic conditional knock-out (*Lis1*^{hc}, formerly referred as *Pafah1b1*^{tm2Awb(loxp)}) alleles were used, which were described previously (Hirotsune et al., 1998, Yingling et al., 2008). To induce Cre recombinase activation to delete *Lis1* conditional allele, the TM-inducible *CreER*TM line (Hayashi and McMahon, 2002) was used to mate with *Lis1* mutant mice.

Cell culture

Primary mouse embryonic fibroblasts (MEFs) were derived from E14.5 embryos and were cultured in DMEM (Mediatech) supplemented with 12.5% FBS (Gibco), penicillin/streptomycin and L-glutamine at 37°C in a 5% CO₂ incubator. All MEFs used in this study were less than passage 4 (Yingling et al., 2008). *CreER*TM recombinase activity was induced by administering 4-hydroxy tamoxifen (Sigma, 100 nM) dissolved in culture media. H293T cells for viral packaging were maintained in 10% FBS (Gibco) in DMEM medium (Mediatech).

Retrovirus production and MEF infection

To produce retroviruses, pMV-GP (gag, pol), pCMV-G (VSV-G env), and pCX retroviral vectors were purified by Endofree Plasmid Maxiprep kit (Qiagen) and transfected in H293T cells with TransIT-LT1 transfection reagent (Mirus). Packaging vectors (pMV-GP, pCMV-G) were gifts from Atsushi Miyano-hara (UCSD). pCLNR-H2BG (H2B-GFP) was a gift from Geoffrey Wahl (Salk institute, Addgene plasmid #17735). To construct pCX-mCherry- α -tubulin retroviral vector, cDNA of mCherry was amplified by PCR from pcDNA3.1-mCherry derived from an

mCherry expression vector (a gift from Roger Tsien, UCSD). The mCherry cDNA PCR product was subcloned into pEGFP- α -tubulin (Clontech) digested with Sall/NotI to generate mCherry- α -tubulin. Then, the PCR product of cDNA encoding mCherry- α -tubulin was ligated into the linearized pCX backbone vector derived from pCX-Centrin2-DsRed (gift from Joseph Gleeson, UCSD) with BamHI/PacI. Other GFP-fusion proteins used for rescue experiments (pCX-GFP-LIS1, pCX-GFP-NDEL1, pCX-GFP-NDE1 and pCX-GFP-DIC1) were generated by cDNA amplification from mammalian expression vectors pCMV-GFP-NDEL1 (described in Toyooka et al., 2003), pCMV-GFP-LIS1, pCMV-GFP-NDE1 (gifts from Shinji Hirotsune, Osaka City University, Japan, described in Sasaki et al., 2005) and pCMV-GFP-DIC1 (gifts from Shinji Hirotsune, described in Yamada et al., 2008), followed by BamHI/PacI digestion for cloning into the pCX retroviral vector. Viral supernatants (in DMEM without antibiotics and FBS) were collected at 48 h post-transfection and filtered through 0.45 μ m filter (Sartorius). MEFs were infected with retrovirus by co-incubating the mixture of viral supernatant and fresh media for 24 h. During infection, 12.5% FBS was supplemented in the viral supernatant media along with 4 μ g/mL polybrene (Sigma).

Western blotting

MEFs were lysed in Tris-Triton buffer (10 mM Tris pH 7.4, 100 mM NaCl, 1 mM EDTA, 1 mM EGTA, 1% Triton X-100, 10% glycerol, 0.1% SDS, 0.5% deoxycholate) with protease/phosphatase inhibitors. Lysates were collected on ice and centrifuged. Supernatants with protein extracts were transferred into new tubes, boiled at 95°C for 5min, then stored at -20°C before use. Protein concentrations were determined by the BCA protein assay kit (Pierce) and equal amounts were loaded on a 10% SDS-PAGE resolving gel (Bio-Rad). After electrophoresis, proteins were transferred to a nitrocellulose membrane (Bio-Rad). The membrane was blocked in TBST (TBS with 0.1% Tween 20) with 2.5% skim milk for 1 h at RT and incubated with the

following primary antibodies at 4°C overnight: rabbit anti-LIS1 (1:1,000, a gift from Shinji Hirotsune), mouse anti- α -tubulin (Sigma, 1:8,000), mouse anti- β -actin (Sigma, 1:5,000). Secondary antibodies used were HRP-conjugated goat anti-rabbit and goat anti-mouse (Jackson Lab, 1:10,000) which were incubated for 1 h. Antibody binding was detected via the ECL kit (Pierce). Relative protein amount was measured using ImageJ software after background subtraction.

Immunocytochemistry

MEFs were grown on acid-washed and 0.2% gelatin (Millipore)-coated glass coverslips and fixed with 4% PFA in PBS for 20 min. For centrosomal protein immunostaining and EB1 staining, MEFs were fixed with -20°C cold methanol for 2 min. 2.5% normal goat serum (or FBS) and 0.1% Triton X-100 in PBS was used for blocking for 1 h at RT. The primary antibodies were diluted in blocking buffer and incubated overnight at 4°C. The primary antibodies used were: rabbit anti-LIS1 (Abcam, 1:250); mouse anti- α -tubulin (Sigma, 1:500); rat anti- α -tubulin (AbD Serotec, 1:1,000); mouse anti- γ -tubulin (Sigma, 1:500); rabbit anti-pericentrin (Covance, 1:1,000); rabbit anti-NDE1 (Proteintech, 1:250); rabbit anti-NDEL1 (Abcam, 1:250); mouse anti-p150^{Glued} (BD bioscience, 1:200); mouse anti-EB1 (BD bioscience, 1:200); mouse anti-GFP (Invitrogen, 1:400); rabbit anti-GFP (Invitrogen, 1:400); mouse anti-centrin (Millipore, 1:200); rabbit cennexin/ODF2 (Abcam, 1:200); rabbit anti-ninein (Abcam, 1:200); and rabbit anti-Cep164 (1:1000, a gift from Erich Nigg, University of Basel, Switzerland). The following goat secondary antibodies were incubated for 1 h at RT: anti-mouse AlexaFluor-488; anti-mouse AlexaFluor-594; anti-rabbit AlexaFluor-488; anti-rabbit AlexaFluor-568; anti-rat AlexaFluor-488; and anti-rat AlexaFluor-647 (Invitrogen). ProLong gold antifade reagent with DAPI (Invitrogen) was used to counterstain the nucleus and as mounting medium. All the fixed sample

images were captured using a Nikon C1si laser-scanning confocal microscope with a 60x 1.4 NA PlanApo oil objective lens (Nikon).

For visualization of astral MTs, MEFs were fixed in 0.25% glutaraldehyde in BRB80 buffer (80 mM PIPES pH 6.8, 1 mM MgCl₂, 1 mM EGTA) for 10 min, then treated with 0.2% sodium borohydride in PBS for 20 min, changing the borohydride solution two times. Primary rat anti- α -tubulin antibody was diluted in blocking buffer (2% FBS, 0.1% Triton X-100 in PBS). To visualize cortical dynactin p150^{Glued}, MEFs were pre-extracted with 0.5% Triton X-100 in PHEM buffer (120 mM PIPES, 50 mM HEPES, 20 mM EGTA, 8 mM MgSO₄) with 5 μ M taxol (Sigma) for 1 min and then fixed with -20°C cold methanol for 2 min.

Mitotic spindle analysis and cell shape analysis

For analysis of the mitotic spindle, MEFs were arrested in metaphase by treatment with proteasome inhibitor, 10 μ M MG132 (EMD biosciences) for 2 h. From the coverslips of MEFs, a series of Z stack images (0.5 μ m apart) of metaphase mitotic spindles stained with anti-pericentrin, anti- α -tubulin antibodies were obtained using the Nikon C1si laser-scanning confocal microscope (Biological Imaging Development Center, UCSF). The linear (x-y plane) and vertical (z-axis) distance between spindle poles was measured from Nikon EZ-C1 imaging software.

Mitotic spindle length (D) and spindle angles (α°) were calculated by 3D trigonometric functions.

The drug treatment in MEFs was performed in following condition : 1 μ M taxol (Sigma) were added to the medium and incubated for 30 min after the treatment of 10 μ M MG132 for 2 h. Cell shape was analyzed from the MEFs incubated with lipophilic dye, DHCC (3,3'-dihexyoxacarbocyanine iodide, Sigma) for 10 min then treated with 10 μ M MG132 for 2 h.

Kinetochores staining and quantification

MEFs were treated with 10 μ M nocodazole (Sigma) for 1 h under normal incubation conditions to accumulate proteins at the kinetochores. Then MEFs were fixed with -20°C cold methanol for 2 min. Confocal images were obtained from an Olympus FV1000 laser scanning confocal microscope. From each genotype, 10 cells were analyzed and compared in softWoRx Explorer (Applied Precision) using 10X10 window in Data Inspector. Interkinetochore distance was determined using the line segment tool across Z-stacks. The total immunofluorescence of 10 kinetochores was averaged for each cell. Primary antibodies were: goat anti-LIS1 (Abcam, 1:200); mouse anti-p150^{glued} (BD bioscience, 1:200); rabbit anti-CLIP170 (Holly Goodson, University of Norte Dame, 1:200); mouse anti-DIC70.1 (Sigma, 1:25); human SH-CREST autoimmune serum (a gift from William Brinkley, Baylor College of Medicine, 1:10,000); and Mad2 (a gift from Don Cleveland, UCSD, 1:200). Secondary antibodies were: donkey anti-rabbit FITC; donkey anti-goat Cy3; donkey anti-human Cy2, and donkey anti-human Cy3 (Jackson Laboratory).

Time-lapse live cell imaging

Glass-bottom 6 well tissue culture plates (MatTek) were used for live cell imaging of mitosis. The plates were pre-incubated with 0.2% gelatin (Millipore) solution before plating MEFs on glass-bottom dishes 24 h prior to live cell imaging. Retroviruses were transduced into primary MEFs by co-incubating with viral supernatants for 24 h. 4-hydroxy TM (100 nM, Sigma) was used for 12 h for *CreERTM* for Cre transgene activation. MEFs expressing both H2B-GFP and mCherry- α -tubulin retroviruses were recorded with a time-lapse Nikon Ti microscope equipped with 5% CO₂ and a 37°C temperature-controlled chamber (Nikon imaging center, UCSF). To monitor long-term mitosis of MEFs, multiple points were selected for acquiring each fluorescence image (GFP/mCherry) with a motorized stage and perfect focus function. Fluorescence was captured with a Coolsnap camera (Roper Scientific) with exposure time of 100 msec for GFP and 200

msec for mCherry. Time-lapse images of cell division were taken every 1 min (up to 12 h). Filters and multipoint scanning were controlled by NIS-Element imaging software (Nikon).

Tracking EB1-GFP

EB1-GFP was amplified using oligos (fwd: caccatggcagtgaacgtataactca and rev: ttactgtacagctcgtccat) and inserted into pTOPO vector and subsequently cloned into pAd/CMV/V5-DEST with Gateway cloning (Invitrogen). Adenovirus particles were purified as described previously (Kumar et al., 2009). 1 μ l of EB1-GFP adenovirus was added to MEF growth media 24 h prior to imaging. Cells were treated with 9 μ M RO-3306 (EMD bioscience), a CDK1 inhibitor, for 18 h to arrest cells at the G2/M transition of the cell cycle. Mitosis of MEFs was imaged after drug release by changing to fresh media containing 20 mM HEPES (Sigma).

EB1-GFP protein dynamics were imaged at 37°C with a 100X NA 1.49 oil-immersed objective lens (CFI Apo TIRF, Nikon) equipped with a spinning-disk confocal scanning unit (Borealis-modified CSU-X1, Spectral Applied Research) using a Nikon Ti microscope (Nikon) with a 488nm laser, electronic shutters, a cool charged-coupled device camera (CoolSnap HQ, Photometrics), and controlled by NIS-Elements software (Nikon). MT plus-ends were tracked in time-lapse images from EB1-GFP expressing MEFs acquired every 30 s using perfect focus function. Three sections of Z stacks (2 μ m apart) were acquired at every time point.

Retrovirus plasmid construction for cytokinesis study

pCLNR-H2BG was a gift from Geoffrey Wahl (Salk institute, Addgene plasmid #17735). pCX-mCherry- α -tubulin was described previously. SEPT6-GFP was amplified from pEGFP-SEPT6, a gift from Matthew Krummel (UCSF, previously described in Gildea et al., 2012) and subcloned into pCX retroviral vector to generate pCX-SEPT6-GFP. MRLC1-GFP was amplified from pEGFP-MRLC1, a gift from Tom Egelhoff (Cleveland Clinic, Addgene plasmid # 35680) and

subcloned into pCX to generate pCX-MRLC1-GFP. H2B encoding cDNA was amplified from pCLNR-H2BG and subcloned into pCX-tdTomato with BamHI to generate pCX-H2B-tdTomato. pCX-tdTomato was first cloned by shuttling tdTomato from pRSET-B-tdTomato plasmid (a gift from Roger Tsien, UCSD) by BamHI/PacI.

Immunocytochemistry of MEFs in cytokinesis

To identify RhoA in the cleavage furrow, MEFs were fixed with 10% trichloroacetic acid (TCA) for 10 min (Yonemura et al., 2004). The primary antibodies used for immunocytochemistry experiments were; Rat anti- α -tubulin (AbD Serotec, 1:1,000), mouse anti-RhoA (Santa Cruz, 1:500), rabbit anti-anillin (Santa Cruz, 1:250), rabbit anti-NMHCII-A (Covance, 1:1,000), rabbit anti-cleaved caspase3 (Cell Signaling, 1:500). The secondary antibodies were; Alexa Fluor 594- (or) 633-conjugated phalloidin (Invitrogen, 1:100) and Alexa Fluor 488-, 568-, 647- conjugated mouse, rabbit, rat antibodies (Invitrogen, 1:500).

Spinning-disk confocal timelapse live-imaging of myosin-II and septin6

Primary MEFs were co-infected a mixture of MRLC1-GFP and H2B-tdTomato retroviruses with 4 μ g/mL polybrene. Lasers with 488 nm and 561 nm emission were used for GFP and tdTomato live-imaging. SEPT6-GFP was also traced by Nikon Ti spinning-disk confocal microscope with 488 nm emission laser. The sequential 2 μ m interval 5~7 Z-stack images were captured every 30 sec. The best Z confocal plane images showing the cleavage furrow were made as timelapse movies.

References

- Alkuraya, F.S., X. Cai, C. Emery, G.H. Mochida, M.S. Al-Dosari, J.M. Felie, R.S. Hill, B.J. Barry, J.N. Partlow, G.G. Gascon, A. Kentab, M. Jan, R. Shaheen, Y. Feng, and C.A. Walsh. 2011. Human mutations in NDE1 cause extreme microcephaly with lissencephaly [corrected]. *Am J Hum Genet.* 88:536-547.
- Assadi, A.H., G. Zhang, U. Beffert, R.S. McNeil, A.L. Renfro, S. Niu, C.C. Quattrocchi, B.A. Antalffy, M. Sheldon, D.D. Armstrong, A. Wynshaw-Boris, J. Herz, G. D'Arcangelo, and G.D. Clark. 2003. Interaction of reelin signaling and *Lis1* in brain development. *Nat Genet.* 35:270-276.
- Aumais, J.P., J.R. Tunstead, R.S. McNeil, B.T. Schaar, S.K. McConnell, S.H. Lin, G.D. Clark, and L.Y. Yu-Lee. 2001. NudC associates with *Lis1* and the dynein motor at the leading pole of neurons. *J Neuroscience.* 21:RC187.
- Aumais, J.P., S.N. Williams, W. Luo, M. Nishino, K.A. Caldwell, G.A. Caldwell, S.H. Lin, and L.Y. Yu-Lee. 2003. Role for NudC, a dynein-associated nuclear movement protein, in mitosis and cytokinesis. *J Cell Sci.* 116:1991-2003.
- Bai, J., R.L. Ramos, J.B. Ackman, A.M. Thomas, R.V. Lee, and J.J. LoTurco. 2003. RNAi reveals doublecortin is required for radial migration in rat neocortex. *Nat Neuro.* 6:1277-1283.
- Bakircioglu, M., O.P. Carvalho, M. Khurshid, J.J. Cox, B. Tuysuz, T. Barak, S. Yilmaz, O. Caglayan, A. Dincer, A.K. Nicholas, O. Quarrell, K. Springell, G. Karbani, S. Malik, C. Gannon, E. Sheridan, M. Crosier, S.N. Lisgo, S. Lindsay, K. Bilguvar, F. Gergely, M. Gunel, and C.G. Woods. 2011. The essential role of centrosomal NDE1 in human cerebral cortex neurogenesis. *Am J Hum Genet.* 88:523-535.

- Basto, R., K. Brunk, T. Vinadogrova, N. Peel, A. Franz, A. Khodjakov, and J.W. Raff. 2008. Centrosome amplification can initiate tumorigenesis in flies. *Cell*. 133:1032-1042.
- Beach, J.R., G.S. Hussey, T.E. Miller, A. Chaudhury, P. Patel, J. Monslow, Q. Zheng, R.A. Keri, O. Reizes, A.R. Bresnick, P.H. Howe, and T.T. Egelhoff. 2011. Myosin II isoform switching mediates invasiveness after TGF-beta-induced epithelial-mesenchymal transition. *PNAS*. 108:17991-17996.
- Beffert, U., G. Morfini, H.H. Bock, H. Reyna, S.T. Brady, and J. Herz. 2002. Reelin-mediated signaling locally regulates protein kinase B/Akt and glycogen synthase kinase 3beta. *J Biol Chem*. 277:49958-49964.
- Bellion, A., J.P. Baudoin, C. Alvarez, M. Bornens, and C. Metin. 2005. Nucleokinesis in tangentially migrating neurons comprises two alternating phases: forward migration of the Golgi/centrosome associated with centrosome splitting and myosin contraction at the rear. *J Neurosci*. 25:5691-5699.
- Bement, W.M., H.A. Benink, and G. von Dassow. 2005. A microtubule-dependent zone of active RhoA during cleavage plane specification. *J Cell Biol*. 170:91-101.
- Berger, M.F., E. Hodis, T.P. Heffernan, Y.L. Deribe, M.S. Lawrence, A. Protopopov, E. Ivanova, I.R. Watson, E. Nickerson, P. Ghosh, H. Zhang, R. Zeid, X. Ren, K. Cibulskis, A.Y. Sivachenko, N. Wagle, A. Sucker, C. Sougnez, R. Onofrio, L. Ambrogio, D. Auclair, T. Fennell, S.L. Carter, Y. Drier, P. Stojanov, M.A. Singer, D. Voet, R. Jing, G. Saksena, J. Barretina, A.H. Ramos, T.J. Pugh, N. Stransky, M. Parkin, W. Winckler, S. Mahan, K. Ardlie, J. Baldwin, J. Wargo, D. Schadendorf, M. Meyerson, S.B. Gabriel, T.R. Golub, S.N. Wagner, E.S. Lander, G. Getz, L. Chin, and L.A. Garraway. 2012. Melanoma genome sequencing reveals frequent PREX2 mutations. *Nature*. 485:502-506.
- Bielas, S.L., F.F. Serneo, M. Chechlacz, T.J. Deerinck, G.A. Perkins, P.B. Allen, M.H. Ellisman, and J.G. Gleeson. 2007. Spinophilin facilitates dephosphorylation of doublecortin by PP1 to mediate microtubule bundling at the axonal wrist. *Cell*. 129:579-591.

- Bienvenu, T., K. Poirier, G. Friocourt, N. Bahi, D. Beaumont, F. Fauchereau, L. Ben Jeema, R. Zemni, M.C. Vinet, F. Francis, P. Couvert, M. Gomot, C. Moraine, H. van Bokhoven, V. Kalscheuer, S. Frints, J. Gecz, K. Ohzaki, H. Chaabouni, J.P. Fryns, V. Desportes, C. Beldjord, and J. Chelly. 2002. ARX, a novel Prd-class-homeobox gene highly expressed in the telencephalon, is mutated in X-linked mental retardation. *Hum Mol Genet.* 11:981-991.
- Bilguvar, K., A.K. Ozturk, A. Louvi, K.Y. Kwan, M. Choi, B. Tatli, D. Yalnizoglu, B. Tuysuz, A.O. Caglayan, S. Gokben, H. Kaymakcalan, T. Barak, M. Bakircioglu, K. Yasuno, W. Ho, S. Sanders, Y. Zhu, S. Yilmaz, A. Dincer, M.H. Johnson, R.A. Bronen, N. Kocer, H. Per, S. Mane, M.N. Pamir, C. Yalcinkaya, S. Kumandas, M. Topcu, M. Ozmen, N. Sestan, R.P. Lifton, M.W. State, and M. Gunel. 2010. Whole-exome sequencing identifies recessive WDR62 mutations in severe brain malformations. *Nature.* 467:207-210.
- Bonneau, D., A. Toutain, A. Laquerriere, S. Marret, P. Saugier-veber, M.A. Barthez, S. Radi, V. Biran-Mucignat, D. Rodriguez, and A. Gelot. 2002. X-linked lissencephaly with absent corpus callosum and ambiguous genitalia (XLAG): clinical, magnetic resonance imaging, and neuropathological findings. *Ann Neurol.* 51:340-349.
- Bornens, M. 2002. Centrosome composition and microtubule anchoring mechanisms. *Curr Opin Cell Biol.* 14:25-34.
- Busson, S., D. Dujardin, A. Moreau, J. Dompierre, and J.R. De Mey. 1998. Dynein and dynactin are localized to astral microtubules and at cortical sites in mitotic epithelial cells. *Curr Biol.* 8:541-544.
- Canman, J.C., L.A. Cameron, P.S. Maddox, A. Straight, J.S. Timnauer, T.J. Mitchison, G. Fang, T.M. Kapoor, and E.D. Salmon. 2003. Determining the position of the cell division plane. *Nature.* 424:1074-1078.
- Canman, J.C., D.B. Hoffman, and E.D. Salmon. 2000. The role of pre- and post-anaphase microtubules in the cytokinesis phase of the cell cycle. *Curr Biol.* 10:611-614.

- Cappello, S., C.R. Bohringer, M. Bergami, K.K. Conzelmann, A. Ghanem, G.S. Tomassy, P. Arlotta, M. Mainardi, M. Allegra, M. Caleo, J. van Hengel, C. Brakebusch, and M. Gotz. 2012. A radial glia-specific role of RhoA in double cortex formation. *Neuron*. 73:911-924.
- Cappello, S., P. Monzo, and R.B. Vallee. 2011. NudC is required for interkinetic nuclear migration and neuronal migration during neocortical development. *Dev Biol*. 357:326
- Cardoso, C., R.J. Leventer, H.L. Ward, K. Toyo-Oka, J. Chung, A. Gross, C.L. Martin, J. Allanson, D.T. Pilz, A.H. Olney, O.M. Mutchinick, S. Hirotsune, A. Wynshaw-Boris, W.B. Dobyns, and D.H. Ledbetter. 2003. Refinement of a 400-kb critical region allows genotypic differentiation between isolated lissencephaly, Miller-Dieker syndrome, and other phenotypes secondary to deletions of 17p13.3. *Am J Hum Genet*. 72:918-930.
- Caspi, M., R. Atlas, A. Kantor, T. Sapir, and O. Reiner. 2000. Interaction between LIS1 and doublecortin, two lissencephaly gene products. *Hum Mol Genet*. 9:2205-2213.
- Caviness, V.S., Jr. 1982. Neocortical histogenesis in normal and reeler mice: a developmental study based upon [3H]thymidine autoradiography. *Brain Res*. 256:293-302.
- Chong, S.S., S.D. Pack, A.V. Roschke, A. Tanigami, R. Carrozzo, A.C. Smith, W.B. Dobyns, and D.H. Ledbetter. 1997. A revision of the lissencephaly and Miller-Dieker syndrome critical regions in chromosome 17p13.3. *Hum Mol Genet*. 6:147-155.
- Colasante, G., A. Sessa, S. Crispi, R. Calogero, A. Mansouri, P. Collombat, and V. Broccoli. 2009. Arx acts as a regional key selector gene in the ventral telencephalon mainly through its transcriptional repression activity. *Dev Biol*. 334:59-71.
- Cooper, J.A. 2008. A mechanism for inside-out lamination in the neocortex. *Trends Neurosci*. 31:113-119.
- Coquelle, F.M., M. Caspi, F.P. Cordelieres, J.P. Dompierre, D.L. Dujardin, C. Koifman, P. Martin, C.C. Hoogenraad, A. Akhmanova, N. Galjart, J.R. De Mey, and O. Reiner. 2002. LIS1, CLIP-170's key to the dynein/dynactin pathway. *Mol Cell Biol*. 22:3089-3102.

- Coquelle, F.M., M. Caspi, F.P. Cordelieres, J.P. Dompierre, D.L. Dujardin, C. Koifman, P. Martin, C.C. Hoogenraad, A. Akhmanova, N. Galjart, J.R. De Mey, and O. Reiner. 2002. LIS1, CLIP-170's key to the dynein/dynactin pathway. *Mol Cell Biol.* 22:3089-3102.
- Corbo, J.C., T.A. Deuel, J.M. Long, P. LaPorte, E. Tsai, A. Wynshaw-Boris, and C.A. Walsh. 2002. Doublecortin is required in mice for lamination of the hippocampus but not the neocortex. *J Neurosci.* 22:7548-7557.
- D'Arcangelo, G., R. Homayouni, L. Keshvara, D.S. Rice, M. Sheldon, and T. Curran. 1999. Reelin is a ligand for lipoprotein receptors. *Neuron.* 24:471-479.
- D'Arcangelo, G., G.G. Miao, S.C. Chen, H.D. Soares, J.I. Morgan, and T. Curran. 1995. A protein related to extracellular matrix proteins deleted in the mouse mutant reeler. *Nature.* 374:719-723.
- D'Avino, P.P., T. Takeda, L. Capalbo, W. Zhang, K.S. Lilley, E.D. Laue, and D.M. Glover. 2008. Interaction between Anillin and RacGAP50C connects the actomyosin contractile ring with spindle microtubules at the cell division site. *J Cell Sci.* 121:1151-1158.
- Derewenda, U., C. Tarricone, W.C. Choi, D.R. Cooper, S. Lukasik, F. Perrina, A. Tripathy, M.H. Kim, D.S. Cafiso, A. Musacchio, and Z.S. Derewenda. 2007. The structure of the coiled-coil domain of Ndel1 and the basis of its interaction with Lis1, the causal protein of Miller-Dieker lissencephaly. *Structure.* 15:1467-1481.
- des Portes, V., J.M. Pinard, P. Billuart, M.C. Vinet, A. Koulakoff, A. Carrie, A. Gelot, E. Dupuis, J. Motte, Y. Berwald-Netter, M. Catala, A. Kahn, C. Beldjord, and J. Chelly. 1998. A novel CNS gene required for neuronal migration and involved in X-linked subcortical laminar heterotopia and lissencephaly syndrome. *Cell.* 92:51-61.
- Deuel, T.A., J.S. Liu, J.C. Corbo, S.Y. Yoo, L.B. Rorke-Adams, and C.A. Walsh. 2006. Genetic interactions between doublecortin and doublecortin-like kinase in neuronal migration and axon outgrowth. *Neuron.* 49:41-53.

- Di Cunto, F., S. Imarisio, E. Hirsch, V. Broccoli, A. Bulfone, A. Migheli, C. Atzori, E. Turco, R. Triolo, G.P. Dotto, L. Silengo, and F. Altruda. 2000. Defective neurogenesis in citron kinase knockout mice by altered cytokinesis and massive apoptosis. *Neuron*. 28:115-127.
- Dobyns, W.B., O. Reiner, R. Carrozzo, and D.H. Ledbetter. 1993. Lissencephaly. A human brain malformation associated with deletion of the LIS1 gene located at chromosome 17p13. *JAMA*. 270:2838-2842.
- Doxsey, S., D. McCollum, and W. Theurkauf. 2005. Centrosomes in cellular regulation. *Annu Rev Cell Dev Biol*. 21:411-434.
- Draviam, V.M., I. Shapiro, B. Aldridge, and P.K. Sorger. 2006. Misorientation and reduced stretching of aligned sister kinetochores promote chromosome missegregation in EB1- or APC-depleted cells. *EMBO J*. 25:2814-2827.
- Dujardin, D.L., and R.B. Vallee. 2002. Dynein at the cortex. *Curr Opin Cell Biol*. 14:44-49.
- Dulabon, L., E.C. Olson, M.G. Taglienti, S. Eisenhuth, B. McGrath, C.A. Walsh, J.A. Kreidberg, and E.S. Anton. 2000. Reelin binds alpha3beta1 integrin and inhibits neuronal migration. *Neuron*. 27:33-44.
- Echard, A., G.R. Hickson, E. Foley, and P.H. O'Farrell. 2004. Terminal cytokinesis events uncovered after an RNAi screen. *Curr Biol*. 14:1685-1693.
- Echeverri, C.J., B.M. Paschal, K.T. Vaughan, and R.B. Vallee. 1996. Molecular characterization of the 50-kD subunit of dynactin reveals function for the complex in chromosome alignment and spindle organization during mitosis. *J Cell Biol*. 132:617-633.
- Efimov, V.P., and N.R. Morris. 2000. The LIS1-related NUDF protein of *Aspergillus nidulans* interacts with the coiled-coil domain of the NUDE/RO11 protein. *J Cell Biol*. 150:681-688.
- Egan, M.J., K. Tan, and S.L. Reck-Peterson. 2012. Lis1 is an initiation factor for dynein-driven organelle transport. *J Cell Biol*. 197:971-982.

- Eggert, U.S., T.J. Mitchison, and C.M. Field. 2006. Animal cytokinesis: from parts list to mechanisms. *Annu Rev Biochem.* 75:543-566.
- Faulkner, N.E., D.L. Dujardin, C.Y. Tai, K.T. Vaughan, C.B. O'Connell, Y. Wang, and R.B. Vallee. 2000. A role for the lissencephaly gene LIS1 in mitosis and cytoplasmic dynein function. *Nat Cell Biol.* 2:784-791.
- Feller, S.M. 2001. Crk family adaptors-signalling complex formation and biological roles. *Oncogene.* 20:6348-6371.
- Feng, Y., E.C. Olson, P.T. Stukenberg, L.A. Flanagan, M.W. Kirschner, and C.A. Walsh. 2000. LIS1 regulates CNS lamination by interacting with mNudE, a central component of the centrosome. *Neuron.* 28:665-679.
- Feng, Y., and C.A. Walsh. 2004. Mitotic spindle regulation by Nde1 controls cerebral cortical size. *Neuron.* 44:279-293.
- Fink, J., N. Carpi, T. Betz, A. Betard, M. Chebah, A. Azioune, M. Bornens, C. Sykes, L. Fetler, D. Cuvelier, and M. Piel. 2011. External forces control mitotic spindle positioning. *Nat Cell Biol.* 13:771-778.
- Fleck, M.W., S. Hirotsune, M.J. Gambello, E. Phillips-Tansey, G. Soares, R.F. Mervis, A. Wynshaw-Boris, and C.J. McBain. 2000. Hippocampal abnormalities and enhanced excitability in a murine model of human lissencephaly. *J Neurosci.* 20:2439-2450.
- Foe, V.E., and G. von Dassow. 2008. Stable and dynamic microtubules coordinately shape the myosin activation zone during cytokinetic furrow formation. *J Cell Biol.* 183:457-470.
- Friocourt, G., P. Marcorelles, P. Saugier-veber, M.L. Quille, S. Marret, and A. Laquerriere. 2011. Role of cytoskeletal abnormalities in the neuropathology and pathophysiology of type I lissencephaly. *Acta Neuropathol.* 121:149-170.
- Frotscher, M. 1998. Cajal-Retzius cells, Reelin, and the formation of layers. *Curr Opin Neurobiol.* 8:570-575.

- Fukasawa, K. 2011. Aberrant activation of cell cycle regulators, centrosome amplification, and mitotic defects. *Hormones & cancer*. 2:104-112.
- Fulp, C.T., G. Cho, E.D. Marsh, I.M. Nasrallah, P.A. Labosky, and J.A. Golden. 2008. Identification of Arx transcriptional targets in the developing basal forebrain. *Hum Mol Genet*. 17:3740-3760.
- Gambello, M.J., D.L. Darling, J. Yingling, T. Tanaka, J.G. Gleeson, and A. Wynshaw-Boris. 2003. Multiple dose-dependent effects of Lis1 on cerebral cortical development. *J Neurosci*. 23:1719-1729.
- Ganem, N.J., S.A. Godinho, and D. Pellman. 2009. A mechanism linking extra centrosomes to chromosomal instability. *Nature*. 460:278-282.
- Gdalyahu, A., I. Ghosh, T. Levy, T. Sapir, S. Sapoznik, Y. Fishler, D. Azoulai, and O. Reiner. 2004. DCX, a new mediator of the JNK pathway. *EMBO J*. 23:823-832.
- Gilden, J.K., S. Peck, Y.C. Chen, and M.F. Krummel. 2012. The septin cytoskeleton facilitates membrane retraction during motility and blebbing. *J Cell Biol*. 196:103-114.
- Gleeson, J.G., K.M. Allen, J.W. Fox, E.D. Lamperti, S. Berkovic, I. Scheffer, E.C. Cooper, W.B. Dobyns, S.R. Minnerath, M.E. Ross, and C.A. Walsh. 1998. Doublecortin, a brain-specific gene mutated in human X-linked lissencephaly and double cortex syndrome, encodes a putative signaling protein. *Cell*. 92:63-72.
- Glotzer, M. 1996. Mitosis: don't get mad, get even. *Curr Biol*. 6:1592-1594.
- Glotzer, M. 2005. The molecular requirements for cytokinesis. *Science*. 307:1735-1739.
- Glotzer, M. 2009. The 3Ms of central spindle assembly: microtubules, motors and MAPs. *Nat Rev Mol Cell Biol*. 10:9-20.
- Gonczy, P. 2002. Mechanisms of spindle positioning: focus on flies and worms. *Trends Cell Biol*. 12:332-339.
- Gonzalez-Billault, C., J.A. Del Rio, J.M. Urena, E.M. Jimenez-Mateos, M.J. Barallobre, M. Pascual, L. Pujadas, S. Simo, A.L. Torre, R. Gavin, F. Wandosell, E. Soriano, and J.

- Avila. 2005. A role of MAP1B in Reelin-dependent neuronal migration. *Cereb Cortex*. 15:1134-1145.
- Graser, S., Y.D. Stierhof, S.B. Lavoie, O.S. Gassner, S. Lamla, M. Le Clech, and E.A. Nigg. 2007. Cep164, a novel centriole appendage protein required for primary cilium formation. *J Cell Biol*. 179:321-330.
- Gregory, S.L., S. Ebrahimi, J. Milverton, W.M. Jones, A. Bejsovec, and R. Saint. 2008. Cell division requires a direct link between microtubule-bound RacGAP and Anillin in the contractile ring. *Curr Biol*. 18:25-29.
- Gupta, A., L.H. Tsai, and A. Wynshaw-Boris. 2002. Life is a journey: a genetic look at neocortical development. *Nat Rev Genet*. 3:342-355.
- Gusnowski, E.M., and M. Srayko. 2011. Visualization of dynein-dependent microtubule gliding at the cell cortex: implications for spindle positioning. *J Cell Biol*. 194:377-386.
- Han, G., B. Liu, J. Zhang, W. Zuo, N.R. Morris, and X. Xiang. 2001. The *Aspergillus* cytoplasmic dynein heavy chain and NUDF localize to microtubule ends and affect microtubule dynamics. *Curr Biol*. 11:719-724.
- Hattori, M., H. Adachi, M. Tsujimoto, H. Arai, and K. Inoue. 1994. Miller-Dieker lissencephaly gene encodes a subunit of brain platelet-activating factor acetylhydrolase [corrected]. *Nature*. 370:216-218.
- Hayashi, S., and A.P. McMahon. 2002. Efficient recombination in diverse tissues by a tamoxifen-inducible form of Cre: a tool for temporally regulated gene activation/inactivation in the mouse. *Dev Biol*. 244:305-318.
- Hendricks, A.G., J.E. Lazarus, E. Perlson, M.K. Gardner, D.J. Odde, Y.E. Goldman, and E.L. Holzbaur. 2012. Dynein tethers and stabilizes dynamic microtubule plus ends. *Curr Biol*. 22:632-637.

- Herzog, D., P. Loetscher, J. van Hengel, S. Knusel, C. Brakebusch, V. Taylor, U. Suter, and J.B. Relvas. 2011. The small GTPase RhoA is required to maintain spinal cord neuroepithelium organization and the neural stem cell pool. *J Neurosci.* 31:5120-5130.
- Hiesberger, T., M. Trommsdorff, B.W. Howell, A. Goffinet, M.C. Mumby, J.A. Cooper, and J. Herz. 1999. Direct binding of Reelin to VLDL receptor and ApoE receptor 2 induces tyrosine phosphorylation of disabled-1 and modulates tau phosphorylation. *Neuron.* 24:481-489.
- Hippenmeyer, S., Y.H. Youn, H.M. Moon, K. Miyamichi, H. Zong, A. Wynshaw-Boris, and L. Luo. 2010. Genetic mosaic dissection of *Lis1* and *Ndel1* in neuronal migration. *Neuron.* 68:695-709.
- Hirotsune, S., M.W. Fleck, M.J. Gambello, G.J. Bix, A. Chen, G.D. Clark, D.H. Ledbetter, C.J. McBain, and A. Wynshaw-Boris. 1998. Graded reduction of *Pafah1b1* (*Lis1*) activity results in neuronal migration defects and early embryonic lethality. *Nat Genet.* 19:333-339.
- Holland, A.J., and D.W. Cleveland. 2009. Boveri revisited: chromosomal instability, aneuploidy and tumorigenesis. *Nat Rev Mol Cell Biol.* 10:478-487.
- Hong, S.E., Y.Y. Shugart, D.T. Huang, S.A. Shahwan, P.E. Grant, J.O. Hourihane, N.D. Martin, and C.A. Walsh. 2000. Autosomal recessive lissencephaly with cerebellar hypoplasia is associated with human *RELN* mutations. *Nat Genet.* 26:93-96.
- Howell, B.J., B.F. McEwen, J.C. Canman, D.B. Hoffman, E.M. Farrar, C.L. Rieder, and E.D. Salmon. 2001. Cytoplasmic dynein/dynactin drives kinetochore protein transport to the spindle poles and has a role in mitotic spindle checkpoint inactivation. *J Cell Biol.* 155:1159-1172.
- Howell, B.W., F.B. Gertler, and J.A. Cooper. 1997. Mouse disabled (*mDab1*): a Src binding protein implicated in neuronal development. *EMBO J.* 16:121-132.

- Ishikawa, H., A. Kubo, S. Tsukita, and S. Tsukita. 2005. Odf2-deficient mother centrioles lack distal/subdistal appendages and the ability to generate primary cilia. *Nat Cell Biol.* 7:517-524.
- Jaglin, X.H., K. Poirier, Y. Saillour, E. Buhler, G. Tian, N. Bahi-Buisson, C. Fallet-Bianco, F. Phan-Dinh-Tuy, X.P. Kong, P. Bomont, L. Castelnau-Ptakhine, S. Odent, P. Loget, M. Kossorotoff, I. Snoeck, G. Plessis, P. Parent, C. Beldjord, C. Cardoso, A. Represa, J. Flint, D.A. Keays, N.J. Cowan, and J. Chelly. 2009. Mutations in the beta-tubulin gene TUBB2B result in asymmetrical polymicrogyria. *Nat Genet.* 41:746-752.
- Jimenez-Mateos, E.M., F. Wandosell, O. Reiner, J. Avila, and C. Gonzalez-Billault. 2005. Binding of microtubule-associated protein 1B to LIS1 affects the interaction between dynein and LIS1. *Biochem J.* 389:333-341.
- Kanai, M., M.S. Crowe, Y. Zheng, G.F. Vande Woude, and K. Fukasawa. 2010. RhoA and RhoC are both required for the ROCK II-dependent promotion of centrosome duplication. *Oncogene.* 29:6040-6050.
- Kanda, T., K.F. Sullivan, and G.M. Wahl. 1998. Histone-GFP fusion protein enables sensitive analysis of chromosome dynamics in living mammalian cells. *Curr Biol.* 8:377-385.
- Kaplan, A., and O. Reiner. 2011. Linking cytoplasmic dynein and transport of Rab8 vesicles to the midbody during cytokinesis by the doublecortin domain-containing 5 protein. *J Cell Sci.* 124:3989-4000.
- Katayama, K., J. Melendez, J.M. Baumann, J.R. Leslie, B.K. Chauhan, N. Nemkul, R.A. Lang, C.Y. Kuan, Y. Zheng, and Y. Yoshida. 2011. Loss of RhoA in neural progenitor cells causes the disruption of adherens junctions and hyperproliferation. *PNAS.* 108:7607-7612.
- Kawauchi, T., K. Chihama, Y. Nabeshima, and M. Hoshino. 2006. Cdk5 phosphorylates and stabilizes p27kip1 contributing to actin organization and cortical neuronal migration. *Nat Cell Biol.* 8:17-26.

Keays, D.A., G. Tian, K. Poirier, G.J. Huang, C. Siebold, J. Cleak, P.L. Oliver, M. Fray, R.J. Harvey, Z. Molnar, M.C. Pinon, N. Dear, W. Valdar, S.D. Brown, K.E. Davies, J.N. Rawlins, N.J. Cowan, P. Nolan, J. Chelly, and J. Flint. 2007. Mutations in alpha-tubulin cause abnormal neuronal migration in mice and lissencephaly in humans. *Cell*. 128:45-57.

Kechad, A., S. Jananji, Y. Ruella, and G.R. Hickson. 2012. Anillin acts as a bifunctional linker coordinating midbody ring biogenesis during cytokinesis. *Curr Biol*. 22:197-203.

Kholmanskikh, S.S., J.S. Dobrin, A. Wynshaw-Boris, P.C. Letourneau, and M.E. Ross. 2003. Disregulated RhoGTPases and actin cytoskeleton contribute to the migration defect in Lis1-deficient neurons. *J Neurosci*. 23:8673-8681.

Kholmanskikh, S.S., H.B. Koeller, A. Wynshaw-Boris, T. Gomez, P.C. Letourneau, and M.E. Ross. 2006. Calcium-dependent interaction of Lis1 with IQGAP1 and Cdc42 promotes neuronal motility. *Nat Neurosci*. 9:50-57.

Kinoshita, M., C.M. Field, M.L. Coughlin, A.F. Straight, and T.J. Mitchison. 2002. Self- and actin-templated assembly of Mammalian septins. *Dev Cell*. 3:791-802.

Kirschner, M.W., and T. Mitchison. 1986. Microtubule dynamics. *Nature*. 324:621.

Kitamura, K., M. Yanazawa, N. Sugiyama, H. Miura, A. Iizuka-Kogo, M. Kusaka, K. Omichi, R. Suzuki, Y. Kato-Fukui, K. Kamiirisa, M. Matsuo, S. Kamijo, M. Kasahara, H. Yoshioka, T. Ogata, T. Fukuda, I. Kondo, M. Kato, W.B. Dobyns, M. Yokoyama, and K. Morohashi. 2002. Mutation of ARX causes abnormal development of forebrain and testes in mice and X-linked lissencephaly with abnormal genitalia in humans. *Nat Genet*. 32:359-369.

Kline-Smith, S.L., and C.E. Walczak. 2004. Mitotic spindle assembly and chromosome segregation: refocusing on microtubule dynamics. *Mol Cell*. 15:317-327.

Konno, D., G. Shioi, A. Shitamukai, A. Mori, H. Kiyonari, T. Miyata, and F. Matsuzaki. 2008. Neuroepithelial progenitors undergo LGN-dependent planar divisions to maintain self-renewability during mammalian neurogenesis. *Nat Cell Biol*. 10:93-101.

- Kosako, H., T. Yoshida, F. Matsumura, T. Ishizaki, S. Narumiya, and M. Inagaki. 2000. Rho-kinase/ROCK is involved in cytokinesis through the phosphorylation of myosin light chain and not ezrin/radixin/moesin proteins at the cleavage furrow. *Oncogene*. 19:6059-6064.
- Kosodo, Y., K. Toida, V. Dubreuil, P. Alexandre, J. Schenk, E. Kiyokage, A. Attardo, F. Mora-Bermudez, T. Arii, J.D. Clarke, and W.B. Huttner. 2008. Cytokinesis of neuroepithelial cells can divide their basal process before anaphase. *EMBO J*. 27:3151-3163.
- Kramer, A., B. Maier, and J. Bartek. 2011. Centrosome clustering and chromosomal (in)stability: a matter of life and death. *Mol Oncol*. 5:324-335.
- Kwon, M., S.A. Godinho, N.S. Chandhok, N.J. Ganem, A. Azioune, M. Thery, and D. Pellman. 2008. Mechanisms to suppress multipolar divisions in cancer cells with extra centrosomes. *Genes Dev*. 22:2189-2203.
- Laan, L., N. Pavin, J. Husson, G. Romet-Lemonne, M. van Duijn, M.P. Lopez, R.D. Vale, F. Julicher, S.L. Reck-Peterson, and M. Dogterom. 2012. Cortical dynein controls microtubule dynamics to generate pulling forces that position microtubule asters. *Cell*. 148:502-514.
- Lam, C., M.A. Vergnolle, L. Thorpe, P.G. Woodman, and V.J. Allan. 2010. Functional interplay between LIS1, NDE1 and NDEL1 in dynein-dependent organelle positioning. *J Cell Sci*. 123:202-212.
- Lee, W.L., M.A. Kaiser, and J.A. Cooper. 2005. The offloading model for dynein function: differential function of motor subunits. *J Cell Biol*. 168:201-207.
- Li, J., W.L. Lee, and J.A. Cooper. 2005. NudEL targets dynein to microtubule ends through LIS1. *Nat Cell Biol*. 7:686-690.
- Liang, Y., W. Yu, Y. Li, Z. Yang, X. Yan, Q. Huang, and X. Zhu. 2004. Nudel functions in membrane traffic mainly through association with Lis1 and cytoplasmic dynein. *J Cell Biol*. 164:557-566.

- Lo Nigro, C., C.S. Chong, A.C. Smith, W.B. Dobyns, R. Carrozzo, and D.H. Ledbetter. 1997. Point mutations and an intragenic deletion in LIS1, the lissencephaly causative gene in isolated lissencephaly sequence and Miller-Dieker syndrome. *Hum Mol Genet.* 6:157-164.
- Ma, Z., M. Kanai, K. Kawamura, K. Kaibuchi, K. Ye, and K. Fukasawa. 2006. Interaction between ROCK II and nucleophosmin/B23 in the regulation of centrosome duplication. *Mol Cell Biol.* 26:9016-9034.
- Maddox, A.S., L. Lewellyn, A. Desai, and K. Oegema. 2007. Anillin and the septins promote asymmetric ingression of the cytokinetic furrow. *Dev Cell.* 12:827-835.
- Mandato, C.A., H.A. Benink, and W.M. Bement. 2000. Microtubule-actomyosin interactions in cortical flow and cytokinesis. *Cell Motil Cytoskel.* 45:87-92.
- Marin, O., M. Valiente, X. Ge, and L.H. Tsai. 2010. Guiding neuronal cell migrations. *Cold Spring Harb Perspect Biol.* 2:a001834.
- Markus, S.M., K.M. Plevock, B.J. St Germain, J.J. Punch, C.W. Meaden, and W.L. Lee. 2011. Quantitative analysis of Pac1/LIS1-mediated dynein targeting: Implications for regulation of dynein activity in budding yeast. *Cytoskeleton (Hoboken).* 68:157-174.
- Markus, S.M., J.J. Punch, and W.L. Lee. 2009. Motor- and tail-dependent targeting of dynein to microtubule plus ends and the cell cortex. *Curr Biol.* 19:196-205.
- Matsuki, T., A. Pramatarova, and B.W. Howell. 2008. Reduction of Crk and CrkL expression blocks reelin-induced dendritogenesis. *J Cell Sci.* 121:1869-1875.
- Matsumura, F., S. Ono, Y. Yamakita, G. Totsukawa, and S. Yamashiro. 1998. Specific localization of serine 19 phosphorylated myosin II during cell locomotion and mitosis of cultured cells. *J Cell Biol.* 140:119-129.
- McKenney, R.J., M. Vershinin, A. Kunwar, R.B. Vallee, and S.P. Gross. 2010. LIS1 and NudE induce a persistent dynein force-producing state. *Cell.* 141:304-314.
- McKenney, R.J., S.J. Weil, J. Scherer, and R.B. Vallee. 2011. Mutually exclusive cytoplasmic dynein regulation by NudE-Lis1 and dynactin. *J Biol Chem.* 286:39615-39622.

- Merdes, A., K. Ramyar, J.D. Vechio, and D.W. Cleveland. 1996. A complex of NuMA and cytoplasmic dynein is essential for mitotic spindle assembly. *Cell*. 87:447-458.
- Mimori-Kiyosue, Y., N. Shiina, and S. Tsukita. 2000. The dynamic behavior of the APC-binding protein EB1 on the distal ends of microtubules. *Curr Biol*. 10:865-868.
- Miyauchi, K., Y. Yamamoto, T. Kosaka, and H. Hosoya. 2006. Myosin II activity is not essential for recruitment of myosin II to the furrow in dividing HeLa cells. *Biochem Biophys Res Comm*. 350:543-548.
- Mogensen, M.M., A. Malik, M. Piel, V. Bouckson-Castaing, and M. Bornens. 2000. Microtubule minus-end anchorage at centrosomal and non-centrosomal sites: the role of ninein. *J Cell Sci*. 113 (Pt 17):3013-3023.
- Moore, J.K., and J.A. Cooper. 2010. Coordinating mitosis with cell polarity: Molecular motors at the cell cortex. *Seminars in cell & Dev Biol*. 21:283-289.
- Mori, D., Y. Yano, K. Toyo-oka, N. Yoshida, M. Yamada, M. Muramatsu, D. Zhang, H. Saya, Y.Y. Toyoshima, K. Kinoshita, A. Wynshaw-Boris, and S. Hirotsune. 2007. NDEL1 phosphorylation by Aurora-A kinase is essential for centrosomal maturation, separation, and TACC3 recruitment. *Mol Cell Biol*. 27:352-367.
- Morris, N.R., V.P. Efimov, and X. Xiang. 1998. Nuclear migration, nucleokinesis and lissencephaly. *Trends Cell Biol*. 8:467-470.
- Morris, S.M., U. Albrecht, O. Reiner, G. Eichele, and L.Y. Yu-Lee. 1998. The lissencephaly gene product Lis1, a protein involved in neuronal migration, interacts with a nuclear movement protein, NudC. *Curr Biol*. 8:603-606.
- Murthy, K., and P. Wadsworth. 2008. Dual role for microtubules in regulating cortical contractility during cytokinesis. *J Cell Sci*. 121:2350-2359.
- Nakagawa, Y., Y. Yamane, T. Okanoue, S. Tsukita, and S. Tsukita. 2001. Outer dense fiber 2 is a widespread centrosome scaffold component preferentially associated with mother centrioles: its identification from isolated centrosomes. *Mol Biol Cell*. 12:1687-1697.

- Nguyen-Ngoc, T., K. Afshar, and P. Gonczy. 2007. Coupling of cortical dynein and G alpha proteins mediates spindle positioning in *Caenorhabditis elegans*. *Nat Cell Biol.* 9:1294-1302.
- Nicholas, A.K., M. Khurshid, J. Desir, O.P. Carvalho, J.J. Cox, G. Thornton, R. Kausar, M. Ansar, W. Ahmad, A. Verloes, S. Passemard, J.P. Misson, S. Lindsay, F. Gergely, W.B. Dobyns, E. Roberts, M. Abramowicz, and C.G. Woods. 2010. WDR62 is associated with the spindle pole and is mutated in human microcephaly. *Nat Genet.* 42:1010-1014.
- Niethammer, M., D.S. Smith, R. Ayala, J. Peng, J. Ko, M.S. Lee, M. Morabito, and L.H. Tsai. 2000. NUDEL is a novel Cdk5 substrate that associates with LIS1 and cytoplasmic dynein. *Neuron.* 28:697-711.
- Nigg, E.A. 2002. Centrosome aberrations: cause or consequence of cancer progression? *Nature reviews. Cancer.* 2:815-825.
- Nigg, E.A., and T. Stearns. 2011. The centrosome cycle: Centriole biogenesis, duplication and inherent asymmetries. *Nat Cell Biol.* 13:1154-1160.
- Nishimura, Y., and S. Yonemura. 2006. Centralspindlin regulates ECT2 and RhoA accumulation at the equatorial cortex during cytokinesis. *J Cell Sci.* 119:104-114.
- O'Connell, C.B., and Y.L. Wang. 2000. Mammalian spindle orientation and position respond to changes in cell shape in a dynein-dependent fashion. *Mol Biol Cell.* 11:1765-1774.
- Oegema, K., M.S. Savoian, T.J. Mitchison, and C.M. Field. 2000. Functional analysis of a human homologue of the *Drosophila* actin binding protein anillin suggests a role in cytokinesis. *J Cell Biol.* 150:539-552.
- Ozcelik, T., N. Akarsu, E. Uz, S. Caglayan, S. Gulsuner, O.E. Onat, M. Tan, and U. Tan. 2008. Mutations in the very low-density lipoprotein receptor VLDLR cause cerebellar hypoplasia and quadrupedal locomotion in humans. *PNAS.* 105:4232-4236.
- Palmer, K.J., H. Hughes, and D.J. Stephens. 2009. Specificity of cytoplasmic dynein subunits in discrete membrane-trafficking steps. *Mol Biol Cell.* 20:2885-2899.

- Park, T.J., K. Boyd, and T. Curran. 2006. Cardiovascular and craniofacial defects in Crk-null mice. *Mol Cell Biol.* 26:6272-6282.
- Park, T.J., and T. Curran. 2008. Crk and Crk-like play essential overlapping roles downstream of disabled-1 in the Reelin pathway. *J Neurosci.* 28:13551-13562.
- Pawlisz, A.S., C. Mutch, A. Wynshaw-Boris, A. Chenn, C.A. Walsh, and Y. Feng. 2008. Lis1-Nde1-dependent neuronal fate control determines cerebral cortical size and lamination. *Hum Mol Genet.* 17:2441-2455.
- Paylor, R., S. Hirotsune, M.J. Gambello, L. Yuva-Paylor, J.N. Crawley, and A. Wynshaw-Boris. 1999. Impaired learning and motor behavior in heterozygous Pafah1b1 (Lis1) mutant mice. *Learn Mem.* 6:521-537.
- Piekny, A., M. Werner, and M. Glotzer. 2005. Cytokinesis: welcome to the Rho zone. *Trends Cell Biol.* 15:651-658.
- Piekny, A.J., and M. Glotzer. 2008. Anillin is a scaffold protein that links RhoA, actin, and myosin during cytokinesis. *Curr Biol.* 18:30-36.
- Pigino, G., G. Paglini, L. Ulloa, J. Avila, and A. Caceres. 1997. Analysis of the expression, distribution and function of cyclin dependent kinase 5 (cdk5) in developing cerebellar macroneurons. *J Cell Sci.* 110 (Pt 2):257-270.
- Poirier, K., D.A. Keays, F. Francis, Y. Saillour, N. Bahi, S. Manouvrier, C. Fallet-Bianco, L. Pasquier, A. Toutain, F.P. Tuy, T. Bienvenu, S. Joriot, S. Odent, D. Ville, I. Desguerre, A. Goldenberg, M.L. Moutard, J.P. Fryns, H. van Esch, R.J. Harvey, C. Siebold, J. Flint, C. Beldjord, and J. Chelly. 2007. Large spectrum of lissencephaly and pachygyria phenotypes resulting from de novo missense mutations in tubulin alpha 1A (TUBA1A). *Hum Mutat.* 28:1055-1064.
- Pramparo, T., O. Libiger, S. Jain, H. Li, Y.H. Youn, S. Hirotsune, N.J. Schork, and A. Wynshaw-Boris. 2011. Global developmental gene expression and pathway analysis of normal brain

- development and mouse models of human neuronal migration defects. *PLoS Genet.* 7:e1001331.
- Pramparo, T., Y.H. Youn, J. Yingling, S. Hirotsune, and A. Wynshaw-Boris. 2010. Novel embryonic neuronal migration and proliferation defects in *Dcx* mutant mice are exacerbated by *Lis1* reduction. *J Neurosci.* 30:3002-3012.
- Quille, M.L., S. Carat, S. Quemener-Redon, E. Hirchaud, D. Baron, C. Benech, J. Guihot, M. Placet, O. Mignen, C. Ferec, R. Houlgatte, and G. Friocourt. 2011. High-throughput analysis of promoter occupancy reveals new targets for *Arx*, a gene mutated in mental retardation and interneuronopathies. *PLoS One.* 6:e25181.
- Quintyne, N.J., J.E. Reing, D.R. Hoffelder, S.M. Gollin, and W.S. Saunders. 2005. Spindle multipolarity is prevented by centrosomal clustering. *Science.* 307:127-129.
- Rakic, P. 1974. Neurons in rhesus monkey visual cortex: systematic relation between time of origin and eventual disposition. *Science.* 183:425-427.
- Rankin, K.E., and L. Wordeman. 2010. Long astral microtubules uncouple mitotic spindles from the cytokinetic furrow. *J Cell Biol.* 190:35-43.
- Reiner, O., R. Carrozzo, Y. Shen, M. Wehnert, F. Faustinella, W.B. Dobyns, C.T. Caskey, and D.H. Ledbetter. 1993. Isolation of a Miller-Dieker lissencephaly gene containing G protein. *Science.* 261:185-188.
- Reiner, O., S. Sapoznik, and T. Sapir. 2006. Lissencephaly 1 linking to multiple diseases: mental retardation, neurodegeneration, schizophrenia, male sterility, and more. *Neuromolecular Med.* 8:547-565.
- Rieder, C.L., and H. Maiato. 2004. Stuck in division or passing through: what happens when cells cannot satisfy the spindle assembly checkpoint. *Dev Cell.* 7:637-651.
- Roszko, I., C. Afonso, D. Henrique, and L. Mathis. 2006. Key role played by RhoA in the balance between planar and apico-basal cell divisions in the chick neuroepithelium. *Dev Biol.* 298:212-224.

- Sapir, T., M. Elbaum, and O. Reiner. 1997. Reduction of microtubule catastrophe events by LIS1, platelet-activating factor acetylhydrolase subunit. *EMBO J.* 16:6977-6984.
- Sapir, T., A. Shmueli, T. Levy, T. Timm, M. Elbaum, E.M. Mandelkow, and O. Reiner. 2008. Antagonistic effects of doublecortin and MARK2/Par-1 in the developing cerebral cortex. *J Neurosci.* 28:13008-13013.
- Sarkisian, M.R., W. Li, F. Di Cunto, S.R. D'Mello, and J.J. LoTurco. 2002. Citron-kinase, a protein essential to cytokinesis in neuronal progenitors, is deleted in the flathead mutant rat. *J Neurosci.* 22:RC217.
- Sasaki, S., D. Mori, K. Toyooka, A. Chen, L. Garrett-Beal, M. Muramatsu, S. Miyagawa, N. Hiraiwa, A. Yoshiki, A. Wynshaw-Boris, and S. Hirotsune. 2005. Complete loss of Ndel1 results in neuronal migration defects and early embryonic lethality. *Mol Cell Biol.* 25:7812-7827.
- Sasaki, S., A. Shionoya, M. Ishida, M.J. Gambello, J. Yingling, A. Wynshaw-Boris, and S. Hirotsune. 2000. A LIS1/NUDEL/cytoplasmic dynein heavy chain complex in the developing and adult nervous system. *Neuron.* 28:681-696.
- Schaar, B.T., K. Kinoshita, and S.K. McConnell. 2004. Doublecortin microtubule affinity is regulated by a balance of kinase and phosphatase activity at the leading edge of migrating neurons. *Neuron.* 41:203-213.
- Schaar, B.T., and S.K. McConnell. 2005. Cytoskeletal coordination during neuronal migration. *PNAS.* 102:13652-13657.
- Schroer, T.A. 2004. Dynactin. *Annu Rev Cell Dev Biol.* 20:759-779.
- Schuyler, S.C., and D. Pellman. 2001. Microtubule "plus-end-tracking proteins": The end is just the beginning. *Cell.* 105:421-424.
- Sedzinski, J., M. Biro, A. Oswald, J.Y. Tinevez, G. Salbreux, and E. Paluch. 2011. Polar actomyosin contractility destabilizes the position of the cytokinetic furrow. *Nature.* 476:462-466.

- Sheeman, B., P. Carvalho, I. Sagot, J. Geiser, D. Kho, M.A. Hoyt, and D. Pellman. 2003. Determinants of *S. cerevisiae* dynein localization and activation: implications for the mechanism of spindle positioning. *Curr Biol.* 13:364-372.
- Siller, K.H., M. Serr, R. Steward, T.S. Hays, and C.Q. Doe. 2005. Live imaging of *Drosophila* brain neuroblasts reveals a role for Lis1/dynactin in spindle assembly and mitotic checkpoint control. *Mol Biol Cell.* 16:5127-5140.
- Smith, D.S., M. Niethammer, R. Ayala, Y. Zhou, M.J. Gambello, A. Wynshaw-Boris, and L.H. Tsai. 2000. Regulation of cytoplasmic dynein behaviour and microtubule organization by mammalian Lis1. *Nat Cell Biol.* 2:767-775.
- Solecki, D.J., L. Model, J. Gaetz, T.M. Kapoor, and M.E. Hatten. 2004. Par6alpha signaling controls glial-guided neuronal migration. *Nat Neurosci.* 7:1195-1203.
- Solecki, D.J., N. Trivedi, E.E. Govek, R.A. Kerekes, S.S. Gleason, and M.E. Hatten. 2009. Myosin II motors and F-actin dynamics drive the coordinated movement of the centrosome and soma during CNS glial-guided neuronal migration. *Neuron.* 63:63-80.
- Stehman, S.A., Y. Chen, R.J. McKenney, and R.B. Vallee. 2007. NudE and NudEL are required for mitotic progression and are involved in dynein recruitment to kinetochores. *J Cell Biol.* 178:583-594.
- Straight, A.F., A. Cheung, J. Limouze, I. Chen, N.J. Westwood, J.R. Sellers, and T.J. Mitchison. 2003. Dissecting temporal and spatial control of cytokinesis with a myosin II Inhibitor. *Science.* 299:1743-1747.
- Straight, A.F., C.M. Field, and T.J. Mitchison. 2005. Anillin binds nonmuscle myosin II and regulates the contractile ring. *Mol Biol Cell.* 16:193-201.
- Strickland, L.I., Y. Wen, G.G. Gundersen, and D.R. Burgess. 2005. Interaction between EB1 and p150glued is required for anaphase astral microtubule elongation and stimulation of cytokinesis. *Curr Biol.* 15:2249-2255.

- Su, S.C., and L.H. Tsai. 2010. Cyclin-Dependent Kinases in Brain Development and Disease. *Annu Rev Cell Dev Biol.*
- Sumigray, K.D., H. Chen, and T. Lechler. 2011. Lis1 is essential for cortical microtubule organization and desmosome stability in the epidermis. *J Cell Biol.* 194:631-642.
- Tai, C.Y., D.L. Dujardin, N.E. Faulkner, and R.B. Vallee. 2002. Role of dynein, dynactin, and CLIP-170 interactions in LIS1 kinetochore function. *J Cell Biol.* 156:959-968.
- Tanaka, T., H. Koizumi, and J.G. Gleeson. 2006. The doublecortin and doublecortin-like kinase 1 genes cooperate in murine hippocampal development. *Cereb Cortex.* 16 Suppl 1:i69-73.
- Tanaka, T., F.F. Serneo, C. Higgins, M.J. Gambello, A. Wynshaw-Boris, and J.G. Gleeson. 2004. Lis1 and doublecortin function with dynein to mediate coupling of the nucleus to the centrosome in neuronal migration. *J Cell Biol.* 165:709-721.
- Tanaka, T., F.F. Serneo, H.C. Tseng, A.B. Kulkarni, L.H. Tsai, and J.G. Gleeson. 2004. Cdk5 phosphorylation of doublecortin ser297 regulates its effect on neuronal migration. *Neuron.* 41:215-227.
- Thery, M., A. Jimenez-Dalmaroni, V. Racine, M. Bornens, and F. Julicher. 2007. Experimental and theoretical study of mitotic spindle orientation. *Nature.* 447:493-496.
- Thoma, C.R., A. Toso, K.L. Gutbrodt, S.P. Reggi, I.J. Frew, P. Schraml, A. Hergovich, H. Moch, P. Meraldi, and W. Krek. 2009. VHL loss causes spindle misorientation and chromosome instability. *Nat Cell Biol.* 11:994-1001.
- Tischfield, M.A., H.N. Baris, C. Wu, G. Rudolph, L. Van Maldergem, W. He, W.M. Chan, C. Andrews, J.L. Demer, R.L. Robertson, D.A. Mackey, J.B. Ruddle, T.D. Bird, I. Gottlob, C. Pieh, E.I. Traboulsi, S.L. Pomeroy, D.G. Hunter, J.S. Soul, A. Newlin, L.J. Sabol, E.J. Doherty, C.E. de Uzcategui, N. de Uzcategui, M.L. Collins, E.C. Sener, B. Wabbels, H. Hellebrand, T. Meitinger, T. de Berardinis, A. Magli, C. Schiavi, M. Pastore-Trossello, F. Koc, A.M. Wong, A.V. Levin, M.T. Geraghty, M. Descartes, M. Flaherty, R.V. Jamieson, H.U. Moller, I. Meuthen, D.F. Callen, J. Kerwin, S. Lindsay, A. Meindl, M.L. Gupta, Jr.,

- D. Pellman, and E.C. Engle. 2010. Human TUBB3 mutations perturb microtubule dynamics, kinesin interactions, and axon guidance. *Cell*. 140:74-87.
- Tokuoka, S.M., S. Ishii, N. Kawamura, M. Satoh, A. Shimada, S. Sasaki, S. Hirotsune, A. Wynshaw-Boris, and T. Shimizu. 2003. Involvement of platelet-activating factor and LIS1 in neuronal migration. *Eur J Neurosci*. 18:563-570.
- Toyo-oka, K., A. Shionoya, M.J. Gambello, C. Cardoso, R. Leventer, H.L. Ward, R. Ayala, L.H. Tsai, W. Dobyns, D. Ledbetter, S. Hirotsune, and A. Wynshaw-Boris. 2003. 14-3-3epsilon is important for neuronal migration by binding to NUDEL: a molecular explanation for Miller-Dieker syndrome. *Nat Genet*. 34:274-285.
- Toyoshima, F., S. Matsumura, H. Morimoto, M. Mitsushima, and E. Nishida. 2007. PtdIns(3,4,5)P3 regulates spindle orientation in adherent cells. *Dev Cell*. 13:796-811.
- Toyoshima, F., and E. Nishida. 2007. Integrin-mediated adhesion orients the spindle parallel to the substratum in an EB1- and myosin X-dependent manner. *EMBO J*. 26:1487-1498.
- Trommsdorff, M., M. Gotthardt, T. Hiesberger, J. Shelton, W. Stockinger, J. Nimpf, R.E. Hammer, J.A. Richardson, and J. Herz. 1999. Reeler/Disabled-like disruption of neuronal migration in knockout mice lacking the VLDL receptor and ApoE receptor 2. *Cell*. 97:689-701.
- Tsai, J.W., Y. Chen, A.R. Kriegstein, and R.B. Vallee. 2005. LIS1 RNA interference blocks neural stem cell division, morphogenesis, and motility at multiple stages. *J Cell Biol*. 170:935-945.
- Tsai, L.H., and J.G. Gleeson. 2005. Nucleokinesis in neuronal migration. *Neuron*. 46:383-388.
- Tsukada, M., A. Prokscha, E. Ungewickell, and G. Eichele. 2005. Doublecortin association with actin filaments is regulated by neurabin II. *J Biol Chem*. 280:11361-11368.
- von Dassow, G. 2009. Concurrent cues for cytokinetic furrow induction in animal cells. *Trends Cell Biol*. 19:165-173.

- Watanabe, S., Y. Ando, S. Yasuda, H. Hosoya, N. Watanabe, T. Ishizaki, and S. Narumiya. 2008. mDia2 induces the actin scaffold for the contractile ring and stabilizes its position during cytokinesis in NIH 3T3 cells. *Mol Biol Cell*. 19:2328-2338.
- Werner, M., E. Munro, and M. Glotzer. 2007. Astral signals spatially bias cortical myosin recruitment to break symmetry and promote cytokinesis. *Curr Biol*. 17:1286-1297.
- Wynshaw-Boris, A. 2007. Lissencephaly and LIS1: insights into the molecular mechanisms of neuronal migration and development. *Clin Genet*. 72:296-304.
- Wynshaw-Boris, A., T. Pramparo, Y.H. Youn, and S. Hirotsune. 2010. Lissencephaly: mechanistic insights from animal models and potential therapeutic strategies. *Seminars in cell & Dev Biol*. 21:823-830.
- Xiang, X., A.H. Osmani, S.A. Osmani, M. Xin, and N.R. Morris. 1995. NudF, a nuclear migration gene in *Aspergillus nidulans*, is similar to the human LIS-1 gene required for neuronal migration. *Mol Biol Cell*. 6:297-310.
- Xie, Z., K. Sanada, B.A. Samuels, H. Shih, and L.H. Tsai. 2003. Serine 732 phosphorylation of FAK by Cdk5 is important for microtubule organization, nuclear movement, and neuronal migration. *Cell*. 114:469-482.
- Xing, Z., X. Tang, Y. Gao, L. Da, H. Song, S. Wang, P. Tiollais, T. Li, and M. Zhao. 2011. The human LIS1 is downregulated in hepatocellular carcinoma and plays a tumor suppressor function. *Biochem Biophys Res Comm*. 409:193-199.
- Xu, H., K. Huang, Q. Gao, Z. Gao, and X. Han. 2001. A study on the prevention and treatment of myopia with nacre on chicks. *Pharmacol Res*. 44:1-6.
- Yamada, M., Y. Yoshida, D. Mori, T. Takitoh, M. Kengaku, H. Umeshima, K. Takao, T. Miyakawa, M. Sato, H. Sorimachi, A. Wynshaw-Boris, and S. Hirotsune. 2009. Inhibition of calpain increases LIS1 expression and partially rescues in vivo phenotypes in a mouse model of lissencephaly. *Nat Med*. 15:1202-1207.

- Yamashiro, S., G. Totsukawa, Y. Yamakita, Y. Sasaki, P. Madaule, T. Ishizaki, S. Narumiya, and F. Matsumura. 2003. Citron kinase, a Rho-dependent kinase, induces di-phosphorylation of regulatory light chain of myosin II. *Mol Biol Cell*. 14:1745-1756.
- Yang, Z., J. Loncarek, A. Khodjakov, and C.L. Rieder. 2008. Extra centrosomes and/or chromosomes prolong mitosis in human cells. *Nat Cell Biol*. 10:748-751.
- Yingling, J., Y.H. Youn, D. Darling, K. Toyo-Oka, T. Pramparo, S. Hirotsune, and A. Wynshaw-Boris. 2008. Neuroepithelial stem cell proliferation requires LIS1 for precise spindle orientation and symmetric division. *Cell*. 132:474-486.
- Yonemura, S., K. Hirao-Minakuchi, and Y. Nishimura. 2004. Rho localization in cells and tissues. *Exp Cell Res*. 295:300-314.
- Youn, Y.H., T. Pramparo, S. Hirotsune, and A. Wynshaw-Boris. 2009. Distinct dose-dependent cortical neuronal migration and neurite extension defects in *Lis1* and *Ndel1* mutant mice. *J Neurosci*. 29:15520-15530.
- Yu, T.W., G.H. Mochida, D.J. Tischfield, S.K. Sgaier, L. Flores-Sarnat, C.M. Sergi, M. Topcu, M.T. McDonald, B.J. Barry, J.M. Felie, C. Sunu, W.B. Dobyns, R.D. Folkerth, A.J. Barkovich, and C.A. Walsh. 2010. Mutations in *WDR62*, encoding a centrosome-associated protein, cause microcephaly with simplified gyri and abnormal cortical architecture. *Nat Genet*. 42:1015-1020.
- Zhang, M.Y., N.N. Huang, G.A. Clawson, S.A. Osmani, W. Pan, P. Xin, M.S. Razzaque, and B.A. Miller. 2002. Involvement of the fungal nuclear migration gene *nudC* human homolog in cell proliferation and mitotic spindle formation. *Exp Cell Res*. 273:73-84.
- Zhao, W.M., and G. Fang. 2005. Anillin is a substrate of anaphase-promoting complex/cyclosome (APC/C) that controls spatial contractility of myosin during late cytokinesis. *J Biol Chem*. 280:33516-33524.
- Zhou, M., and Y.L. Wang. 2008. Distinct pathways for the early recruitment of myosin II and actin to the cytokinetic furrow. *Mol Biol Cell*. 19:318-326.

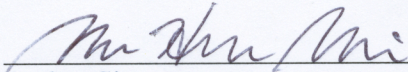
- Zhou, T., J.P. Aumais, X. Liu, L.Y. Yu-Lee, and R.L. Erikson. 2003. A role for Plk1 phosphorylation of NudC in cytokinesis. *Dev Cell*. 5:127-138.
- Zimmerman, W., and S.J. Doxsey. 2000. Construction of centrosomes and spindle poles by molecular motor-driven assembly of protein particles. *Traffic*. 1:927-934.
- Zimmerman, W.C., J. Sillibourne, J. Rosa, and S.J. Doxsey. 2004. Mitosis-specific anchoring of gamma tubulin complexes by pericentrin controls spindle organization and mitotic entry. *Mol Biol Cell*. 15:3642-3657.
- Zylkiewicz, E., M. Kijanska, W.C. Choi, U. Derewenda, Z.S. Derewenda, and P.T. Stukenberg. 2011. The N-terminal coiled-coil of Ndel1 is a regulated scaffold that recruits LIS1 to dynein. *J Cell Biol*. 192:433-445.

Publishing Agreement

It is the policy of the University to encourage the distribution of all theses, dissertations, and manuscripts. Copies of all UCSF theses, dissertations, and manuscripts will be routed to the library via the Graduate Division. The library will make all theses, dissertations, and manuscripts accessible to the public and will preserve these to the best of their abilities, in perpetuity.

Please sign the following statement:

I hereby grant permission to the Graduate Division of the University of California, San Francisco to release copies of my thesis, dissertation, or manuscript to the Campus Library to provide access and preservation, in whole or in part, in perpetuity.



Author Signature

11/7/2012
Date